

**POLITECNICO DI MILANO**  
SCHOOL OF INDUSTRIAL AND INFORMATION ENGINEERING  
MASTER OF SCIENCE IN SPACE ENGINEERING  
DEPARTMENT OF AEROSPACE SCIENCE AND TECHNOLOGY



# Adaptive Hybrid System Framework for unified Admittance and Impedance Control of Manipulators

**Advisor:** Prof. Mauro MASSARI  
**Co-Advisor:** Prof. Ranjan MUKHERJEE

**Master's Thesis of:**  
Francesco CAVENAGO 815771  
Lorenzo VOLI 824385

ACADEMIC YEAR 2014-2015

---

## Abstract

Manipulation is an important area in the robotic field since it is employed in many applications. An increasing number of activities requires the support of robots to humans in order to guarantee safety or to improve the performance, above all in demanding challenges typical of space research, humanoid development and health-care assistance. Therefore many efforts have been concentrated on developing new control strategies to deal with the interaction with different environments. In this context, the impedance control in its two typical implementations, known as "Admittance Control" and "Impedance Control", has been widely used since it is capable of taking into account the dynamic coupling between the robot and the environment. Admittance and Impedance Control show different stability requirements and for this reason they are employed in different scenarios. In the present work a new impedance control algorithm is proposed aimed at unifying these two formulations. It is an Adaptive Hybrid System that interpolates the features between Admittance and Impedance Control by rapidly switching between them. Acting on the duty cycle of the switching system, it is able to guarantee good performance and robustness in unknown environment, even time variant. The adaptive component is realized with a Multilayer Feedforward Neural Network that receives the states of the system and the interaction force as inputs and gives a proper duty cycle as output. The proposed new controller is developed for 1 d.o.f. and 2 d.o.f.s systems. The performance and robustness to uncompensated friction, delay and uncertainties are proved by means of numerical simulations.

**Keywords:** Impedance Control, Admittance Control, switching system, adaptive system, neural network, genetic algorithm, unknown environment, manipulation.



## Sommario

Nel campo della robotica il problema della manipolazione è da sempre di particolare interesse: un crescente numero di attività richiedono l'affiancamento di robot a operatori umani per garantire la sicurezza e incrementare le performance. In ambiti quali la ricerca spaziale, lo sviluppo di umanoidi e l'assistenza sanitaria questo bisogno diventa più impellente per far fronte alle nuove sfide che si impongono. Per questo motivo molti sforzi sono stati fatti per sviluppare nuove strategie di controllo volte a gestire l'interazione tra l'automa e l'oggetto manipolato. In questo contesto il controllo di impedenza nelle sue due formulazioni, note come "Controllo di Ammettenza" e "Controllo di Impedenza", è stato largamente utilizzato in quanto capace di gestire l'accoppiamento dinamico tra robot e ambiente interagente. Il Controllo di Ammettenza e il Controllo di Impedenza mostrano requisiti di stabilità opposti, di conseguenza viene usato rispettivamente uno o l'altro a seconda dello scenario in cui ci si trova ad operare. Nel presente lavoro è proposto un nuovo algoritmo per il controllo di impedenza che ha lo scopo di unificare le due differenti implementazioni. Il sistema ibrido adattativo è in grado di interpolare le caratteristiche del Controllo di Ammettenza e di Impedenza commutando rapidamente tra i due. Agendo sul duty cycle dello switch, il sistema è in grado di garantire ottime performance e un alto livello di robustezza durante l'interazione con ambienti sconosciuti, anche tempo-varianti. La componente adattativa è realizzata sfruttando una rete neurale feedforward che riceve gli stati del sistema e la forza di interazione come ingressi e fornisce un adeguato duty cycle come output. La strategia di controllo presentata è sviluppata su sistemi ad uno e due gradi di libertà. Le performance e la robustezza sono provate attraverso simulazioni numeriche.

**Parole chiave:** Controllo di Impedenza, Controllo di Ammettenza, switch, sistema adattativo, reti neurali, algoritmo genetico, ambiente sconosciuto, manipolazione, manipolatori.

---

# Contents

<b>1</b>	<b>Introduction</b>	<b>15</b>
<b>2</b>	<b>Background</b>	<b>21</b>
2.1	Impedance control framework . . . . .	21
2.2	Problem statement . . . . .	22
2.3	Impedance Control . . . . .	23
2.4	Admittance Control . . . . .	23
2.5	Comparison of Impedance and Admittance Control . . . . .	24
2.6	Hybrid system . . . . .	26
2.6.1	Motivations . . . . .	26
2.6.2	Structure . . . . .	27
2.7	Simulation examples . . . . .	29
<b>3</b>	<b>Hybrid System Framework in the 2 d.o.f.s case</b>	<b>35</b>
3.1	Dynamic model . . . . .	36
3.2	Control law . . . . .	37
3.3	Simulation results . . . . .	39
<b>4</b>	<b>Adaptive strategy: introduction and applications</b>	<b>43</b>
4.1	Applications . . . . .	43
4.1.1	Industry . . . . .	43
4.1.2	Space . . . . .	44
4.1.3	Healthcare . . . . .	46
4.2	Problem overview . . . . .	47
4.3	Possible solutions and limitations . . . . .	49
4.4	Neural Network adaptive solution . . . . .	54
4.5	Neural Network: basic concepts . . . . .	55
4.6	Genetic Algorithm . . . . .	58
<b>5</b>	<b>Adaptive system: Neural Network model and training</b>	<b>61</b>
5.1	Neural Network structure in the 1 d.o.f. system . . . . .	61

5.2	Neural Network training in the 1 d.o.f. system . . . . .	65
5.2.1	Command position . . . . .	65
5.2.2	Stiffness set selection . . . . .	68
5.2.3	Fitness function . . . . .	68
5.2.4	Population size and weights boundaries . . . . .	70
5.3	Neural Network structure in the 2 d.o.f.s system . . . . .	76
5.4	Neural Network training in the 2 d.o.f.s system . . . . .	77
<b>6</b>	<b>Results</b>	<b>81</b>
6.1	Fixed environment stiffness . . . . .	81
6.2	Time-variant stiffness . . . . .	92
6.3	Robustness analysis . . . . .	99
6.4	Specialized training . . . . .	105
<b>7</b>	<b>Conclusions</b>	<b>107</b>



# List of Tables

5.1	Starting Upper Boundaries (UB) and Lower Boundaries (LB) for the weights and biases . . . . .	73
5.2	Intermediate solution for the network weights and biases .	73
5.3	Refined Upper Boundaries (UB) and Lower Boundaries (LB) for the weights and biases . . . . .	74
5.4	Starting Upper Boundaries (UB) and Lower Boundaries (LB) for the weights and biases . . . . .	78



# List of Figures

2.1	Impedance Control system structure . . . . .	23
2.2	Admittance Control system structure . . . . .	24
2.3	Concept of Impedance Control . . . . .	25
2.4	Concept of Admittance Control . . . . .	26
2.5	Qualitative illustration of the performance of Impedance Control and Admittance Control for different environment stiffness . . . . .	26
2.6	Concept of Hybrid Control . . . . .	27
2.7	Single degree-of-freedom system interacting with an environment . . . . .	30
2.8	Re-scaled ideal trajectories of the single d.o.f. system for a step change in the virtual equilibrium position for a soft and a stiff environment . . . . .	31
2.9	Deviation from the ideal trajectory for Impedance, Admittance and Hybrid Control for the soft environment $k_e = 10N/m$ . . . . .	32
2.10	Deviation from the ideal trajectory for Impedance, Admittance and Hybrid Control for the stiff environment $k_e = 3200N/m$ . . . . .	32
2.11	Deviation from the ideal trajectory for Impedance, Admittance and Hybrid Control for intermediate environment $k_e = 1300N/m$ . . . . .	33
3.1	2 dofs system graphic representation . . . . .	35
3.2	2 d.o.f.s system error response with Hybrid Control for the soft environment $k_e = 10N/m$ . . . . .	41
3.3	2 d.o.f.s system error response with Hybrid Control for the intermediate environment stiffness $k_e = 1400N/m$ . . . . .	42
3.4	2 d.o.f.s system error response with Hybrid Control for the stiff environment $k_e = 3200N/m$ . . . . .	42

4.1	DLR Justin humanoid cleaning a window . . . . .	44
4.2	Artistic representation that shows an OOS mission . . . . .	45
4.3	Manipulation task representation . . . . .	45
4.4	Rehabilitation device representation . . . . .	46
4.5	Switching concept . . . . .	47
4.6	Deviation from the reference response with $k_e = 10N/m$ considering models with and without uncertainties, delays and uncompensated friction. . . . .	50
4.7	Mapping $n_{optimal} - k_e$ . . . . .	51
4.8	Comparison between Impedance, Admittance and Hybrid Control with optimal $n$ for environment stiffness $k_e = 10N/m$	52
4.9	Comparison between Impedance, Admittance and Hybrid Control with optimal $n$ for environment stiffness $k_e = 1500N/m$	52
4.10	Comparison between Impedance, Admittance and Hybrid Control with optimal $n$ for environment stiffness $k_e = 3200N/m$	53
4.11	Structure of neuron $k$ . . . . .	56
4.12	Multilayer feedforward architecture . . . . .	57
4.13	Single-point crossover operator . . . . .	59
5.1	Neural Network adaptive system diagram . . . . .	62
5.2	Neuron implemented in Simulink . . . . .	63
5.3	Neural Network implemented in Simulink . . . . .	64
5.4	Double step in a single command trajectory . . . . .	66
5.5	Two separate step command trajectories . . . . .	66
5.6	Two separate step command trajectories: one positive and one negative . . . . .	66
5.7	Responses of the solutions of two different classes trained with the same command position trajectory $x_0$ . . . . .	67
5.8	Optimal time invariant $n$ relative to the selected $k_e$ discretization . . . . .	69
5.9	Flowchart of the procedure for the weights boundaries and population size setting . . . . .	72
5.10	Comparison between the error response trends of the intermediate and final sets of coefficients with $k_e = 10N/m$ . . . . .	74
5.11	Final network weights and biases for the single d.o.f. system	75
5.12	Neural Network adaptive system diagram in 2 d.o.f.s case . . . . .	77
5.13	Final network weights and biases for the two d.o.f.s system	79
6.1	Error responses of the single d.o.f. system to a step command position from 0 to 0.5m for $k_e = 10N/m$ . . . . .	83

List of Figures

---

6.2	Error responses of the single d.o.f. system to a step command position from 0 to $0.5m$ for $k_e = 700N/m$ . . . . .	84
6.3	Error responses of the single d.o.f. system to a step command position from 0 to $0.5m$ for $k_e = 2100N/m$ . . . . .	85
6.4	Error responses of the single d.o.f. system to a step command position from 0 to $0.5m$ for $k_e = 3200N/m$ . . . . .	86
6.5	Error responses of the 2 d.o.f.s system to a step command position from 0 to $0.5m$ for $k_e = 10N/m$ . . . . .	87
6.6	Error responses of the 2 d.o.f.s system to a step command position from 0 to $0.5m$ for $k_e = 700N/m$ . . . . .	88
6.7	Error responses of the 2 d.o.f.s system to a step command position from 0 to $0.5m$ for $k_e = 2100N/m$ . . . . .	89
6.8	Error responses of the 2 d.o.f.s system to a step command position from 0 to $0.5m$ for $k_e = 3200N/m$ . . . . .	90
6.9	Joints coordinates of the 2 d.o.f.s system to a step command position from 0 to $0.5m$ for $k_e = 10N/m$ and $k_e = 3200N/m$	91
6.10	Time varying contact stiffness $k_e$ , command position $x_0$ and adapted $n$ trend for the single d.o.f. system . . . . .	93
6.11	Comparison of errors for the time varying $k_e$ for the single d.o.f. system . . . . .	94
6.12	Time varying contact stiffness $k_e$ with exponential trend and related command position $x_0$ for the simulation in the single d.o.f. system cases . . . . .	95
6.13	Comparison of errors for the time variant $k_e$ , with exponential trend, in the single d.o.f. system case . . . . .	96
6.14	Time varying contact stiffness $k_e$ with exponential trend and related command position $x_{e0}$ for the simulation in the 2 d.o.f.s system cases . . . . .	97
6.15	Comparison of errors for the time variant $k_e$ , with exponential trend, in the 2 d.o.f.s system case . . . . .	98
6.16	Error responses of the single d.o.f. system to a step command position from 0 to $0.5m$ for $k_e = 5000N/m$ out of the training range . . . . .	100
6.17	Error responses of the single d.o.f. system with increased uncertainties respectively for $k_e = 10N/m$ and $k_e = 1200N/m$	101
6.18	Error responses of the single d.o.f. system with increased uncertainties respectively for $k_e = 2600N/m$ and $k_e = 3200N/m$ . . . . .	102
6.19	Error responses of the 2 d.o.f.s system with increased uncertainties respectively for $k_e = 10N/m$ and $k_e = 1200N/m$	103

6.20	Error responses of the 2 d.o.f.s system with increased uncertainties respectively for $k_e = 2600N/m$ and $k_e = 3200N/m$	104
6.21	Comparison between error responses of Hybrid Control and Adaptive Hybrid Control for $k_e = 1600N/m$	106

# Chapter 1

## Introduction

In the last 40 years, impact of robots in human life has increased significantly. Advances in mechatronics and robotics have enabled the development of many machines capable of supporting human beings in a growing number of activities.

Robotic capabilities have moved from simple operations to more advanced and difficult tasks carrying considerable improvements in many different fields, such as industrial manufacturing, commercial services, space exploration, medical and military applications.

Nowadays many efforts are focused on manipulation tasks involving dynamic interaction between robot and environment, since they would open to new and fascinating perspectives.

The dynamic coupling between manipulator and environment generates reaction forces that must be handled properly to avoid undesired effects. Pure position control fails in this situation. Contact forces cause deviations from the desired trajectory that the control system tries to compensate. This leads to a build-up of that forces, until breakage of robot hardware or manipulated object.

This is a crucial aspect in many applications from the industrial ones to more demanding challenges typical of space operations, health applications and humanoids development.

Today space research efforts are concentrated on topics like On Orbit Servicing (OOS) [31, 32] and assistance to astronauts for intra-vehicular and extra-vehicular activities [33] where many robotic devices are exploited. They have to be able to manipulate objects with different features and conditions, often unknown *a priori* for the OOS.

As regards healthcare, exoskeletons and manipulators require control approaches capable of guaranteeing appropriate and safe dynamic interaction between human and robot.

The work here presented is a new controller that wants to respond to these needs. It is a new way to deal with the interaction between robots and unknown environment. It unifies in a single framework two impedance control implementations having opposite features. Thanks to this hybrid nature it can work properly in different scenarios. Moreover the adaptivity of this system makes it capable of guaranteeing good performance even in situations where informations about the manipulated object are poor.

Historically two fundamentals control methodologies have been proposed to deal with the manipulation issue.

The first strategy is known as "Hybrid Position and Force Control", it was proposed by Raibert and Craig [1] and then developed by Mason [2]. It is based on formal models of the manipulator and the task geometry. Since it is not possible to control both position and force along the same d.o.f., in this approach the task space is split into two domains, the position and the force subspaces. The reaction force is controlled in the force subspace and the position of the end effector is controlled in the position subspace. The main drawback of this approach is its failure to recognize the importance of the manipulator impedance, i.e. it does not consider the dynamic coupling between robot and environment.

On the other hand, Hogan [3, 4, 5] suggested a method to face this dynamic issue. It is based on the control of the relation between position and force and it is known as "Impedance Control". He started from the observation that two interacting physical systems must be physically complementary. Since the environment typically behaves like an admittance, i.e. it receives forces as input and it gives displacements as output, the controller must be an impedance, which accepts motion inputs and yields force outputs. This approach aims to regulate mechanical impedance of the manipulator.

Hogan [6] observed that actually any control algorithm implements a relation between measured quantities and actuator forces. This produces a change in robot dynamic behavior, i.e. at the end effector the output impedance is modified. Therefore it makes sense to design the controller to do what it naturally does.

Impedance control can be realized in two different ways depending on the causality of the controller. They are known as "Impedance Control" and "Admittance Control".

In Impedance Control the controller is an impedance and consequently the controlled plant is treated as an admittance. Conversely in Admittance Control the plant is position-controlled so it behaves as impedance and hence the controller must be an admittance.



---

Some hybrid systems were introduced in order to combine qualities of the Hogan and Raibert and Craig methodologies. Anderson and Spong [7] pointed out the force control inability of handling unmodeled dynamics due to coupling and impedance control inadequacy in following a commanded force trajectory. Therefore their solution is based on an inner feedback linearization loop with force cancelation and an outer loop which joins Impedance and Hybrid Force\Position Control in one strategy. Similarly to Craig and Raibert, they divided the task space in two; in the position subspace they adopted impedance control, whereas in force subspace they used a force control.

Liu and Goldenberg [8] pushed forward the idea of Anderson and Spong. They proposed to add desired inertia and damping terms in force control subspace in order to improve the dynamic behavior, in addition they introduced a PI controller to tackle the uncertainties of the manipulator dynamic model. These approaches start with the assumption that the environment features are known, therefore they could be inefficient in case of lack of informations about the environment.

Recently Ott, Nakamura and Mukherjee [9, 10] have developed a new way to implement impedance control. They proposed a control strategy that is an hybrid between Impedance and Admittance Control and it aims to combine the advantages of the two solutions rapidly switching between them.

Indeed the two strategies have complementary performances, as shown by Lawrence [11], who investigated their stability properties in the presence of non ideal effects, such as time delay. Starting from Eppinger and Seering observations [12] about the effects of high feedback gains on stability, he pointed out opposite requirements for Impedance and Admittance control. For Admittance Control, low values of stiffness and damping produce high feedback gains, therefore it suffers the inability to provide soft impedance, giving as a result instability during interaction with stiff environment. As concern Impedance Control, high feedback gains are consequences of high values of stiffness and damping, and so it is difficult to provide large stiffness, causing poor accuracy in soft environment and free motion.

Many efforts have been made in order to improve performances of both Impedance and Admittance Control. Impedance Control has been implemented in DLR's light-weight robot [13] and ATR's Humanoid built by Sarcos [14], by adding an inner force loop that allows to decrease undesired effects due to friction and unmodeled dynamics. Another possibility is hardware modification such as low friction joints or direct drive actuators. Regarding Admittance Control the problem of instability during the interaction with stiff environment can be eliminated using series elas-

tic actuation or compliant end effectors, but this also causes decrease in performances.

Overcoming of the two control laws limitations has been investigated through the application of adaptive strategies to either Impedance or Admittance Control. Slotine and Li [15], Lu and Meng [16] proposed the adaptation of unknown parameters in robot and payload models in order to mitigate the effects of uncertainties on the Impedance Control. Singh and Popa [17] exploited a Model Reference Adaptive Control (MRAC) applied to Impedance Control and combined impedance and force control. The idea is to adapt an input parameter in order to minimize the error between the actual and the reference model. As concern the combined impedance and force control it is required the knowledge of the environment stiffness that is estimated online, thanks to the measurement of the interaction force. Since the robot and the environment are dynamically coupled, this estimation can improve the overall system performances. In the same direction, Book and Love [18] suggested the adaptation of impedance parameters based on an estimation of the environment stiffness, since it affects the natural frequencies and damping ratio of the coupled system. The identification is performed with a Recursive Least Square method (RLS). On the other hand Seraji [19] applied adaptive PID and PD controllers to Admittance Control in an unknown environment.

Contrary to the previous studies, the aim of the strategy proposed by Ott, Nakamura and Mukherjee is not to improve the performances of either Impedance or Admittance Controls; in fact the system is a unified framework for Impedance and Admittance Controls that can take advantage of advanced implementations of each of the two controllers. Nowadays systems that switch between different control laws are not widespread in industrial applications, since they appear more complex and less reliable than common regulators. However the Hybrid System could lead to improvements in performances and to an high versatility, i.e. a new class of robots that can be suitable for different manipulatory tasks. Needless to say, a system capable of adapting itself to unknown and variable environments would be a great advancement in this direction.

The following study proposes a way to accomplish this goal. The duty cycle of the switching system is selected as adaptive parameter since it determines how much Impedance and Admittance Control are used. Hence, varying this parameter, it is possible to modify the controller features exploiting more a control law with respect to the other one in order to provide certain performance in different environments.

It should be noted that this parameter is embedded in the system and it does not show any explicit relation with the states and the control action.

---

Moreover the system is highly nonlinear due to its switching nature. For these reasons classical approaches for adaptive problems that require the knowledge of the dependance of the control force or the states on the adaptive parameter fail. Even solutions exploiting tools like maximum principle or Bellman equation are not adequate since the resulting problem would be extremely hard if not impossible to be solved. These facts led to the decision of exploiting a feedforward artificial neural network (ANN) to achieve the desired result.

ANNs are a powerful tools inspired by the human brain structure and functionality. They are particularly suitable to deal with very highly nonlinear systems; indeed they are capable of approximating any function with a desired accuracy, as proved by Cybenko [20] and Hornik and al. [21]. For this reason they are extensively used in the identification or in input-output mapping of complex systems [22, 23, 24]. In a control problem scenario, they can be exploited directly as controllers [25, 26], indirectly to set properly some parameters, i.e. realizing an adaptive system [27, 23, 24] or even to solve non-linear optimal problem i.e. dynamic programming [23, 28, 29, 30]. Their strength lies in the fact that their application does not require high-level knowledge of the system and they can guarantee good performances when the surrounding environment changes. The constitutive element of a ANN is the neuron, which is a simple processing unit. Neurons are organized in layers and they are linked each other through weighted connections, creating a net. The weights are selected in order to minimize a desired cost function; this operation can be performed online or offline and it is called respectively learning or training. Many different algorithms can be used to minimize the cost function, the solution here proposed exploits a genetic algorithm (GA).

The designed ANN accepts as input from the system the measurements of the states and interaction force and it returns as output the design parameter at each sample time. In this way the adaptive system can promptly react to deviations from the desired behavior, also in unknown and time varying external environment.

Firstly the Adaptive Hybrid System is developed for a single d.o.f. system in order to highlight the main issues and explain how to overcome them. Afterwards the same concepts are extended to a 2 d.o.f.s system.

The current work is organized in the following way: in chapter 2 what was already done in the development of the Hybrid System is reported and then in chapter 3 the 2 d.o.f.s model is presented. In chapter 4 the problem of making the hybrid system adaptive is introduced. The proposed solution is discussed in chapter 5. Finally the results are shown in chapter 6 and in chapter 7 the main conclusions of the work are summarized.



# Chapter 2

## Background

In this chapter the basic concepts of Impedance and Admittance Control and the way they are implemented in this work, are presented. Afterwards an overview of the hybrid system is given together with a discussion of its performances with respect to the first two controllers, as motivation for the new framework.

### 2.1 Impedance control framework

The manipulation problem typically involves a mechanical interaction between the robot and the manipulated object resulting in an energy exchange between the two sides.

In two particular cases this work is or tends to zero, i.e. when the interaction force or the displacement are absent or negligible.

When the first condition occurs the manipulator behaves as an isolated system, so the suggested controlled variable(s) is the motion. This solution has been widely utilized in industrial applications where an accurate positioning is required.

On the other hand, in the second situation, the robot encounters physical constraints involving the generation of forces and a limitation for the motion. The system results kinematically coupled to the environment, but not dynamically. Along the constrained d.o.f. a force control is used, whereas along the free ones, again, a position control is preferred.

However the most general operative framework, that includes the previous cases, involves a dynamic coupling and a not null energy exchange as a consequence. The manipulator can not be treated as an isolated system anymore and solutions aiming to control only position or force are inadequate to handle the work exchanged.

The impedance control is an extension of the conventional position control directed to manage the force/motion relation overcoming the above-mentioned issue.

The concept is based on the fact that a physical system can be described as an impedance or an admittance. The former accepts flow inputs and yields effort outputs, the latter behaves in the opposite way. In a linear system these two representations can be interchanged, but this is not true in the general case of a nonlinear system. Therefore the distinction between the two causalities is fundamental since a system can be usually described in only one of the two ways.

Another important aspect, that must be taken into account, regards the fact that two interacting systems must be complementary; therefore along any d.o.f. if one behaves as an impedance the other one must be an admittance. Since the environment is properly described as an admittance, the controller must work as an impedance.

Typically impedance control can be implemented in two ways, commonly known as Impedance and Admittance Control. They are presented in the next sections.

## 2.2 Problem statement

Before introducing Impedance and Admittance Control the considered system is presented. The system is a single d.o.f. mass interacting with the environment; it is governed by the equation of motion 2.1.

$$m\ddot{x} = F + F_{ext} \quad (2.1)$$

Where  $x$  is the mass position,  $F$  is the control action and  $F_{ext}$  is the interaction force with the environment.

Both the controllers should provide an action force such that it satisfies the relation 2.2 between external force and the system dynamic quantities.

$$F_{ext} = M_d\ddot{e} + D_d\dot{e} + K_d e \quad (2.2)$$

with:

$$e = x - x_0 \quad (2.3)$$

$M_d$ ,  $D_d$  and  $K_d$  are positive constants representing the desired inertia, damping and stiffness of the system, while  $x_0$  is the commanded virtual position. The command position represents nominal equilibrium position at steady state in absence of external forces, however in contact situations

it may go to positions beyond the reachable workspace and therefore it is called virtual.

## 2.3 Impedance Control

In the Impedance Control the plant is an admittance, i.e. it receives force as input and gives position as output, on the other hand the controller behaves as an impedance. The expression of the desired control force can be derived from equations 2.1 and 2.2.

$$F = (m - M_d)\ddot{x} + (M_d\ddot{x}_0 - D_d\dot{e} - K_de) \quad (2.4)$$

Since from a practical point of view measurements of position, velocity and interaction force are more advisable than acceleration, taking into account the equation of motion, the control force can be rewritten as in 2.5.

$$F = \left( \frac{m}{M_d} - 1 \right) F_{ext} + m\ddot{x}_0 - \frac{m}{M_d}(D_d\dot{e} + K_de) \quad (2.5)$$

In an ideal case, without friction, uncertainties and measurement delays the controlled system satisfies exactly the desired impedance relation 2.2.

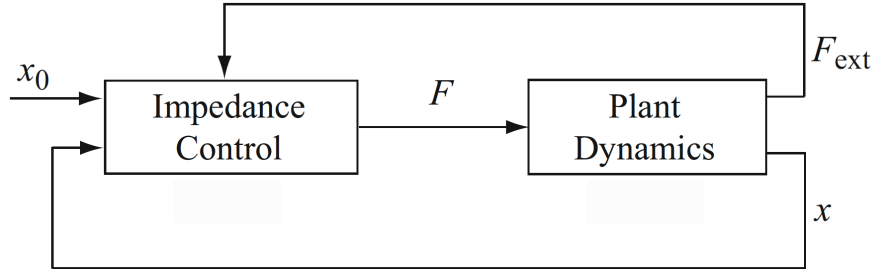


Figure 2.1: Impedance Control system structure

## 2.4 Admittance Control

In the Admittance Control the motion control problem and the impedance control problem are separated. One controller generates a motion trajectory from the interaction force measurement, guaranteeing the desired

dynamic behavior 2.2. A second controller receives that trajectory and provides the related control force to the plant.

Different kind of control law can be implemented to realize the position controller. In this case it is used a simple PD regulator of the form:

$$F = k_p(x_d - x) - k_v\dot{x} \quad (2.6)$$

where  $k_p$  and  $k_d$  are the proportional and derivative coefficients of the controller,  $x_d$  represents the desired trajectory and it is the input of the controller.

Combining the dynamic equation 2.1, the impedance relation 2.2 and the equation 2.6 it is possible to derive the complete system dynamics.

$$m\ddot{x} + k_v\dot{x} + k_p(x - x_d) = F_{ext} \quad (2.7)$$

$$M_d(\ddot{x}_d - \ddot{x}) + D_d(\dot{x}_d - \dot{x}) + K_d(x_d - x) = F_{ext} \quad (2.8)$$

As it can be noticed from equations 2.7 and 2.8, two additional states  $x_d$  and  $\dot{x}_d$  are introduced with respect to the Impedance Control formulation due to the inner position control loop.

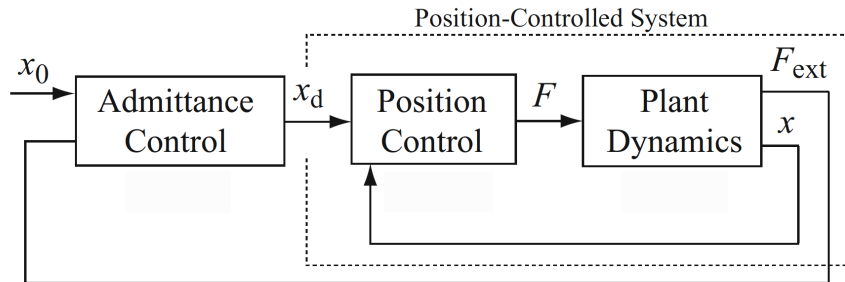


Figure 2.2: Admittance Control system structure

## 2.5 Comparison of Impedance and Admittance Control

Impedance and Admittance Control have different stability and performance characteristics due to their different implementations and causalities [11].

The main limitation in Impedance Control concerns the impossibility of providing stiff behaviour, i.e. large values of  $K_d$ , and/or large inertia



## 2.5 Comparison of Impedance and Admittance Control

---

rescaling  $m/M_d$ . They would lead to an increase of the feedback gains that can amplify noise causing instabilities. Moreover in systems where significant uncompensated friction is present, position accuracy is greatly affected by the desired stiffness and damping that should be high[34]. Consequently, Impedance Control, with its low  $K_d$ , results in poor positioning performance in soft environment or in free motion.

Conversely it is robust to uncertainties in model parameters and can guarantee very good performance and stability in very stiff environments thanks to its soft behaviour that can limit the interaction forces.

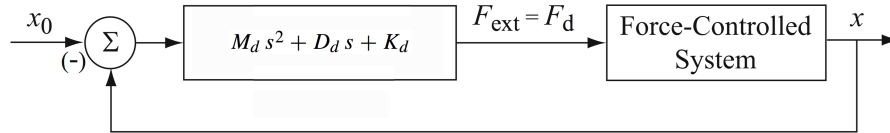


Figure 2.3: Concept of Impedance Control

Regarding the Admittance Control, it is made up of two control loops, as already shown.

The inner one is a position controller that accomplishes the task of compensating unmodeled frictions and for this reason it presents high gains lending the system a stiff behavior.

On the other hand the second one "soften" the overall system. However this action is limited by its stability constraints. Indeed, compliant behavior is difficult to provide because it brings to an high feedback gains, as it can be deduced from figure 2.4, and the result would be persistent oscillations in the response.

As a direct consequence, Admittance Control can assure better performances in the interaction with soft environments; in fact in this situation stiff features are preferable.

The impedance loop works also as a filter for the force feedback noise limiting its influence on the system.

Finally it must be noted that the quality of the position controller largely affects the overall Admittance performance and stability characteristics as shown by Pelletier and Doyon [35].

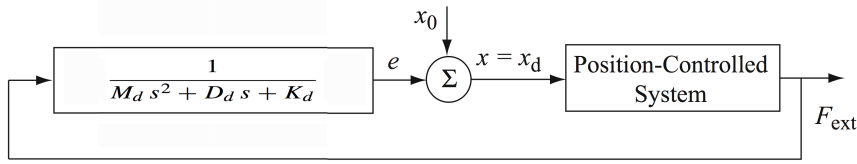


Figure 2.4: Concept of Admittance Control

## 2.6 Hybrid system

### 2.6.1 Motivations

The two control laws described so far have as main constraint their fixed causality. This fact implies their incapability of providing good performances in a large spectrum of environment stiffnesses as illustrated in figure 2.5. An ideal controller should provide consistently good performance, independent of the environment stiffness. The Hybrid Control wants to accomplish this task by rapidly switching between Impedance and Admittance Control. In this way the fixed causality is overcome and the benefits from both the controller are united in one single framework.

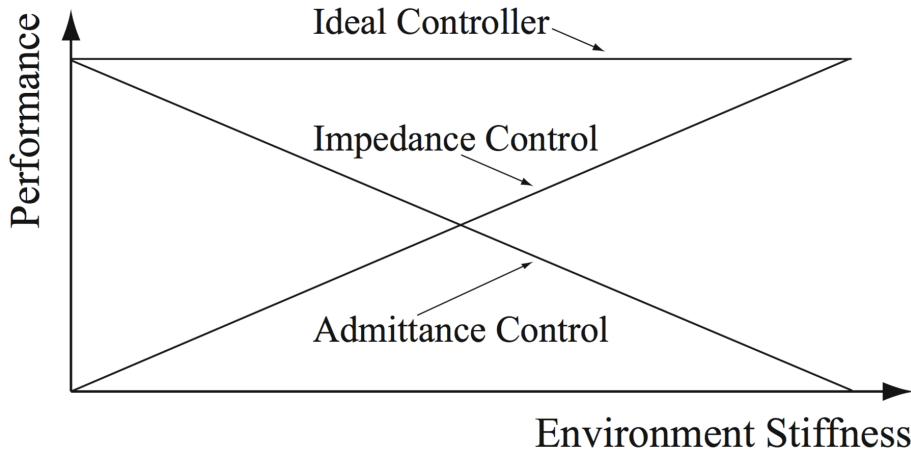


Figure 2.5: Qualitative illustration of the performance of Impedance Control and Admittance Control for different environment stiffness

It should be noticed that the switching approach is different from using averaged control effort, like  $F = (1 - n)F_{imp} + nF_{adm}$ , with  $F_{imp}$  and  $F_{adm}$  the control input from Impedance and Admittance Control respectively.

Indeed Ott and al. [9] showed that this kind of control does not provide good results. They observed that in the averaged control the impedance controller, with its low gain, works as a disturbance to the admittance controller that presents high gains. This fact leads to a depletion of the stability with respect to the pure admittance controller.

### 2.6.2 Structure

The figure 2.6 shows the scheme of the proposed controller.

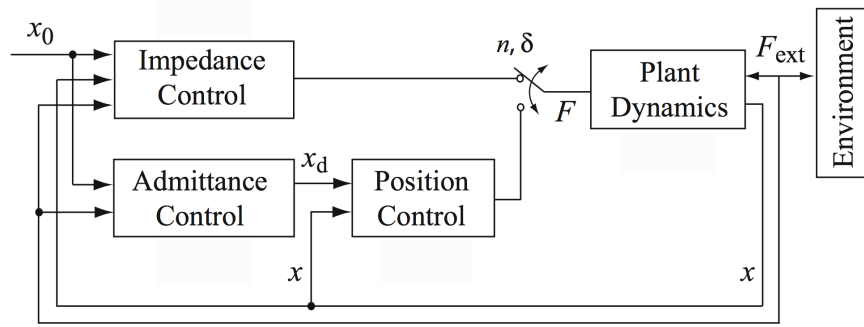


Figure 2.6: Concept of Hybrid Control

The hybrid system switches between Impedance and Admittance Control providing the control action  $F$  as shown in equation 2.9.

$$F = \begin{cases} F_{imp} & : t_0 + k\delta \leq t \leq t_0 + (k+1-n)\delta \\ F_{adm} & : t_0 + (k+1-n)\delta \leq t \leq t_0 + (k+1)\delta \end{cases} \quad (2.9)$$

Where  $F_{imp}$  and  $F_{adm}$  are the control forces provided respectively by Impedance and Admittance Control,  $t_0$  is the initial time,  $\delta$  is the switching period,  $n \in [0, 1]$  is the duty cycle and  $k$  is an integer that takes on values  $0, 1, \dots$ . Therefore the controlled dynamics can be described by the system 2.10.

$$\begin{aligned} \dot{X}_i &= A_i X_i + B_i u & : t_0 + k\delta \leq t \leq t_0 + (k+1-n)\delta \\ \dot{X}_a &= A_a X_a + B_a u & : t_0 + (k+1-n)\delta \leq t \leq t_0 + (k+1)\delta \end{aligned} \quad (2.10)$$

with:

$$X_i = \begin{bmatrix} x \\ \dot{x} \end{bmatrix}$$

$$X_a = \begin{bmatrix} x \\ \dot{x} \\ x_d \\ \dot{x}_d \end{bmatrix}$$

$$\mathbf{A}_i = \begin{bmatrix} 0 & 1 \\ -\frac{K_d+k_e}{M_d} & -\frac{D_d}{M_d} \end{bmatrix}, \quad \mathbf{B}_i = \begin{bmatrix} 0 \\ K_d \end{bmatrix}$$

$$\mathbf{A}_a = \begin{bmatrix} 0 & 1 & 0 & 0 \\ -\frac{k_p+k_e}{m} & -\frac{k_v}{m} & \frac{k_p}{m} & 0 \\ 0 & 0 & 0 & 1 \\ -\frac{k_e}{M_d} & 0 & -\frac{K_d}{M_d} & -\frac{D_d}{M_d} \end{bmatrix}, \quad \mathbf{B}_a = \begin{bmatrix} 0 \\ 0 \\ 0 \\ K_d \end{bmatrix}$$

and  $u = x_0$ .

The equations are derived considering the environment modeled as a linear spring with stiffness  $k_e$  and setting  $\dot{x}_0 = \ddot{x}_0 = 0$ . The external force results:

$$F_{ext} = -k_e(x - x_e) \quad (2.11)$$

Without loss of generality  $x_e$  can be imposed equal to zero, i.e. the environment is at rest at  $x = 0$ .

In the transition from Impedance to Admittance Control the additional states introduced with the latter can be chosen in order to maintain the continuity in the control force  $F$  and its derivative. Equation 2.6 can be written as follows

$$x_d = x + \frac{1}{k_p}(F + k_v\dot{x}) \quad (2.12)$$

with derivative:

$$\dot{x}_d = \dot{x} + \frac{1}{k_p}(\dot{F} + k_v\ddot{x}) = \dot{x} + \frac{1}{k_p}\left[\dot{F} + \frac{k_v}{m}(F + F_{ext})\right] \quad (2.13)$$

Substituting the control force from equation 2.5 in 2.13 it is possible to derive the relation between  $X_a$  and  $X_i$ :

$$X_a = S_{ai}X_i, \quad S_{ai} = \begin{bmatrix} I \\ S \end{bmatrix} \quad (2.14)$$

$I$  is the identity matrix and  $S$  is a 2 x 2 matrix the elements of which have the following expressions.

## 2.7 Simulation examples

---

$$\begin{aligned}
s_{11} &= 1 - \frac{k_e}{k_p} \left( \frac{m}{M_d} - 1 \right) - \frac{K_d}{k_p} \frac{m}{M_d} \\
s_{12} &= \frac{k_v}{k_p} - \frac{D_d}{k_p} \frac{m}{M_d} \\
s_{21} &= -\frac{m}{M_d} \frac{(K_d + k_e)}{k_p} \left( \frac{k_v}{m} - \frac{D_d}{M_d} \right) \\
s_{22} &= 1 - \frac{k_e}{k_p} \left( \frac{m}{M_d} - 1 \right) - \frac{D_d}{M_d} \left( \frac{k_v}{k_p} - \frac{D_d}{k_p} \frac{m}{M_d} \right) - \frac{K_d}{k_p} \frac{m}{M_d}
\end{aligned} \tag{2.15}$$

On the other hand, the map of the state variables from Admittance to Impedance Control can be obtained with the relation:

$$X_i = S_{ia} X_a, \quad S_{ia} = [I \quad O] \tag{2.16}$$

where  $O$  is a 2 x 2 zero matrix.

The stability analysis of the presented controller is discussed in [9].

The stability region of the system decreases as the switching period  $\delta$  increases. Moreover instabilities can occur in very stiff environment with  $n$  close to one. This fact was expected since the well known Admittance Control characteristics.

Finally it should be noted that with  $n = 1$  the hybrid system behaves like an Admittance Control with a resetting action that improves the stability with respect to the pure one. In fact the control force of the hybrid control in this case differs from the pure admittance one because every  $\delta$  period the Impedance Control law is used for a time instant.

## 2.7 Simulation examples

In order to illustrate the performances of the three controllers presented so far, simulation results are shown in this section.

The single d.o.f. system described in section 2.2 is considered; friction, model uncertainties, time delays and noise are introduced. Therefore the equation of motion becomes:

$$m\ddot{x} = F + F_{ext} + F_f \tag{2.17}$$

with the unmodelled friction term:

$$F_f = -sign(\dot{x})(c_v|\dot{x}| + F_c) \tag{2.18}$$

where  $c_v$  and  $F_c$  represent respectively the viscous coefficient and the Coulomb friction.

The parameter values used in the simulation are as follows:

$$\begin{aligned}
 m &= 1.0kg, & \hat{m} &= 0.8kg \\
 c_v &= 1.0Ns/m, & F_c &= 3.0N \\
 k_p &= 10^6N/m, & k_v &= 2 \cdot 0.7\sqrt{k_p m}Ns/m \\
 M_d &= 0.8kg, & K_d &= 100N/m \\
 D_d &= 2 \cdot 0.7\sqrt{K_d M_d}Ns/m
 \end{aligned}$$

$\hat{m}$  is the estimated mass introduced in both impedance and admittance implementations.

The PD gains are set to high values as it is common practice, the uncertainty of  $m$  is not considered since the position controller is supposed to be tuned independently.

The time delays considered are  $2ms$  and the noise on the external force measurement is Gaussian with zero mean and unity variance. Taking into account the stability analysis results, the selected value for  $\delta$  is  $20ms$ .

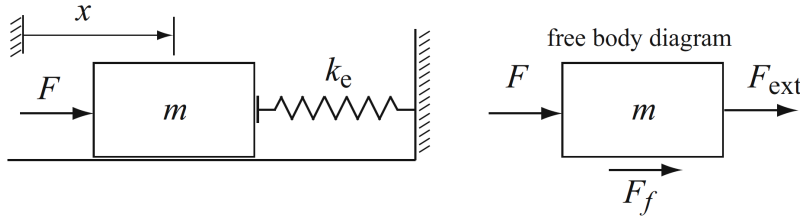


Figure 2.7: Single degree-of-freedom system interacting with an environment

At the initial time instant the mass is considered to be already in contact with the environment. The environment stiffnesses chosen are  $10N/m$ ,  $1300N/m$  and  $3200N/m$ , in order to represent respectively a soft, an intermediate and a stiff environment.

The responses of all controllers are compared with the ideal behaviour of the closed loop system  $x_{ref}$ , derived from equation 2.19 and shown in figure 2.8.

$$\begin{aligned}
 M_d \ddot{e} + D_d \dot{e} + K_d e &= -k_e x \\
 M_d \ddot{x}_{ref} + D_d \dot{x}_{ref} + (K_d + k_e)x_{ref} &= K_d x_0
 \end{aligned} \tag{2.19}$$

## 2.7 Simulation examples

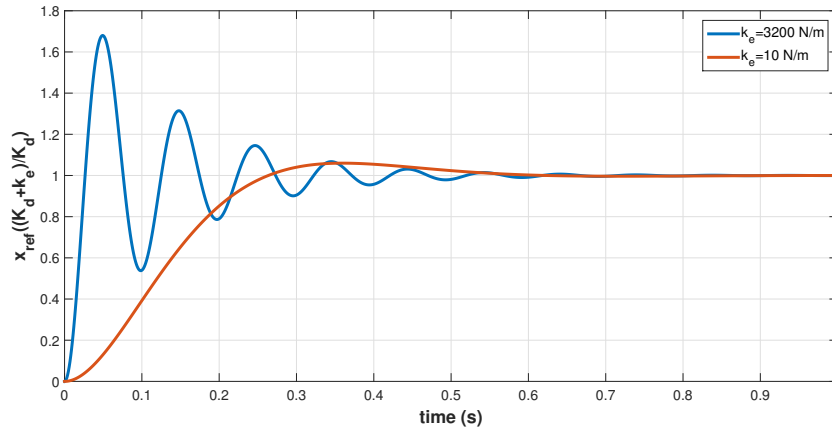


Figure 2.8: Re-scaled ideal trajectories of the single d.o.f. system for a step change in the virtual equilibrium position for a soft and a stiff environment

Figure 2.9 shows the deviation from the ideal trajectory in a soft environment. It can be noticed that the Admittance Control presents better performances than Impedance Control; indeed in the latter case unmodeled friction effect produces a tracking and steady state error. Actually the error for the Impedance Control goes to zero too, but in a very large time window.

On the other hand when the stiffness increases Admittance Control performances deteriorates resulting in large oscillations as represented in figure 2.10. This fact can be attributed to the high feedback gains of the position controller and the time delay of the force feedback. However there is not steady state error thanks to the compensating action of the PD controller. In this case Impedance Control guarantees well damped oscillations and negligible steady state error.

As concern the hybrid system, it can be observed that it can interpolate between the responses of Admittance and Impedance Control by properly selecting the value of  $n$ . As expected in a soft environment the performances improve as  $n$  tends to 1, on the contrary as  $k_e$  increases the best  $n$  decreases. This results are in accordance with what stated in section 2.5. Figures 2.9 and 2.10 also confirm the enhancement of the stability of the admittance controller in the hybrid framework thanks to the resetting action (see section 2.6.2).

One can easily imagine that for intermediate values of environment stiffness an appropriate choice of  $n$  can provide the best performances, as exemplified in figure 2.11 where an intermediate stiffness of  $1300N/m$  is assumed.

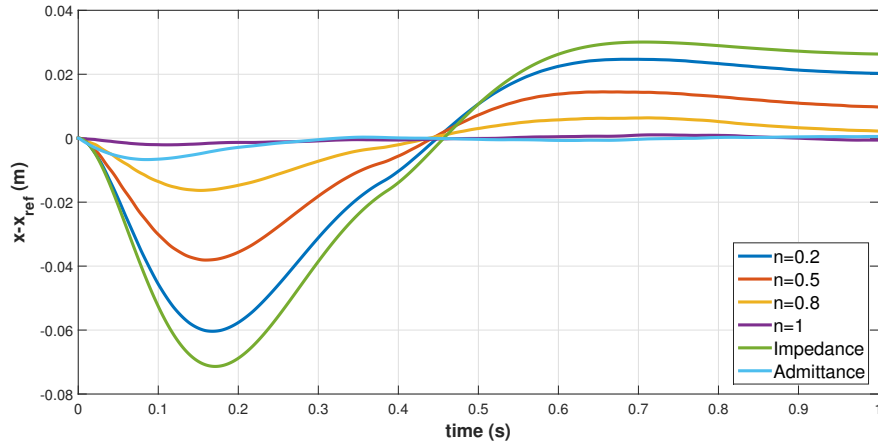


Figure 2.9: Deviation from the ideal trajectory for Impedance, Admittance and Hybrid Control for the soft environment  $k_e = 10N/m$

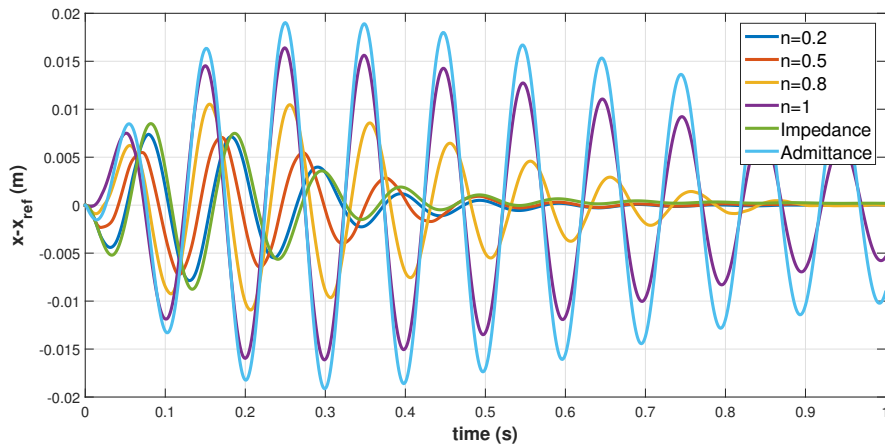


Figure 2.10: Deviation from the ideal trajectory for Impedance, Admittance and Hybrid Control for the stiff environment  $k_e = 3200N/m$



## 2.7 Simulation examples

---

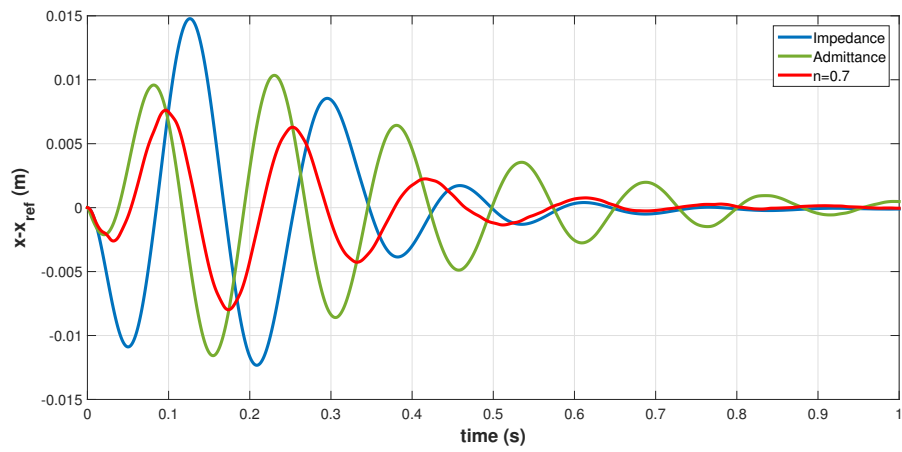


Figure 2.11: Deviation from the ideal trajectory for Impedance, Admittance and Hybrid Control for intermediate environment  $k_e = 1300N/m$



## Chapter 3

# Hybrid System Framework in the 2 d.o.f.s case

In this chapter the Hybrid System Framework for unified Impedance and Admittance Control is applied to a 2 d.o.f.s system. A manipulator made up of 2 rigid joints connected by as much rigid links is considered. It interacts with an environment that is modeled as an inclined frictionless wall with a certain stiffness  $k_e$ . Figure 3.1 represents the system under analysis.

As for the 1 d.o.f. case, a comparison with Impedance and Admittance Control with different environment stiffness is shown.

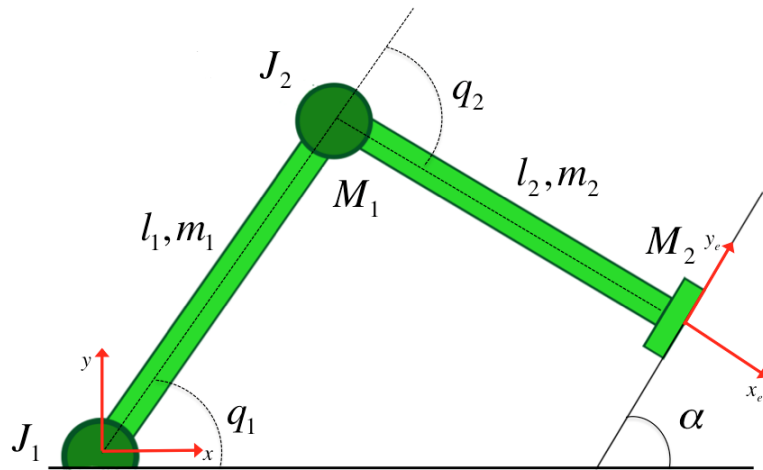


Figure 3.1: 2 dofs system graphic representation

### 3.1 Dynamic model

The equations of motion in the joint space that govern the 2 d.o.f.s system can be derived in different ways, like the Principle of Virtual Work (PVW) or the Lagrange equation, and they are expressed as follows:

$$\mathbf{M}(\mathbf{q})\ddot{\mathbf{q}} + \mathbf{C}(\mathbf{q}, \dot{\mathbf{q}})\dot{\mathbf{q}} + \mathbf{G}(\mathbf{q}) = \boldsymbol{\tau} + \boldsymbol{\tau}_{\text{ext}} \quad (3.1)$$

where the  $\mathbf{q}$ ,  $\dot{\mathbf{q}}$  and  $\ddot{\mathbf{q}}$  are respectively the joints position, velocity and acceleration vectors,  $\boldsymbol{\tau}$  is the control action and  $\boldsymbol{\tau}_{\text{ext}}$  the interaction force vector.  $\mathbf{M}$ ,  $\mathbf{C}$  and  $\mathbf{G}$  represent correspondingly the system inertia matrix, the centrifugal and Coriolis matrix and the gravitational terms. With:

$$\mathbf{q} = \begin{bmatrix} q_1 \\ q_2 \end{bmatrix}, \quad \mathbf{M} = \begin{bmatrix} M_{11} & M_{12} \\ M_{21} & M_{22} \end{bmatrix}, \quad \mathbf{C} = \begin{bmatrix} C_{11} & C_{12} \\ C_{21} & C_{22} \end{bmatrix}, \quad \mathbf{G} = \begin{bmatrix} G_1 \\ G_2 \end{bmatrix}$$

$$\begin{aligned} M_{11} &= \left( M_1 + M_2 + \frac{m_1}{3} + m_2 \right) l_1^2 + \left( M_2 + \frac{m_2}{3} \right) l_2^2 + \\ &\quad + (2M_2 + m_2) l_1 l_2 \cos(q_2) + J_1 \\ M_{22} &= \left( M_2 + \frac{m_2}{3} \right) l_2^2 + J_2 \\ M_{12} &= \left( M_2 + \frac{m_2}{3} \right) l_2^2 + \left( M_2 + \frac{m_2}{2} \right) l_1 l_2 \cos(q_2) \\ M_{21} &= M_{12} \end{aligned} \quad (3.2)$$

$$\begin{aligned} C_{11} &= - \left( M_2 + \frac{m_2}{2} \right) l_1 l_2 \sin(q_2) \dot{q}_2 \\ C_{12} &= - \left( M_2 + \frac{m_2}{2} \right) l_1 l_2 \sin(q_2) (\dot{q}_2 + \dot{q}_1) \\ C_{21} &= \left( M_2 + \frac{m_2}{2} \right) l_1 l_2 \sin(q_2) \dot{q}_1 \\ C_{22} &= 0 \end{aligned} \quad (3.3)$$

$$\begin{aligned} G_1 &= g \left[ \left( M_1 + M_2 + \frac{m_1}{2} + m_2 \right) l_1 \cos(q_1) + \left( M_2 + \frac{m_2}{2} \right) l_2 \cos(q_1 + q_2) \right] \\ G_2 &= g \left( M_2 + \frac{m_2}{2} \right) l_2 \cos(q_1 + q_2) \end{aligned} \quad (3.4)$$

where  $M_1$  is the joint mass and  $M_2$  is the end effector one,  $J_1$  and  $J_2$  represent the motor inertia of the joints,  $m_1$ ,  $m_2$  are the masses of the links of length  $l_1$  and  $l_2$ . The joint coordinates are positive in clockwise direction.

## 3.2 Control law

First of all it is necessary to define the impedance and admittance control laws to be added in the hybrid framework.

The desired impedance relation is expressed as:

$$\mathbf{M}_{\mathbf{d-e}}\ddot{\mathbf{x}}_e + \mathbf{D}_{\mathbf{d-e}}\dot{\mathbf{x}}_e + \mathbf{K}_{\mathbf{d-e}}(\mathbf{x}_e - \mathbf{x}_{0-e}) = \mathbf{F}_{\mathbf{ext-e}} \quad (3.5)$$

where  $\mathbf{M}_{\mathbf{d-e}}$ ,  $\mathbf{D}_{\mathbf{d-e}}$  and  $\mathbf{K}_{\mathbf{d-e}}$  are respectively the desired inertia, damping and stiffness matrices while  $\mathbf{F}_{\mathbf{ext-e}}$  is the interaction force vector. All the quantities are expressed in the environment reference frame, illustrated in figure 3.1. Indeed the desired impedance relation is considered in the interaction force direction, orthogonal to the wall.

Once the quantities are rotated in the base reference frame  $x - y$ , the desired end-effector acceleration can be computed as follows:

$$\ddot{\mathbf{x}} = \mathbf{M}^{-1}(-\mathbf{D}_d\dot{\mathbf{x}} - \mathbf{K}_d(\mathbf{x} - \mathbf{x}_0) + \mathbf{F}_{\mathbf{ext}}) \quad (3.6)$$

Since a control action expressed in the joint space is required, the joint acceleration can be derived from the velocities relationship encoded by the Jacobian.

$$\dot{\mathbf{q}} = \mathbf{J}\dot{\mathbf{x}} \quad (3.7)$$

then

$$\ddot{\mathbf{q}} = \mathbf{J}^{-1}(\ddot{\mathbf{x}} - \dot{\mathbf{J}}\dot{\mathbf{q}}) \quad (3.8)$$

with:

$$\mathbf{J} = \begin{bmatrix} -l_1 \sin q_1 - l_2 \sin (q_1 + q_2) & -l_2 \sin (q_1 + q_2) \\ l_1 \cos q_1 + l_2 \cos (q_1 + q_2) & l_2 \cos (q_1 + q_2) \end{bmatrix}$$

At this point the end-effector acceleration is substituted by the desired one reported in equation 3.6.

$$\ddot{\mathbf{q}} = \mathbf{J}^{-1} \mathbf{M}^{-1} (-\mathbf{D}_d \dot{\mathbf{x}} - \mathbf{K}_d (\mathbf{x} - \mathbf{x}_0) + \mathbf{F}_{\text{ext}}) - \mathbf{J}^{-1} \dot{\mathbf{J}} \dot{\mathbf{q}} \quad (3.9)$$

From the dynamics 3.1 the control torque can be derived as:

$$\boldsymbol{\tau} = \mathbf{M}(\mathbf{q}) \ddot{\mathbf{q}} + \mathbf{C}(\mathbf{q}, \dot{\mathbf{q}}) \dot{\mathbf{q}} + \mathbf{G}(\mathbf{q}) - \boldsymbol{\tau}_{\text{ext}} \quad (3.10)$$

where:

$$\boldsymbol{\tau}_{\text{ext}} = \mathbf{J}^T \mathbf{F}_{\text{ext}} \quad (3.11)$$

Combining 3.9 with 3.10 the Impedance Control torque can be obtained.

$$\begin{aligned} \boldsymbol{\tau} = & \mathbf{M}(\mathbf{q}) \mathbf{J}^{-1} \mathbf{M}_d^{-1} (-\mathbf{D}_d \dot{\mathbf{x}} - \mathbf{K}_d (\mathbf{x} - \mathbf{x}_0) + \mathbf{F}_{\text{ext}}) + \\ & -\mathbf{M}(\mathbf{q}) \mathbf{J}^{-1} \dot{\mathbf{J}} \dot{\mathbf{q}} + \mathbf{C}(\mathbf{q}, \dot{\mathbf{q}}) \dot{\mathbf{q}} + \mathbf{G}(\mathbf{q}) - \mathbf{J}^T \mathbf{F}_{\text{ext}} \end{aligned} \quad (3.12)$$

This is called *computed torque control law*. The  $\mathbf{C}(\mathbf{q}, \dot{\mathbf{q}}) \dot{\mathbf{q}}$  and  $\mathbf{G}(\mathbf{q})$  terms are necessary in order to compensate the centrifugal, Coriolis and gravitational effects.

As concerns the Admittance Control, the desired position transported in the base reference can be derived from equation 3.6. Afterwards, considering the problem geometry, the desired position of the joints that realizes the requested end-effector trajectory can be computed as follows:

$$q_{2d} = \text{atan2} \left[ -\sqrt{1 - \frac{x_d^2 + y_d^2 - l_1^2 - l_2^2}{2l_1 l_2}}, \frac{x_d^2 + y_d^2 - l_1^2 - l_2^2}{2l_1 l_2} \right] \quad (3.13)$$

### 3.3 Simulation results

---

$$q_{1d} = \text{atan2}[y_d, x_d] - \text{atan2}[k_2, k_1] \quad (3.14)$$

where:

$$\begin{aligned} k_1 &= l_1 + l_2 \cos q_{2d} \\ k_2 &= l_2 \sin q_{2d} \end{aligned} \quad (3.15)$$

Finally for the position controller, again a simple PD control law is used. In this case centrifugal, Coriolis and gravitational compensating terms are added.

$$\tau = \mathbf{k}_p(\mathbf{q}_d - \mathbf{q}) - \mathbf{k}_v\dot{\mathbf{q}} + \mathbf{C}(\mathbf{q}, \dot{\mathbf{q}})\dot{\mathbf{q}} + \mathbf{G}(\mathbf{q}) \quad (3.16)$$

Once the impedance and admittance control laws are derived, the formulation for the hybrid system control is the same presented in chapter 2.

$$\tau = \begin{cases} \tau_{imp} & : t_0 + k\delta \leq t \leq t_0 + (k+1-n)\delta \\ \tau_{adm} & : t_0 + (k+1-n)\delta \leq t \leq t_0 + (k+1)\delta \end{cases} \quad (3.17)$$

Where  $\delta$  and  $n$  are again the period and the duty cycle of the switching system.

### 3.3 Simulation results

As already done for the single d.o.f., the performances of the 2 d.o.f.s system are here illustrated. In the simulation uncompensated friction, model uncertainties, time delays and noise are introduced. The resulting equation of motion is:

$$\mathbf{M}(\mathbf{q})\ddot{\mathbf{q}} + \mathbf{C}(\mathbf{q}, \dot{\mathbf{q}})\dot{\mathbf{q}} + \mathbf{G}(\mathbf{q}) = \tau + \tau_{\text{ext}} + \tau_{\text{f}} \quad (3.18)$$

with the unmodelled friction term for each joint:

$$\tau_{fi} = -sign(\dot{q}_i)(c_v|\dot{q}_i| + \tau_c) \quad (3.19)$$

where  $c_v$  and  $\tau_c$  represent respectively the viscous coefficient and the Coulomb friction for  $i^{th}$  the joint.

The parameter values used in the simulation are the following:

$$\begin{array}{ll} M_1 = 1.0kg, & M_2 = 1.0kg \\ m_1 = 0.8kg, & m_2 = 0.8kg \\ l_1 = 0.7m, & l_2 = 0.5m \\ J_1 = 0.001kgm^2, & J_2 = 0.001kgm^2 \\ c_v = 4Ns/m & \tau_c = 1N/m \\ \alpha = 45deg & q_{01} = 90deg \\ \delta = 0.02s & q_{02} = -120deg \end{array}$$

$q_{01}$  and  $q_{02}$  are the considered initial positions for the joints.

The uncertainties are simulated using the following mass and inertia parameters in the control law:

$$\begin{array}{ll} \hat{M}_1 = M_1 * 0.8, & \hat{M}_2 = M_2 * 0.8 \\ \hat{m}_1 = m_1 * 0.9, & \hat{m}_2 = m_2 * 0.9 \\ \hat{J}_1 = J_1 * 0.8, & \hat{J}_2 = J_2 * 0.8 \end{array}$$

The control coefficients are:

$$\mathbf{M}_{d-e} = \begin{bmatrix} 1 & 0 \\ 0 & 1 \end{bmatrix}, \quad \mathbf{K}_{d-e} = \begin{bmatrix} 100 & 0 \\ 0 & 100 \end{bmatrix}, \quad \mathbf{D}_{d-e} = 2*0.7*\sqrt{\mathbf{K}_{d-e} * \mathbf{M}_{d-e}}$$

$$\mathbf{k}_p = \begin{bmatrix} 10^6 & 0 \\ 0 & 10^6 \end{bmatrix}, \quad \mathbf{k}_v = \begin{bmatrix} 500 & 0 \\ 0 & 500 \end{bmatrix}$$

The time delays ( $T_d$ ) is set to  $2ms$ . Again the noise on the external force measurement is Gaussian with zero mean and unity variance and the



### 3.3 Simulation results

---

selected value for  $\delta$  is  $20ms$ . At the initial time the end-effector is considered in contact with the wall and the environment stiffness is expressed with:

$$\mathbf{K}_e = \begin{bmatrix} k_e & 0 \\ 0 & 0 \end{bmatrix}$$

in the environment reference frame, and so:

$$\mathbf{F}_{\text{ext-e}} = -\mathbf{K}_e \mathbf{x}_e \quad (3.20)$$

Figures 3.2, 3.3 and 3.4 show the Hybrid Control System performances with different fixed  $n$  values, respectively in soft, intermediate and stiff environments. The reported results show trends similar to the single d.o.f. case, with better error responses for  $n = 1$  in soft environment and for  $n = 0$  in stiff one. Again it can be noted that the Hybrid Control can interpolate between the responses of Admittance and Impedance Control. An adaptive strategy could allow to find a proper  $n$  value for different environment stiffness leading to lower oscillations in stiff environment than the Admittance Control and negligible overshoots and steady state errors with respect to the Impedance Control in low  $k_e$  values.

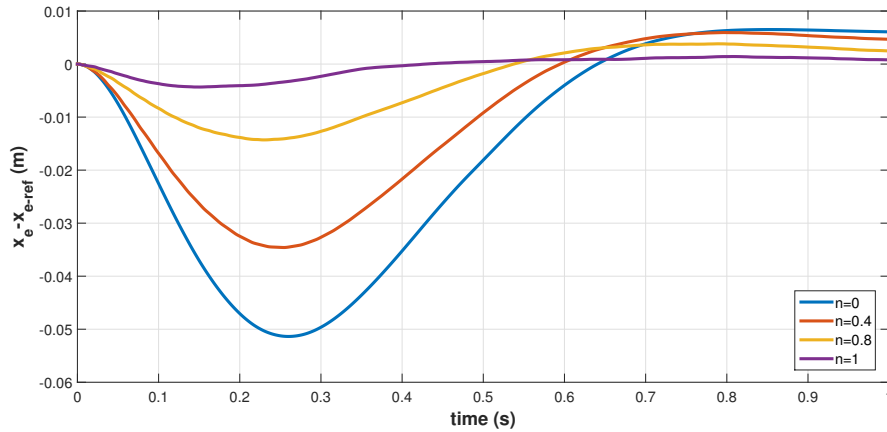


Figure 3.2: 2 d.o.f.s system error response with Hybrid Control for the soft environment  $k_e = 10N/m$

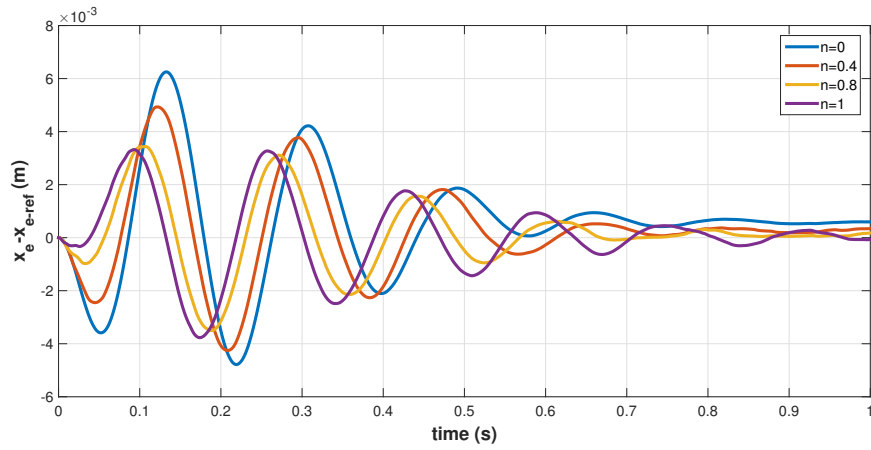


Figure 3.3: 2 d.o.f.s system error response with Hybrid Control for the intermediate environment stiffness  $k_e = 1400N/m$

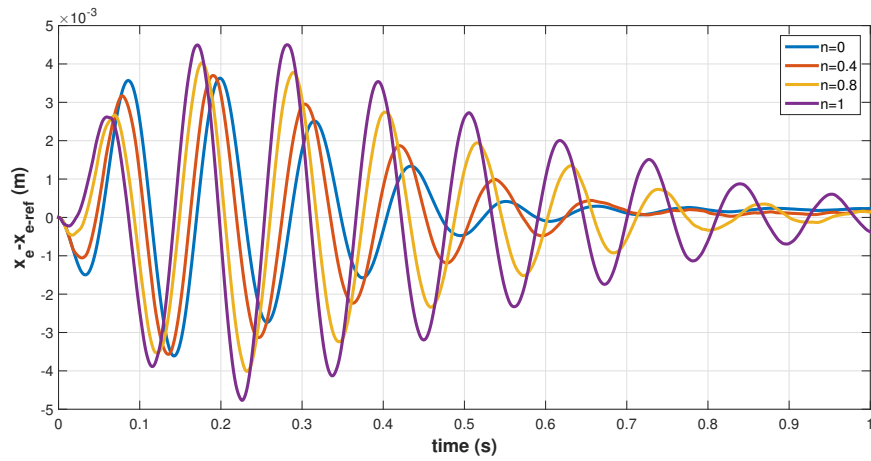


Figure 3.4: 2 d.o.f.s system error response with Hybrid Control for the stiff environment  $k_e = 3200N/m$

# Chapter 4

## Adaptive strategy: introduction and applications

The Hybrid System presented in previous chapters (see sec. 2.6) seems to be a promising solution capable of unifying Impedance and Admittance Control benefits.

However some issues still remain open. How can the duty cycle  $n$  be selected in order to guarantee the best performances? How can the environment stiffness be dealt with? Is it possible to manage a time-variant environment?

This chapter wants to show the potentiality and possible applications of making the Hybrid Control adaptive, discuss the relative problematics and propose answers to these questions. This introductive analysis is done considering the single d.o.f. system presented in 2.2, but the same conclusions are valid for the 2 d.o.f.s one. Finally the basic concepts of Artificial Neural Networks (ANN) and Genetic Algorithm (GA) used in the proposed solution are introduced.

### 4.1 Applications

Before proceeding with the analysis of the adaptivity problem, an overview of its possible applications is presented in this section.

#### 4.1.1 Industry

In the industrial field, robots usually work in structured environments where unforeseen disturbances and interaction with human rarely occur, since geometrical and physical characteristics are mostly known *a priori*.

However they must be machines with significant features of versatility and flexibility [36]. The hardware requirements for Impedance Control and Admittance Control are typically different; this means that once a control law and the associated hardware are selected the other controller can not be used, limiting the duties carried out by a single robot. On the other hand the Hybrid Control could lead to a class of robots capable of accomplishing different tasks with a single custom hardware structure and a single control system, answering to the versatility need.

Moreover the adaptive system discussed in next chapters can enhance the duties in charge of robots, especially the ones where the environment could change during the operations. A trivial example could be the task of wiping a surface constrained at the boundaries; indeed the surface stiffness in the normal direction varies moving from the center to edges.



Figure 4.1: DLR Justin humanoid cleaning a window

### 4.1.2 Space

As concern space activities, more and more robots are asked to assist and in some case completely replace humans. A space robot has to facilitate manipulation, assembling and servicing functions either inside or outside the spacecraft.

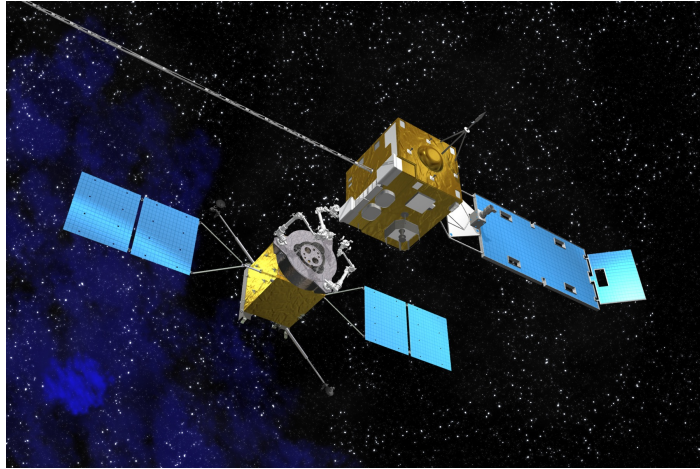


Figure 4.2: Artistic representation that shows an OOS mission

Nowadays space community is focusing its attention on the on-orbit servicing (OOS).

In this scenario the interaction with non-cooperative satellites is highly challenging. It is already shown [31, 32] that impedance control is particularly suitable in the contact phase. In fact during the contact between the end effector and the grasping point there is the risk that the target and the robot can be pushed away from each other. This issue can be overcome if the chaser's hand is controlled to have impedance that is equivalent or smaller than the target mass. In this context future development of the Adaptive Hybrid Control, able to handle collision phenomena, could improve the performances since it could adapt itself to abrupt changes in the external force.

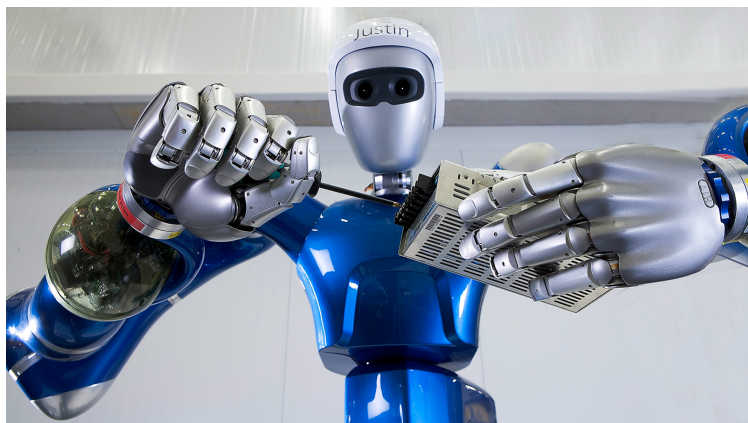


Figure 4.3: Manipulation task representation

Anyway the most common risks in autonomous OOS can occur when the two spacecrafts come together, unpredictable conditions of the target could lead to off-design situations with the possibility of damaging expensive space assets [32]. Therefore it is clear that this task requires a control system that can remain stable and guarantee good response in these unknown environments.

Another important application regards the human support in vehicular activities, where manipulation plays a key role. The robot has to be able to work with many different objects with wide variety of physical characteristics. An example is Robonaut [33] that is designed to accomplish all these requirements. It could be thought to exploit also the flexibility of Adaptive Hybrid Control to create suitable controllers for space humanoids.

### 4.1.3 Healthcare

A further field where this control law could be applied is physical therapy. Robotic appliances are used for rehabilitation purposes to help people recovering from limbs movement disorders or injuries. For instance active devices are exploited to re-educate muscles and articulations to perform common movements. This activity is typically called passive exercise since it is not required active work of the patient, indeed the machine guides the motion of the limb in a proper way. This means that it is necessary to consider robot and patient as a coupled mechanical system. The application of force or position control is not enough to ensure appropriate and safe dynamic interaction between human and manipulator. Impedance and Admittance Control are usually implemented to accomplish these kind of tasks [37], the Adaptive Hybrid System could combine together these



Figure 4.4: Rehabilitation device representation

approaches in a single controller capable of facing variable interaction conditions and guaranteeing the safety of the person.

## 4.2 Problem overview

As already explained, the idea behind the design of the Hybrid System is the development of a general framework capable of unifying Impedance and Admittance Control. This means that, in order to reach the desired impedance relation, potentially, every already existent Impedance or Admittance Control formulation can be added to the hybrid system, depending on the application. Therefore this analysis considers two basic and fixed controllers aiming to provide a prescribed force/motion behavior characterized by opposite causality. The whole study wants to achieve the best possible interpolation of the two control algorithms through a proper command of the switching signal.

The two quantities that govern the switching system are the switching period  $\delta$  and the duty cycle  $n$ .

The selection of the former directly influences the stability region of the system and it must be chosen depending on the expected stiffness range of operations. Instead the latter, as figure 4.5 shows, plays the role of deciding the contribution of each control law in the  $\delta$  period and so it represents the design parameter to be adapted.

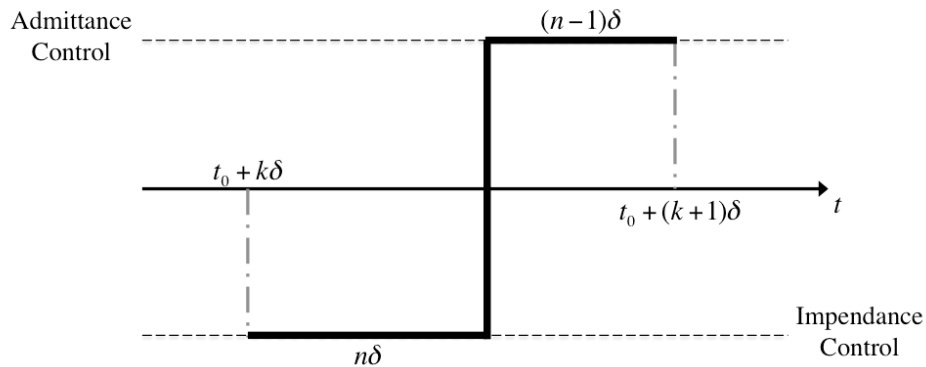


Figure 4.5: Switching concept

In order to make a system adaptive it is necessary to identify a quantity to be minimized, i.e. setting an optimal problem. Since it is required that

the control system follows a prescribed behavior, it is straightforward to consider the deviation from its reference trajectory in the definition of that quantity. Once the desired impedance parameters are defined, the ideal response of the system is described by equation 2.19. As a consequence the error to be minimized can be defined as the difference between the actual position and the reference one. Hence a quadratic cost function is chosen as follows:

$$J = \frac{1}{2} \int_{t_0}^{t_f} (x - x_{ref})^2 d\tau \quad (4.1)$$

Afterwards a relation that links the defined cost function to the chosen design parameter must be identified.

In chapters 2-3 it is highlighted that in soft environments the error response with  $n$  close to zero presents a large overshoot and steady state error, whereas in stiff environments when  $n$  is set near to 1 underdamped oscillations can be observed.

Even though the effects of varying the duty cycle  $n$  in different environments are clear, it should be noted that it is embedded in the system and explicit expressions that relate  $n$  to the force input or the continuous states of the system can not be found.

The only analytical relation which can be derived regards a discretization of the system; indeed, knowing the states of the system at  $t = t_0 + k\delta$ , the states at time  $t = t_0 + (k + 1)\delta$ , with  $k = 0, 1, 2, \dots$ , can be obtained exploiting equations 2.10, 2.14 and 2.16.

$$\begin{aligned} \mathbf{x}_i(t_0 + (k + 1 - n)\delta) &= e^{\mathbf{A}_i(1-n)\delta} \mathbf{x}_i(t_0 + k\delta) + \\ &+ \int_{t_0+k\delta}^{t_0+(k+1-n)\delta} e^{\mathbf{A}_i(t_0+(k+1-n)\delta-\tau)} \mathbf{B}_i K_d x_0 d\tau \end{aligned} \quad (4.2)$$

$$\begin{aligned} \mathbf{x}_a(t_0 + (k + 1)\delta) &= e^{\mathbf{A}_a n\delta} \mathbf{x}_a(t_0 + (k + 1 - n)\delta) + \\ &+ \int_{t_0+(k+1-n)\delta}^{t_0+(k+1)\delta} e^{\mathbf{A}_a(t_0+(k+1)\delta-\tau)} \mathbf{B}_a K_d x_0 d\tau \end{aligned} \quad (4.3)$$

$$\mathbf{x}_a(t_0 + (k + 1 - n)\delta) = \mathbf{S}_{ai} \mathbf{x}_i(t_0 + (k + 1 - n)\delta) \quad (4.4)$$

$$\mathbf{x}_i(t_0 + (k + 1)\delta) = \mathbf{S}_{ia} \mathbf{x}_a(t_0 + (k + 1)\delta) \quad (4.5)$$



Assumed a constant equilibrium position  $x_0 = \bar{x}_0$ , the discrete dynamic of the system becomes:

$$\begin{aligned} \mathbf{x}_{k+1} = & \mathbf{S}_{ia} \left\{ e^{\mathbf{A}_a n \delta} \mathbf{S}_{ai} \left[ e^{\mathbf{A}_i (1-n) \delta} \mathbf{x}_k + \right. \right. \\ & + \left. \int_{t_0+k\delta}^{t_0+(k+1-n)\delta} e^{\mathbf{A}_i (t_0+(k+1-n)\delta-\tau)} \mathbf{B}_i K_d x_0 d\tau \right] + \\ & \left. + \int_{t_0+(k+1-n)\delta}^{t_0+(k+1)\delta} e^{\mathbf{A}_a (t_0+(k+1)\delta-\tau)} \mathbf{B}_a K_d x_0 d\tau \right\} \end{aligned} \quad (4.6)$$

and so:

$$\mathbf{x}_{k+1} = \mathbf{f}(\mathbf{x}_k, \mathbf{u}_k) \quad (4.7)$$

Integral terms could be approximated and discretized, for example using the trapezoidal rule. In this way it would be possible to have a complete discrete representation of the system.

In any case it can be easily seen that  $f$  is a nonlinear system in the  $n$  parameter. Moreover an adaptive solution could take into account the possibility of changing  $n$  continuously in time, making the whole problem more complex.

It could be thought to consider the problem as a control one where the system gives the states as output and receives the duty cycle as input. However it would be a non-affine system, nonlinear in  $n$  and for this reason really hard to manage.

In addition, as already observed in sec. 2.3, Impedance Control can guarantee exactly the behavior described by equation 2.19 in absence of uncertainties, delay and uncompensated friction, as shown in figure 4.6. This is true in any environment, with any stiffness. Therefore the already-complex model should include at least a good estimations of the delay in the measurements and the possible friction.

At this point it should be clear that exploiting adaptive solutions that require precise analytical relations could be extremely demanding to handle.

### 4.3 Possible solutions and limitations

Approaching the problem the very first idea that could come to mind is to consider a constant duty cycle for the Hybrid System and a time-invariant stiffness of the environment.

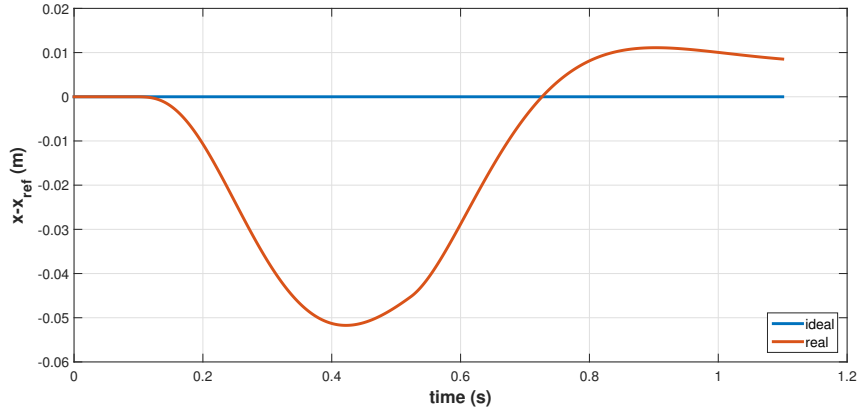


Figure 4.6: Deviation from the reference response with  $k_e = 10N/m$  considering models with and without uncertainties, delays and uncompensated friction.

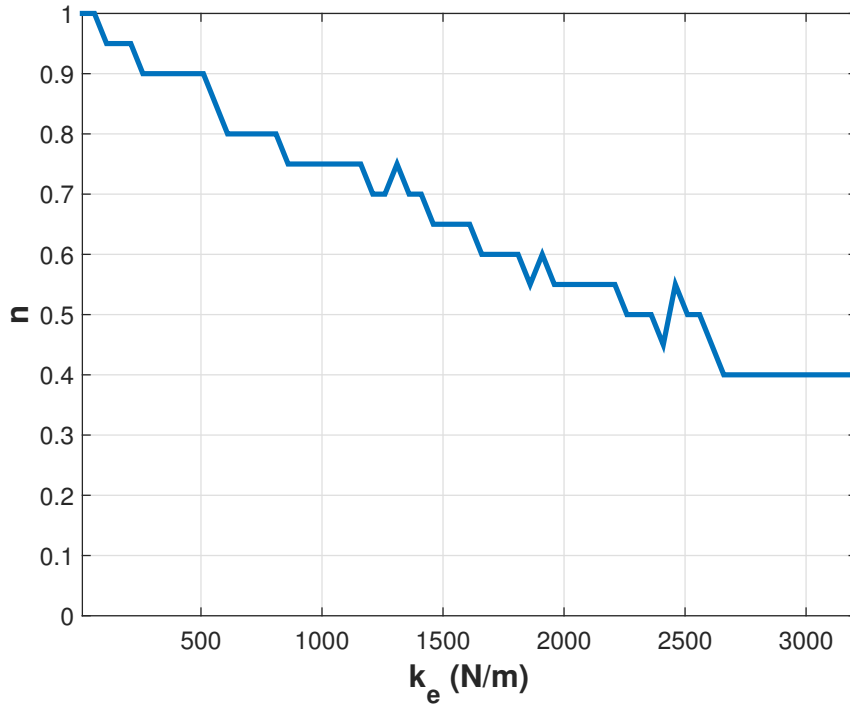
Once the range of operative stiffnesses is defined it can be discretized and the cost function 4.1 can be evaluated by means of simulations varying  $n$  in any situation.

Figure 4.7 shows a possible mapping between stiffnesses and design parameter  $n$ . The switching period is set to  $20ms$  and so the value of  $n$  is discretized with step size of 0.05, whereas  $k_e$  can assume values from  $10N/m$  to  $3210N/m$ . Considering the same stiffness range it should be noted that the mapping can vary if different  $\delta$  periods are chosen.

The optimal response obtained by the cost function 4.1 are characterized by small overshoots, damped behavior and short transient periods. This results underline the fact that the Hybrid System can combine the robustness properties of Impedance Control in stiff environments with the accuracy of Admittance Control in soft contact, as it is shown in figures 4.8, 4.9 and 4.10.

In particular the case with  $k_e = 10N/m$  (see fig. 4.8) exemplifies this property; indeed the resetting action of the states every  $20ms$  given by switching action from Admittance to Impedance improves the performances of the pure Admittance Control.

Once this mapping is defined, if the environment stiffness is known *a-priori* it is possible to select the duty cycle accordingly, however in the most typical situations this information is not available or not accurate. Therefore it would be necessary to estimate the stiffness online and consequently select the  $n$  from an embedded database built up offline with the already explained procedure.

Figure 4.7: Mapping  $n_{optimal} - k_e$ 

There are different ways to obtain informations about the environment from the measurements of the states of the system and the interaction force.

Book and Love [18] estimated the environment stiffness using a Recursive Least-Square algorithm. They discretized the robot workspace and measured the tip force and position each sample period of the controller. The output vector of the RLS algorithm is built up with the force measurements, whereas the regression vector is based on the position ones. Three different time instants are considered for the estimation process. Afterwards the parameter computed is scaled and averaged with the previous estimations exploiting some weights.

RLS method can be used also with more complex environment models as shown in [38]. The environment is represented with a nonlinear function that relates force and system states by means of three parameters. These parameters are computed with two RLS estimators interconnected via feedback. A persistent excitation of the environment is suggested in order to have the best accuracy in the estimation.

Another possible solution is the use of an extended Kalman filter [39]. The

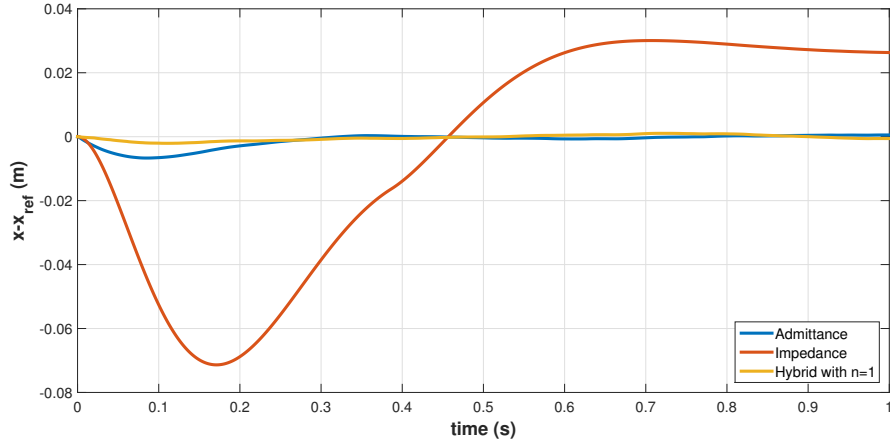


Figure 4.8: Comparison between Impedance, Admittance and Hybrid Control with optimal  $n$  for environment stiffness  $k_e = 10N/m$

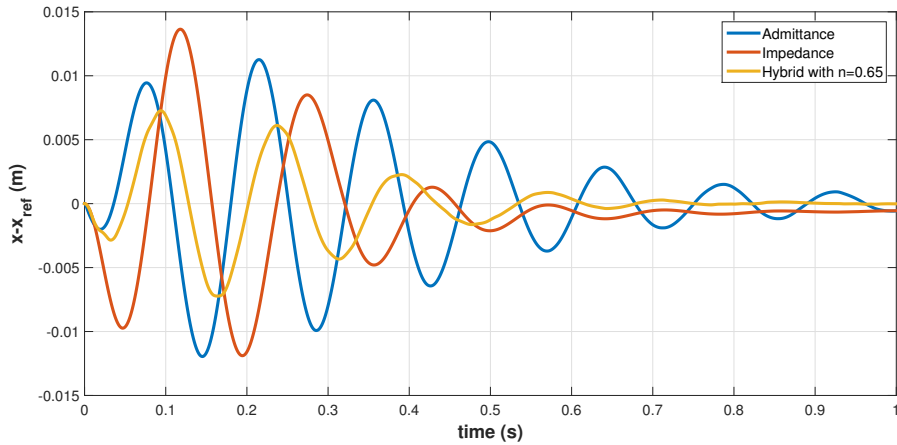


Figure 4.9: Comparison between Impedance, Admittance and Hybrid Control with optimal  $n$  for environment stiffness  $k_e = 1500N/m$

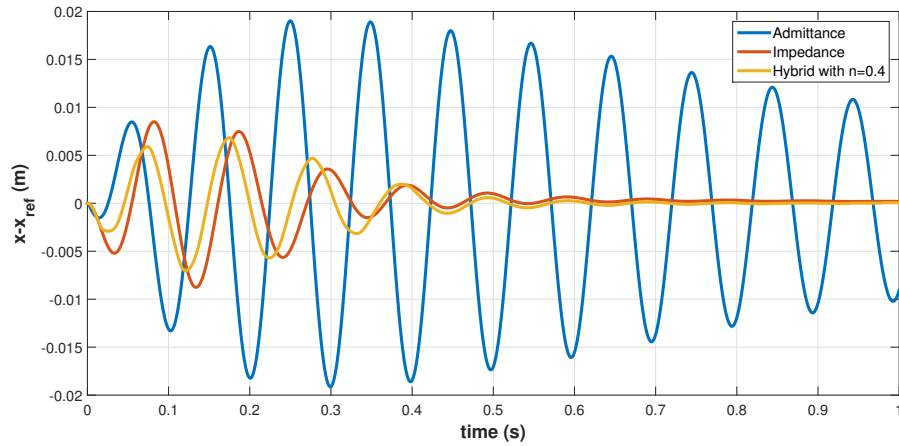


Figure 4.10: Comparison between Impedance, Admittance and Hybrid Control with optimal  $n$  for environment stiffness  $k_e = 3200N/m$

robot-environment interaction is defined by the filter states augmented with environment properties. A spring-damper model is considered and the stiffness and damping parameters are estimated.

A completely different approach is the exploitation of a neural network in order to create a linear mapping from position and velocity to force [40]. The authors proposed a neural network, with the states of the system as input and a force as output. It is trained online using a sliding mode learning algorithm that exploits the error between the output of the network and the measured environmental reaction force. Then the environment stiffness is estimated as the partial derivative of the network output with respect to the position.

An issue that can be immediately pointed out regarding the online computation of the stiffness concerns the inevitable delay in the estimation. A proper setting of the algorithm can minimize this phenomenon, however it still remains and could be problematic if the environment changes continuously in time. The described algorithms could have some difficulties in following these continuous variations leading to bad performances.

From what has been discussed so far, it can be noticed that the environment can be modeled in different ways depending on the application and the desired accuracy. It is easy to imagine that the presented solution based on stiffness estimation and mapping of the  $n$  parameter could result more complex whenever the environment model involves more than one parameter.

Then differences in the performances of Impedance and Admittance Control are mostly caused by uncertainties, uncompensated frictions and delays, as reminded in the previous section. Consequently the mapping solution depends on the simulation of these phenomena, therefore it could result in unrobustness to variations with respect to numerical reproductions.

It is preferable to have a robust controller that can react more promptly to whole system state evolution adapting rapidly itself to possible environment variations. Moreover the performance can be improved if the duty cycle is let to vary for the same environment stiffness. This means that it is not exclusively dependent only on the value of  $k_e$ , but it can follow the system evolution and guarantee a better tracking of the reference response.

As it will be explained in next chapters the solution proposed in this work goes in this direction.

## 4.4 Neural Network adaptive solution

The Adaptive Hybrid System presented in this work exploits a Neural Network in order to define the most suitable  $n$  evolution guaranteeing the smallest deviations from the reference response in a prescribed operative range of environment stiffnesses.

The network receives the measured states and interaction force as inputs and provides a consequent duty cycle. Then the signal is quantized according to the selected  $\delta$  period and sample time and discretized in time in such a way to have one fixed value for each period.

The training is done offline using a Genetic Algorithm as optimization method for the definition of the weights and biases.

In chapter 6 it will be shown that this solution is robust to uncertainties in the model of the robot, and that it works in an unknown environment and provides good performance even in the case of time variant stiffness. Moreover if the environment stiffness is known a specific training of the Neural Network system can give an improvement in the response with respect to the optimal fixed  $n$  solution.

Before proceeding with the analysis of the proposed strategy, some basic concepts about Neural Network and the chosen optimization algorithm are discussed in the next sections.

## 4.5 Neural Network: basic concepts

Artificial Neural Network (ANN) gets inspiration from the way in which the human brain processes the informations, that is completely different from conventional digital computer. The brain is a highly nonlinear and parallel system able to organize its structural constituents, neurons, in order to perform certain computations efficiently.

It has the peculiar ability to build up its own rules of behavior through what usually refers to as experience. It can learn and develop adapting itself to its surrounding environment.

In a similar way, as reported in [24], a neural network is a massively parallel distributed processor made up of simple processing units that has a natural propensity for storing experiential knowledge and making it available for use. The knowledge is acquired by the network from its environment through a learning process and stored in the interneuron connection strengths, known as synaptic weights. These latter elements of the network are modified in such a way to obtain certain desired design objective by means of a procedure called learning algorithm.

The strengths of the Neural Network are, first, the computation power thanks to the massively parallel distributed structure and, second, the generalization property derived from its ability to learn. This last feature means that Neural Network can produce reasonable outputs for inputs different from the ones received during the training. Thanks to these two capabilities the Neural Network are an useful tool to find good approximate solution to complex problems that would be intractable.

In this work, the explained characteristics of the Neural Network are used to create a link between the interaction force and the states of the system and the design parameter, the duty cycle  $n$ . Indeed the ANN can be trained in such a way to guarantee desired performance minimizing a prescribed fitness function, as it will be explained in the next chapter.

The fundamental constituent of a Neural Network is the neuron which is an information-processing unit.

It is possible to identify four basic elements in its structure, shown in figure 4.11:

- *Synapses* or *connecting links* characterized by some weights.
- An *adder* for summing all the weighted inputs of the neuron.
- An *activation function* for limiting the output of a neuron and allowing computation of non trivial problem with a small number of nodes.

- *Bias* that increases or decreases the net input of the activation function.

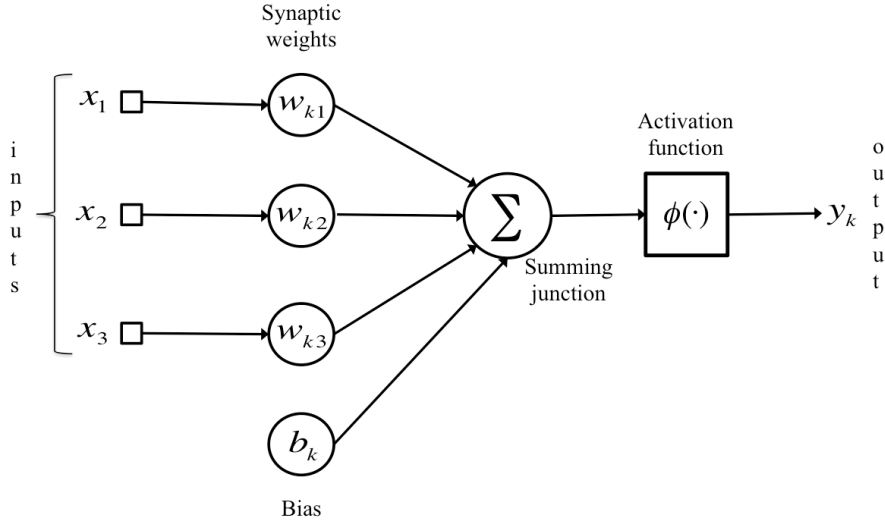


Figure 4.11: Structure of neuron  $k$ .

The most common activation function used in the construction of Neural Network is the sigmoid function. It is a strictly increasing function defined as follows:

$$\sigma(x) = \frac{1}{1 + e^{-a(x-c)}} \quad (4.8)$$

where  $a$  and  $c$  are two parameters.

In this work the sigmoid function is adopted, however other functions have been used in Neural Network such as Heaviside function, hyperbolic tangent function, etc.

The neurons can be organized in different structures from the simpler Single-layer Feedforward Neural Network to more complex solutions like Multi-layers Recurrent Neural Network. For the adaptive system of the Hybrid Control a multilayers feedforward architecture has been selected. This class of ANN are made up of three different parts: an input layer, one or more middle layers and an output layer. Each layer contains a certain number of neurons depending on the task that the neural network has to accomplish. The middle layers are called *hidden layers* and the computation nodes are correspondingly the *hidden neurons* or *hidden units*. They



are named in this way because this part is not seen directly from either input or output of the network.

The term "feedforward" refers to the fact that the neurons of a layer communicate only with the neurons of the next layer. The source nodes in the input layer of the network supply elements of the activation pattern, which represent the input signals applied to the neurons in the first hidden layer. The output signals of the second layer are the inputs of the next hidden layer and so on for the other layers until the output one. The set of signals of this latter layer constitutes the overall response of the network to the activation pattern supplied by the source nodes. If every node in each layer is connected to every node of the next layer the network is defined *fully connected*, otherwise it is said to be *partially connected*.

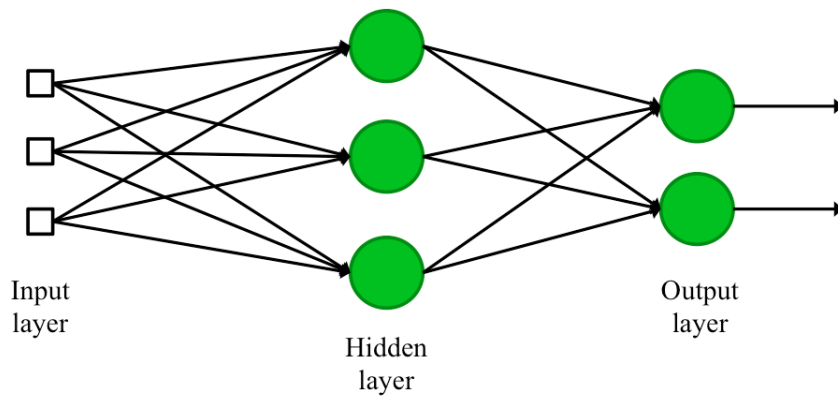


Figure 4.12: Multilayer feedforward architecture

As regards the training or learning phase, it can be done either online or offline. In the former case the neural network learns how to accomplish its task in real time, therefore it is required a certain transition time to reach the convergence of the weights, depending on the efficiency of the selected optimization algorithm. On the other hand in the latter situation the training is done in a phase before the real application of the network and after that the weights typically are fixed.

According to the needs of the designer and the nature of the problem, different optimization algorithm can be selected and different procedures can be followed. For the Adaptive Hybrid System, a Genetic Algorithm is found to be suitable to achieve the goal. The manner adopted for the training will be explained in chapter 5.

## 4.6 Genetic Algorithm

A Genetic Algorithm is a stochastic global maximum (or minimum) search method inspired by the natural biological evolution. In the natural world the reproduction mechanism of the species allows to give birth to new generations preserving those characteristics that are suitable for the survival to the external conditions. It results that, hopefully, for an increasing number of generations the species tend to adapt to the environment.

The algorithm starts considering a population of potential solution, called individuals, that are encoded as strings, called *chromosomes*. The *phenotype* belongs to the decision variable domain in which all the *genotypes* (chromosome values) are discerned. This means that the analysis of the genotype does not give information about the fitting property of the individual. Only the decoding of the chromosome string into its phenotypic value allows to understand how much the individual is suitable as solution of the problem. Once these performance are evaluated a fitting value is assign to every individual, then according to this a part of the population is selected with a certain probability to produce the next generation.

In order to create the next generation some genetic operators are applied to the selected solutions modifying directly the chromosomic content. First of all the recombination operator is applied to a percentage of individuals selected with a probability depending on their fitness value. There are different recombination operators; the simplest one is the single-point crossover that acts on two individuals, called parents, selects a random position  $i$  in the chromosome string and then switches the whole next chromosomic content of the parents (see figure 4.13).

The second operator is the mutation and it is applied to the remaining part of the population. Mutation changes the genetic content of the individual, that for example can be expressed in the binary representation, according to some probabilistic rules. This operator is used to ensure that the investigation covers the whole space of possible solutions and to converge to the global minimum instead of a local one.

A small number of individuals can pass to the next generation without being affected by these operators and they are called *elite children*.

After these operations are applied, the new generation is decoded and fitness values are associated to each individual. Then the process restart with the selection of those individuals which will be the parents for the next generation. When some criteria are satisfied the GA is stopped. Since this method is stochastic it is very difficult to define precise convergence criteria. Commonly the search is terminated after a predefined number of

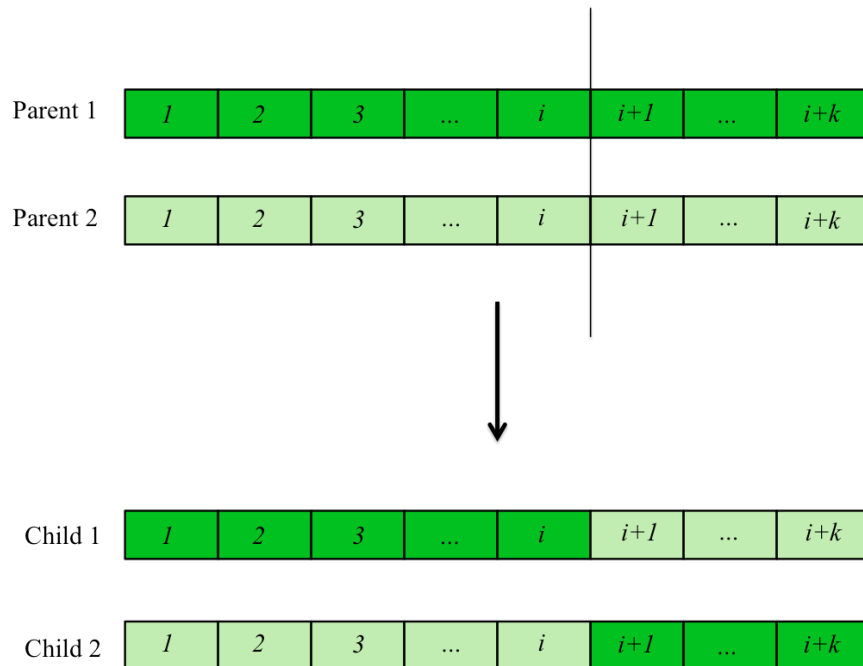


Figure 4.13: Single-point crossover operator

generations and then the quality of the final solution is checked. A good mark to understand if the solution has effectively reached the desired extremum is the convergence of the value of the best individual fitness function with the population mean value of the fitness function. In case the performances are not satisfying the GA may be restarted modifying some parameters.

The GA is particularly suitable in those cases in which the dependence of the fitness function with respect to the parameters to be set is unknown or if it is not regular and presents discontinuities. The main differences between GA and traditional search and optimization methods are represented by the facts that the GA analyzes a population of points in parallel, not a single point, then it does not require knowledge of derivatives or other auxiliary informations. Then it has to be highlighted that it exploits probabilistic transition rules rather than deterministic and it does not work directly on the parameter set but on an encoding of them. The GA method can be useful also for problem that does not have one individual solution. For these reasons it is decided to use this kind of optimization algorithm in this work.



# Chapter 5

## Adaptive system: Neural Network model and training

In this chapter the details of the Neural Network adaptive system model are presented, focusing firstly on the single d.o.f. problem and then on the two d.o.f.s one.

The Neural Network structure motivations and the settings of the optimization algorithm are discussed for the single d.o.f. system, presented in chapter 2, in order to highlight the main criticalities and how they have been taken into account. Then the same concepts are applied to the two d.o.f.s model introduced in chapter 3 with proper modifications.

### 5.1 Neural Network structure in the 1 d.o.f. system

A multilayer feedforward network was selected for the adaptive system. The input layer is made up of three source nodes that are the measured position and velocity of the system and the measurement of its interaction force with the environment.

In a first attempt the possibility of using also the control action on the system and the virtual position  $x_0$ , provided to the controller, was considered. However this solution brings to an higher number of coefficients to be determined by the optimization algorithm, resulting in longer computational times. Moreover it does not provide improvements in the solution. Indeed the control force does not give any additional information about the system dynamics and the feature of the environment, that are completely described by the states and the interaction force. On the other hand  $x_0$  is excluded because it is preferable a system independent of the command

position that during the operations can assume different profiles.

As concern the number of hidden layers, the selection is the result of a trade off between simplicity and performances, in particular single and two hidden layers solutions with comparable overall number of weights and biases were compared. The same methodology was used for the selection of the neurons number per layer. The analysis pointed out that a good compromise is a fully connected structure with just one hidden layer composed of four neurons. The output layer is constituted by only one neuron that receives the hidden layer outputs as inputs and provide the overall response of the network.

The final structure of the adopted Neural Network is shown in figure 5.1.

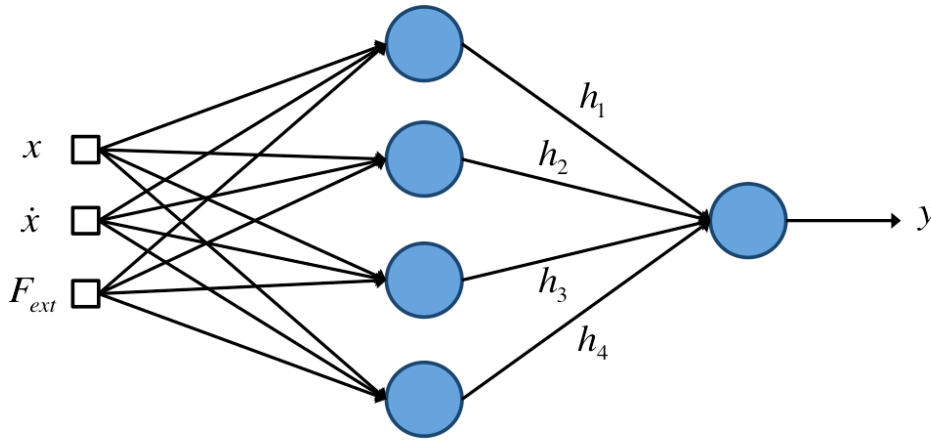


Figure 5.1: Neural Network adaptive system diagram

In order to simplify the optimization problem a single bias common to all the neurons of the hidden layer was used, this consequently decreases the number of coefficients to be evaluated. It was observed that this operation does not deplete the performance.

The activation function adopted in all the neurons is the sigmoid function reported in equation 4.8 with coefficients  $a = 1$  and  $c = 0$ .

In mathematical terms, the output of the  $k^{th}$  hidden neuron can be expressed as follows:

$$h_k = \sigma(w_{1k}x + w_{2k}\dot{x} + w_{3k}F_{ext} + b_h) \quad (5.1)$$

where  $\sigma$  is the sigmoid function,  $w_{ik}$  are the weights and  $b_h$  is the layer bias. Then  $h_k$  enters in the output neuron where again the sigmoid function is

## 5.1 Neural Network structure in the 1 d.o.f. system

---

applied:

$$y = \sigma \left( \sum_{k=1}^4 w_k h_k + b_o \right) \quad (5.2)$$

where  $w_k$  are the weights and  $b_o$  is the output bias.

It should be noted that  $y$  tends asymptotically to 1 or 0 when the argument goes respectively to  $+\infty$  or  $-\infty$ . Therefore the outputs  $n = 0$  or  $n = 1$  could not be reached by the network and this would mean excluding possible solutions. For this reason an additional weight  $w_f$  was added on the output of the neural network and then the constraint on the duty cycle  $n$ , that can vary only between 0 and 1, was recovered applying a  $\sin^2$ , as expressed in equation 5.3.

$$n = \sin^2(w_f y) \quad (5.3)$$

Since the sample time of the simulation is  $T = 0.001s$  and the considered switching period is  $\delta = 0.02s$  the minimum variation of the duty cycle that the switching system can read is  $T/\delta = 0.05$ , therefore a quantizer was added on the output of the neural network.

Finally a sample and hold was applied in order to reproduce the correct switch mode of operation, i.e. a constant value of the duty cycle is maintained during each  $\delta$  period. Figures 5.2 and 5.3 show how each neuron and the whole network were implemented in Simulink.

In brief, the selected structure is characterized by 3 weights for each of the 4 neurons and a single bias for the hidden layer, then 4 weights and a bias for the output layer and a final weight on the network output. This means that the optimization algorithm has to define 19 coefficients.

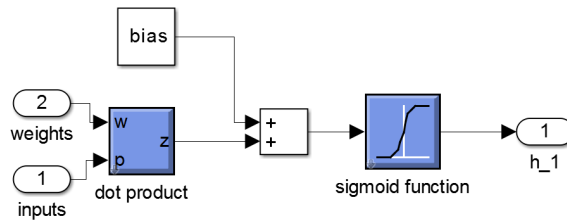


Figure 5.2: Neuron implemented in Simulink

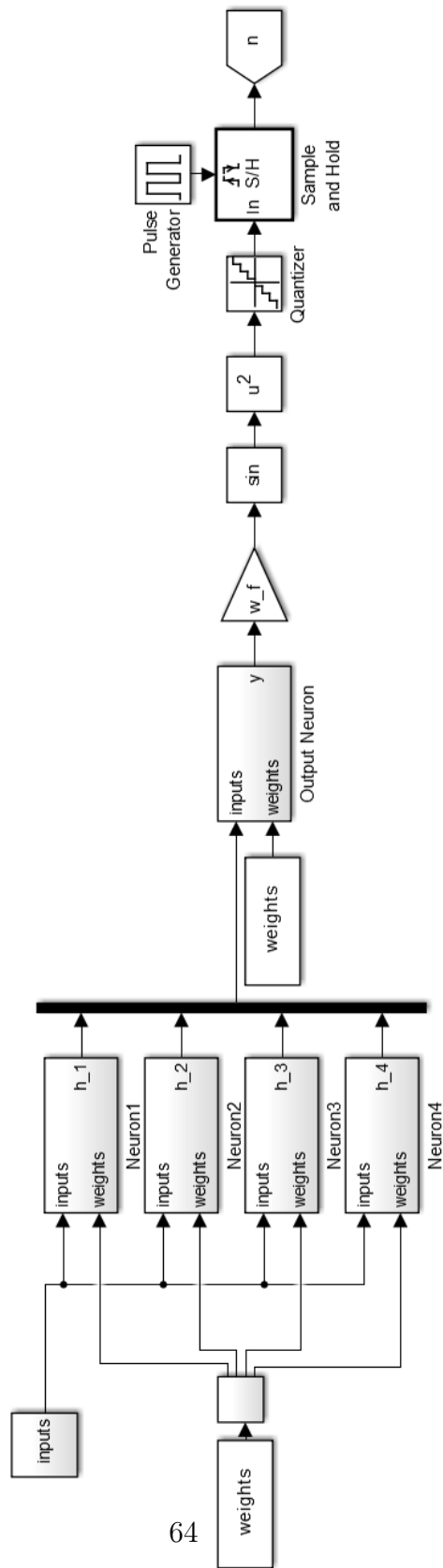


Figure 5.3: Neural Network implemented in Simulink



## 5.2 Neural Network training in the 1 d.o.f. system

The Neural Network training is executed exploiting a Genetic Algorithm as optimization method.

The method's goal is to minimize an *ad hoc* fitness function derived simulating the system response over a certain time interval and for a prescribed set of fixed  $k_e$ . For each  $k_e$  the cost function 4.1 is evaluated and finally all the values are used to create an appropriate fitness function.

It is necessary to pay particularly attention to the setting of some parameters, i.e. the command position for the controller and selection of the stiffnesses set for what concerns the system simulation and the fitness function, the weights boundaries and the population size as regards the Genetic Algorithm.

### 5.2.1 Command position

In the decision of an appropriate command position for the training it is necessary to consider that the system has to be robust to different situations and commands.

It was found that a training performed giving a step command to the system is the strategy that provides the best results. Indeed it provides a good level of generalization guaranteeing a proper behavior when the operations involve other possible command trajectories such as ramps, triangle or trapezoidal profiles.

The first idea was training the network considering the system response to a single step forward from a contact position  $x_0 = 0m$  to  $x_0 = 1m$ . This situation leads to poor performances when the command position moves backward. In fact the behavior of the system is slightly different in the two cases and the Neural Network has to learn the two evolutions of states and interaction force to be able to react properly.

As a consequence the step backward circumstance should be added in the training phase. This could be done in two different ways: either with two consecutive steps (fig. 5.4) or with two separated steps, i.e. two simulations (fig. 5.5).

In the former case the genetic algorithm fails in converging to a good solution. Indeed it is possible to find three classes of solutions, i.e. different sets of weights and biases, with comparable fitness functions but that lead the system to behave in different ways.

With two of these classes the system response is underdamped in cor-

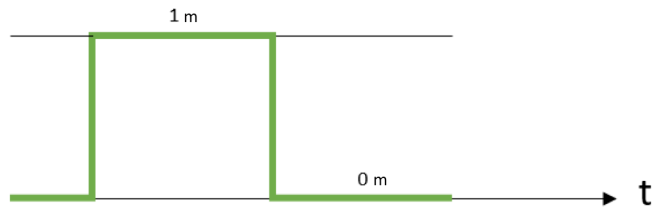


Figure 5.4: Double step in a single command trajectory

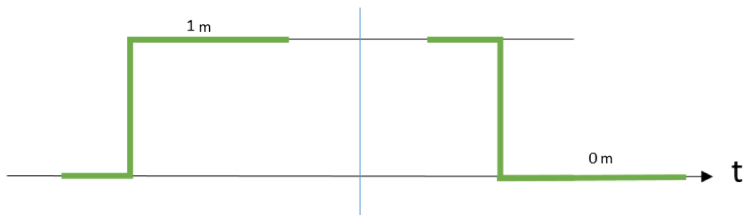


Figure 5.5: Two separate step command trajectories

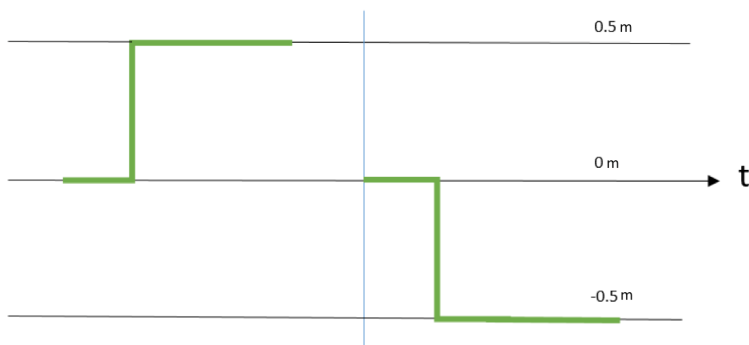


Figure 5.6: Two separate step command trajectories: one positive and one negative

## 5.2 Neural Network training in the 1 d.o.f. system

---

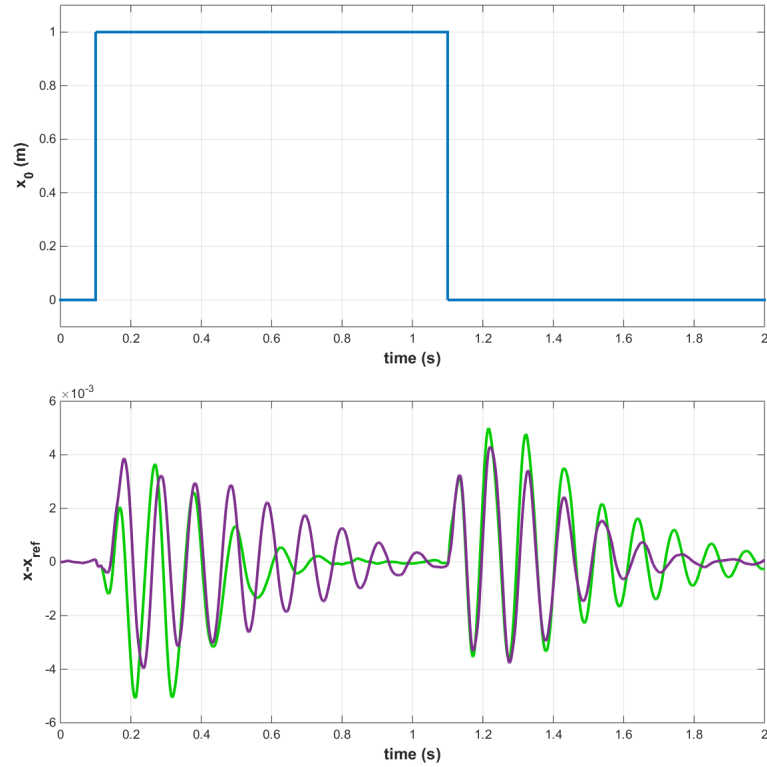


Figure 5.7: Responses of the solutions of two different classes trained with the same command position trajectory  $x_0$

response of respectively the first and the second step, as illustrated in figure 5.7.

The third class instead is middle way between the two. Theoretically it could be a good solution but the main problem is the fact that it remains difficult to be individuated since the algorithm can give one of the three kind of solutions with the same probability, so it would be necessary many attempts to find it. Moreover it should be noted that the result of the research is affected by the fact that in each simulation the system response to the second step has different initial conditions influenced by the response to the first step.

Hence the most suitable strategy is training the network considering two separated steps.

It was decided to consider a positive command and a negative one (fig 5.6). This choice is motivated by the fact that if the control system is a joint it can move in both direction so the Neural Network has to be able to manage this situation. Even if the commanded position is the end

effector one, the considered situation results more general, including both circumstances where the interaction force is positive or negative.

As regards the position to be reached, it was decided to use a step forward from  $x_0 = 0m$  to  $x_0 = 0.5m$  and a step backward from  $x_0 = 0m$  to  $x_0 = -0.5m$ . Needless to say that in operative situation this decision has to take into account the positions that the system has to reach. However it will be shown in next chapter that, even if the command position is not included in the selected training range, the Adaptive Hybrid System can guarantee good performance. Of course if the profile of the command signal is always the same in the operation, it can be used during the training instead of the step.

### 5.2.2 Stiffness set selection

For the training, first of all an operative range has to be selected. In this case it was decided to consider it from  $10N/m$  to  $3210N/m$  in continuity with the previous work on the Hybrid System by Ott, Nakamura, Mukherjee [10]. However this decision is not binding, indeed it can be modified depending on the application needs.

The stiffness set was created discretizing the range with a step of  $200N/m$  as a trade off between the necessity of training the network on a sufficiently wide number of stiffnesses, in which different  $n$  trends are required, and the need of reasonable training time.

Figure 5.8 shows that the time invariant optimal  $n$  distribution relative to the chosen discretization is quite uniform. It can be imagined that this fact can be useful for the Neural Network training since it is facilitated to understand better the relation between the stiffness and the duty cycle. The time invariant optimal  $n$  is derived as already explained in section 4.3.

### 5.2.3 Fitness function

It is now clear that, for the training phase, two simulations for each  $k_e$  value in the selected set are necessary. The time simulation  $T_{sim}$  is  $1s$ . This choice was made because in this time interval all the main characteristics of the response can be recognized, i.e. it takes into account both the whole transient period and the possible steady state error.

The fitness function for the Genetic Algorithm has to be defined in order to achieve the goal of minimizing over the entire range of stiffnesses the cost function defined in section 4.2 and reported here for simplicity:

## 5.2 Neural Network training in the 1 d.o.f. system

---

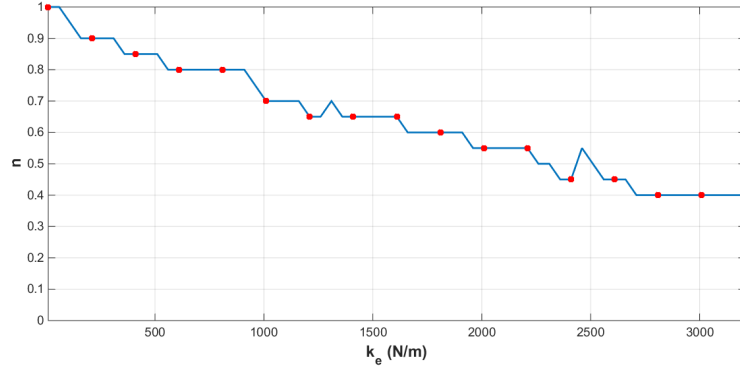


Figure 5.8: Optimal time invariant  $n$  relative to the selected  $k_e$  discretization

$$J = \frac{1}{2} \int_0^{T_{sim}} (x - x_{ref})^2 d\tau \quad (5.4)$$

where  $x$  is the actual position of the system and  $x_{ref}$  is the reference one derived from the desired impedance relation 5.5.

$$M_d \ddot{x}_{ref} + D_d \dot{x}_{ref} + K_d (x_{ref} - x_0) = F_{ext} \quad (5.5)$$

Then a natural consequence is to base the fitness function on the summations of all cost functions evaluated for each system response simulation with the step in both directions.

Therefore, for the step forward, the summation results in the reward function:

$$R_{forward} = \sum_{i=1}^N J_{fi} \quad (5.6)$$

where  $N$  is the number of stiffnesses belonging to the selected set,  $J_{fi}$  is the cost function evaluated for the response with the step forward in the environment characterized by the  $i^{th}$  stiffness.

In the same way for the step backward:

$$R_{backward} = \sum_{i=1}^N J_{bi} \quad (5.7)$$

The resulting fitness function for the Genetic Algorithm is defined as follows:

$$F = \max(R_{forward}, R_{backward}) \quad (5.8)$$

In this way the algorithm looks for a solution that at each generation minimizes the worst reward function keeping the other one bounded. Moreover another advantage of this formulation consists in the fact that the two rewards functions tend to assume similar values leading to analogous dynamic behaviors of the controlled system either for command in the forward or backward direction.

One could think to set a multi-objective minimization problem and exploit the Pareto solution using the two reward functions as objectives. However this strategy is more demanding from computational and time point of view and it does not provide better solutions. In addition it results more difficult to establish whether the convergence is reached or not.

#### 5.2.4 Population size and weights boundaries

The Genetic Algorithm also requires a correct setting of the population size and the weights and biases boundaries to assure the solution convergency. These two parameters are strictly correlated; indeed the wider the boundaries are the more numerous the population has to be in order to guarantee a certain density of individuals in the range. As one can easily imagine, too big population threaten the velocity of the method. Therefore it is extremely important to individuate a proper research region where the best solution could be found.

If the knowledge of the system is poor, this operation is a trial and error procedure and it is performed analyzing the input signals nature of the considered problem and assuming an initial guess for the boundaries to be verified later. Then the results should be examined in order to understand how the inputs are used by the network. If the weight associated to a certain input by the Genetic Algorithm results particularly near to zero

or to initial guessed boundaries, it can mean that this input is respectively less or more useful to the neuron with respect to the other ones and as a consequence a new guess for the boundaries can be done.

In the case here dealt with, since the different natures of the inputs, it is straightforward to focus the attention on the order of magnitude of the network inputs to set the boundaries. Indeed, since all the inputs of the network are necessary to describe the dynamic of the interaction between the environment and the system, it is reasonable to presume that they all should contribute in the same way to the output of the neurons in the first layer of the network and therefore the weights have to scale the source nodes signal properly. Consequently initial guess is done following this criterium. Then the algorithm results show certain weights trends that suggest how to refine the guess. Once a good candidate solution is individuated the boundaries can be restricted around it in order to increase the accuracy of the solution.

It is opportune that the population number related to the first boundaries guess follows the already stated rule, then as the boundaries are narrowed it is possible to decrease it obtaining faster convergence of the algorithm. However it is important to pay attention on guaranteeing a number of individuals sufficiently higher than the number of coefficients to be found. Figure 5.9 illustrates the followed procedure.

As concern the single d.o.f. problem, considering the worst combinations of fixed  $n$  and  $k_e$ , the system response to a unit step pointed out a proportion among the magnitudes of position, velocity and force respectively in the order of 100,10 and 1. Following the explained procedure the boundaries giving an initial good solution were the ones reported in table 5.1. Wherever a boundary is not specified the assumed value is the default ones of the Matlab genetic algorithm.

The resulting coefficients found out with the search method are reported in table 5.2.

In a second step the boundaries were restricted around this solution, as table 5.3 shows, to improve the accuracy. The designed structure of the adaptive system with the final weights is represented in the diagram 5.11. Figure 5.10 shows the improvement in the system performances with the coefficients of the final solution with respect to those of table 5.2 taking as example an environment stiffness of  $10N/m$ .

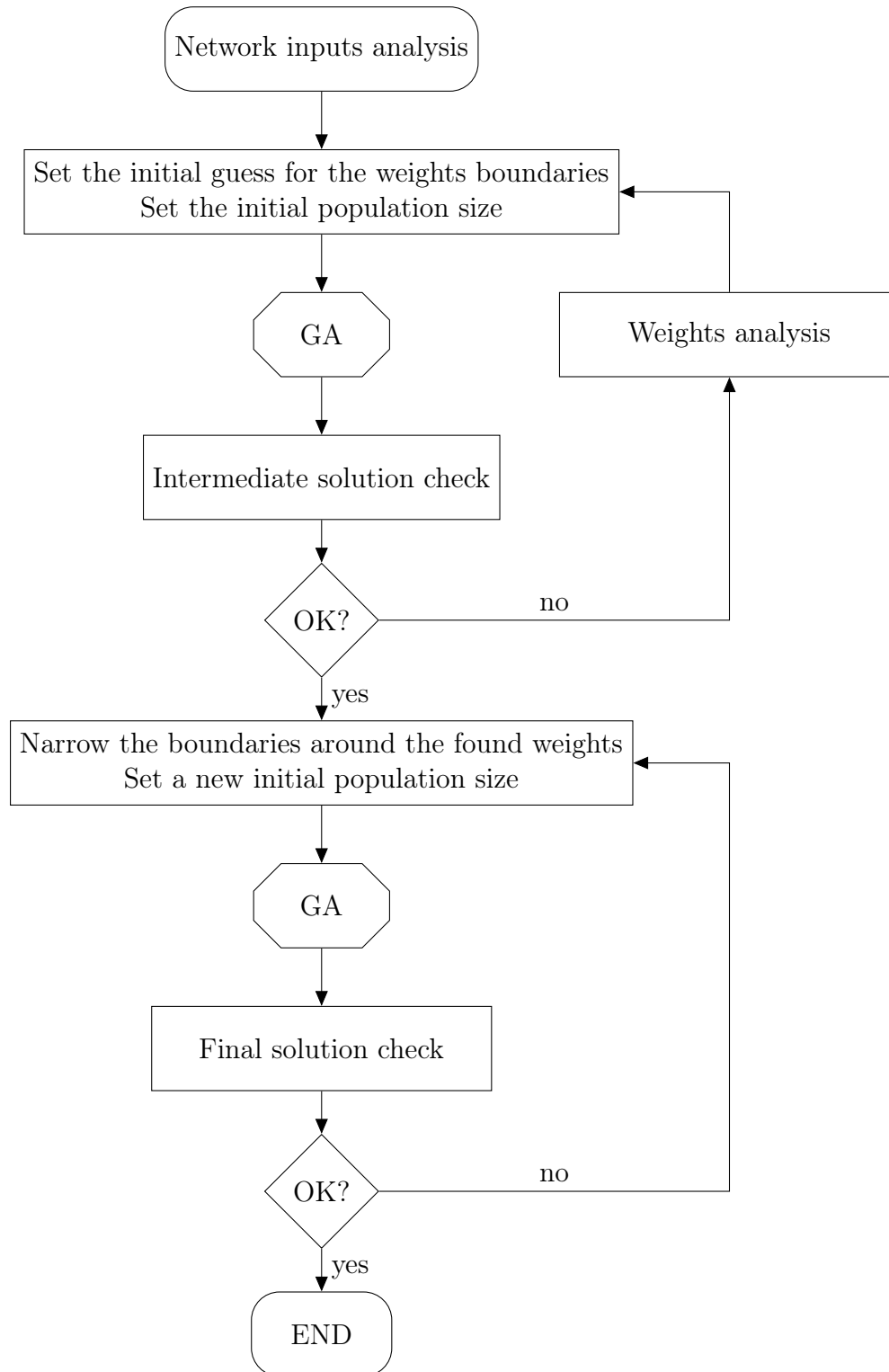


Figure 5.9: Flowchart of the procedure for the weights boundaries and population size setting



5.2 Neural Network training in the 1 d.o.f. system

---

weights	Hidden layer				Output layer					
	$w_{1k}$	$w_{2k}$	$w_{3k}$	$b_h$	$w_1$	$w_2$	$w_3$	$w_4$	$b_o$	$w_f$
UB	1500	100	10	-	-	-	-	-	-	-
LB	-1500	-100	-10	-	-	-	-	-	-	-

Table 5.1: Starting Upper Boundaries (UB) and Lower Boundaries (LB) for the weights and biases

	Neuron 1					
	$w_{11}$	$w_{21}$	$w_{31}$	$b_h$		
	-1338.19	-50.85	3.08	9.94		
	Neuron 2					
	$w_{12}$	$w_{22}$	$w_{32}$	$b_h$		
Hidden layer	-1479.27	-33.98	-6.09	9.94		
	Neuron 3					
	$w_{13}$	$w_{23}$	$w_{33}$	$b_h$		
	1284.81	43.52	0.22	9.94		
	Neuron 4					
	$w_{14}$	$w_{24}$	$w_{34}$	$b_h$		
	412.88	40.00	0.26	9.94		
	Neuron					
Output Layer	$w_1$	$w_2$	$w_3$	$w_4$	$b_o$	$w_f$
	1.71	-2.62	3.26	4.13	0.46	-4.37

Table 5.2: Intermediate solution for the network weights and biases

Hidden layer								
Neuron 1					Neuron 2			
weights	$w_{11}$	$w_{21}$	$w_{31}$	$b_h$	$w_{12}$	$w_{22}$	$w_{32}$	$b_h$
UB	-1100	-40	5	15	-1300	-20	0	15
LB	-1500	-60	0	0	-1500	-45	-10	0

Hidden layer								
Neuron 3				Neuron 4				
weights	$w_{13}$	$w_{23}$	$w_{33}$	$b_h$	$w_{14}$	$w_{24}$	$w_{34}$	$b_h$
UB	1400	60	2	15	500	60	2	15
LB	1100	40	-1	0	350	40	-1	0

Output layer						
Neuron						
weights	$w_1$	$w_2$	$w_3$	$w_4$	$b_o$	$w_f$
UB	3	1	6	7	3	0
LB	-1	-5	0	0	-2	-7

Table 5.3: Refined Upper Boundaries (UB) and Lower Boundaries (LB) for the weights and biases

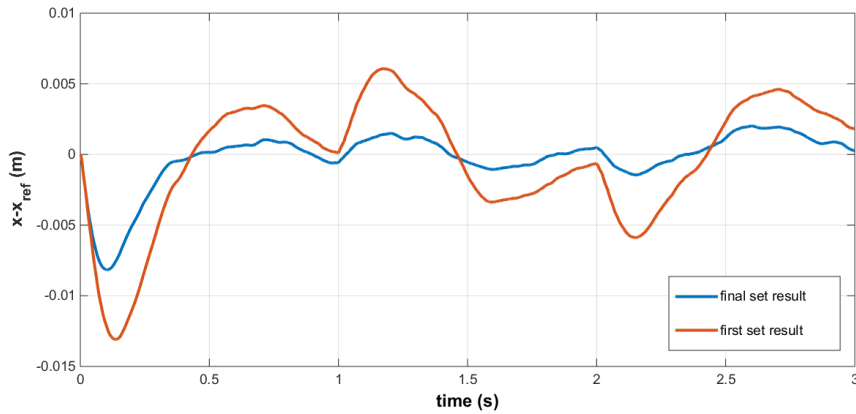


Figure 5.10: Comparison between the error response trends of the intermediate and final sets of coefficients with  $k_e = 10N/m$

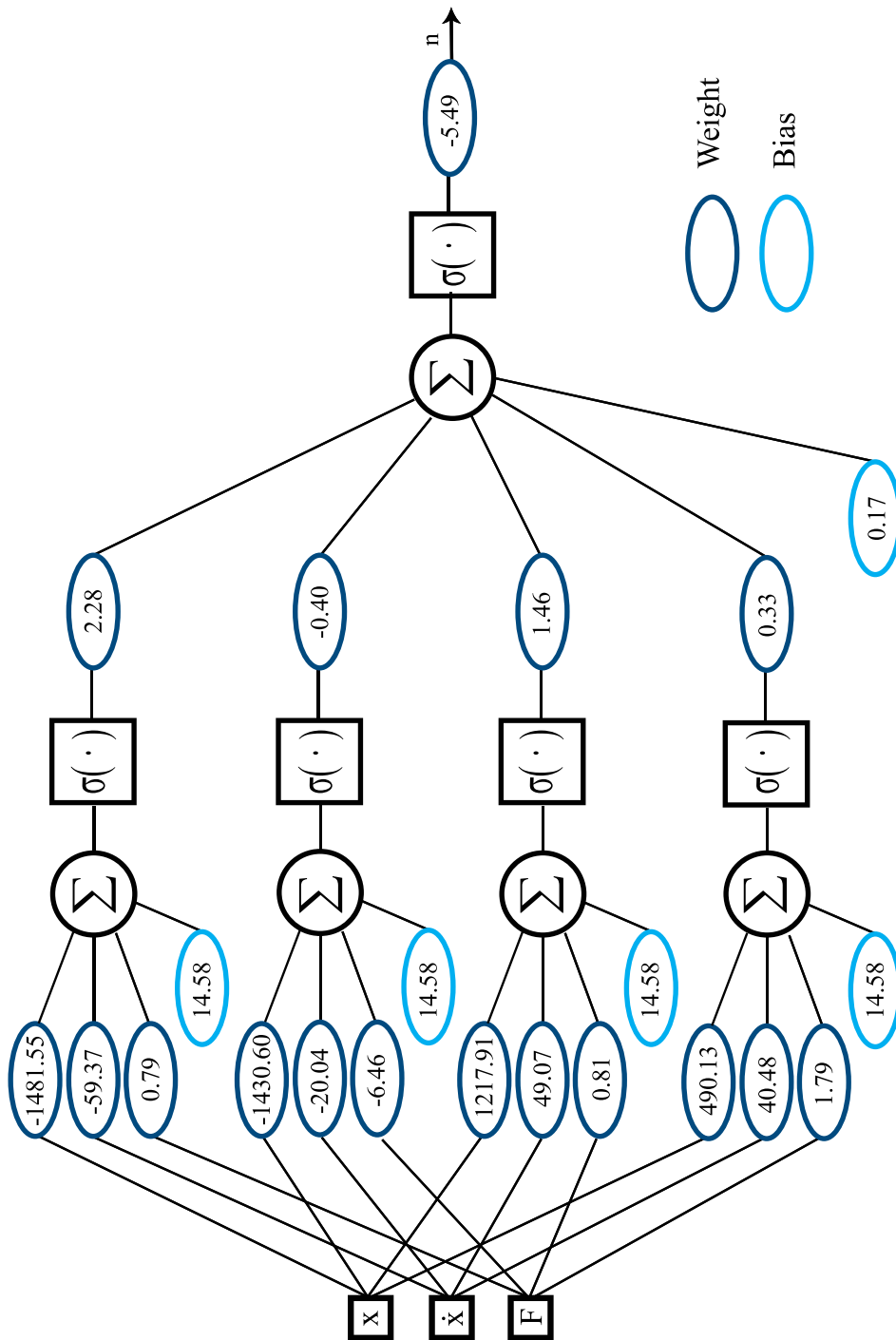


Figure 5.11: Final network weights and biases for the single d.o.f. system

### 5.3 Neural Network structure in the 2 d.o.f.s system

As for the 1 d.o.f. case, the adopted structure is a Multilayer Feedforward Neural Network with only one hidden layer made up of 4 neurons. The source nodes are the position, the velocity and the interaction force of the end-effector and the output, of course, is again the duty cycle  $n$ .

The choice of the inputs for the network is not straightforward since in the case of the 2 d.o.f.s system many possibilities can be selected. Indeed it can be decided to work in the base reference frame or in the joint space or considering some measurements in the first space and the others in the second one. This latter option could be motivated by the fact that typically the quantities related to the joints are measured whereas the force at the wrist can be obtained in the other space. The two reference frames are linked by nonlinear expressions. As can be easily imagined, this could lead to a more complex structure requiring an high number of neurons in order to manage the nonlinearity.

The decision of using the quantities in the base reference frame is motivated by three facts. First of all, it can be considered as a naturally extension of the simpler 1 d.o.f system. Then if a more complex manipulator is taken into account, the degrees of freedom related to the joint space are more than the ones of the end-effector. This means that an higher number of coefficients in each neuron would be necessary making the optimization problem harder and longer to solve, even with the same total amount of hidden neurons. Finally the objective is the control of the position of the end-effector interacting with the environment, therefore the Neural Network is facilitated in learning how to behave if it receives directly the necessary informations. This can be seen observing that with an equal structure it is easier to obtain better results with this network than with the one in the joint space.

The followed procedure to determine the number of layers and neurons per layer is the same already explained in section 5.1.

The proposed Neural Network is equal to the 1 d.o.f. case with a single layer of 4 neurons and a single bias, an output layer made up of 1 neuron and a single bias and a final weight that multiply the overall output signal. In this situation the inputs are 6: position, velocity and force in both  $x$ -direction and  $y$ -direction. Therefore the coefficients that the optimization algorithm has to find become 31. The structure is reported in figure 5.12. It can be immediately noticed that the addition of another end-effector degree of freedom lead to an increase of the coefficients independently on

the number of joints. For instance if a network with 4 hidden neurons results sufficient, the total weights would be 43 either the manipulator has 3 or 7 joints.

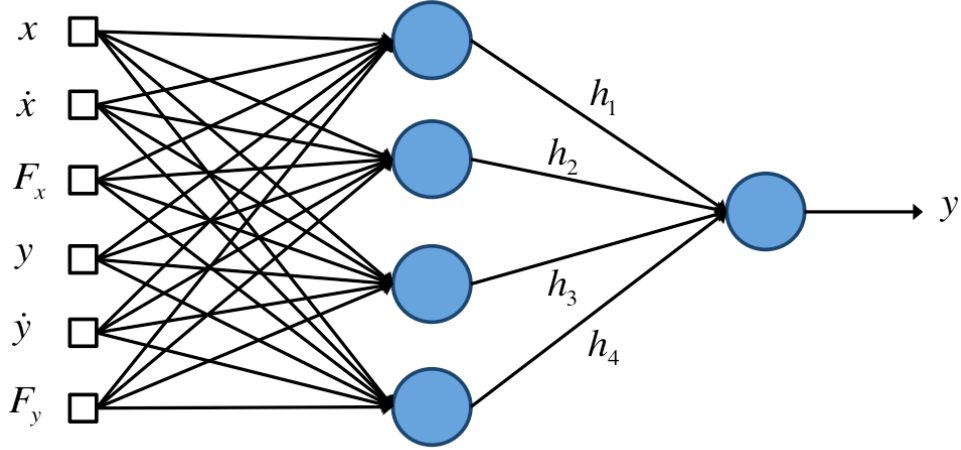


Figure 5.12: Neural Network adaptive system diagram in 2 d.o.f.s case

In mathematical term, the output of the network can be expressed as in equation 5.3.  $w_f$  is again the final weight and  $y$  has the same formulation reported in 5.2. In this case  $h_k$  is defined as in 5.9, whereas  $w_k$  and  $b_o$  are the weights and output bias.

$$h_k = \sigma(w_{1k}x + w_{2k}\dot{x} + w_{3k}F_x + w_{4k}y + w_{5k}\dot{y} + w_{6k}F_y + b_h) \quad (5.9)$$

$\sigma$  is the sigmoid function,  $w_{ik}$  are the weights and  $b_h$  is the layer bias. For the same reasons explained for the single d.o.f. case (see sec. 5.1), the output of the network passes through a quantizer and a sample and hold.

## 5.4 Neural Network training in the 2 d.o.f.s system

The indications emerged in the single d.o.f. analysis were followed for the training of the 2 d.o.f.s case.

Command positions for the end-effector were given in order to have two separated step along the direction orthogonal to the wall (for the geometry

of the problem see chapter 3). The first step is from  $0m$  to  $0.5m$  and the other one from  $0m$  to  $-0.5m$ .

As regards the stiffness set selection, the attention was concentrated on the range between  $10N/m$  and  $3210N/m$  in order to have a comparison with the results of the 1 d.o.f. For the same reasons already explained in section 5.2 the discretization was done with a step of  $200N/m$ .

The considered fitness function was built as shown in equation 5.8. Again two reward functions were defined based on the error with respect to the reference trajectory, as in 5.6-5.7. In this case the impedance relation that has to be satisfied is the one reported in equation 3.5 in the environment reference frame. Since neither interaction forces or commands are considered along the direction parallel to the wall, the error used in the definition of the reward functions is the error in the trajectory orthogonal to the wall.

The procedure for the definition of the coefficients boundaries is illustrated in 5.9. Therefore an initial magnitude analysis of the inputs was done and it led to conclusions similar to the single d.o.f. case, i.e. a relation between position, velocity and force in the order of 100, 10, 1. Afterwards a further analysis suggested to enlarge a little the boundaries for the coefficients of the position and velocity. In table 5.4 are reported the selected boundaries. Once a solution was found, as in the single d.o.f. case, these boundaries were narrowed around the weights set in order to improve the quality of the result. The final weights and biases used for the Neural Network in the 2 d.o.f.s system are reported in 5.13.

Hidden layer							
weights	$w_{1k}$	$w_{2k}$	$w_{3k}$	$w_{4k}$	$w_{5k}$	$w_{6k}$	$b_h$
UB	1500	1500	1000	1000	10	10	—
LB	-1500	-1500	-1000	-1000	-10	-10	—

Output layer						
weights	$w_1$	$w_2$	$w_3$	$w_4$	$b_o$	$w_f$
UB	—	—	—	—	—	—
LB	—	—	—	—	—	—

Table 5.4: Starting Upper Boundaries (UB) and Lower Boundaries (LB) for the weights and biases

5.4 Neural Network training in the 2 d.o.f.s system

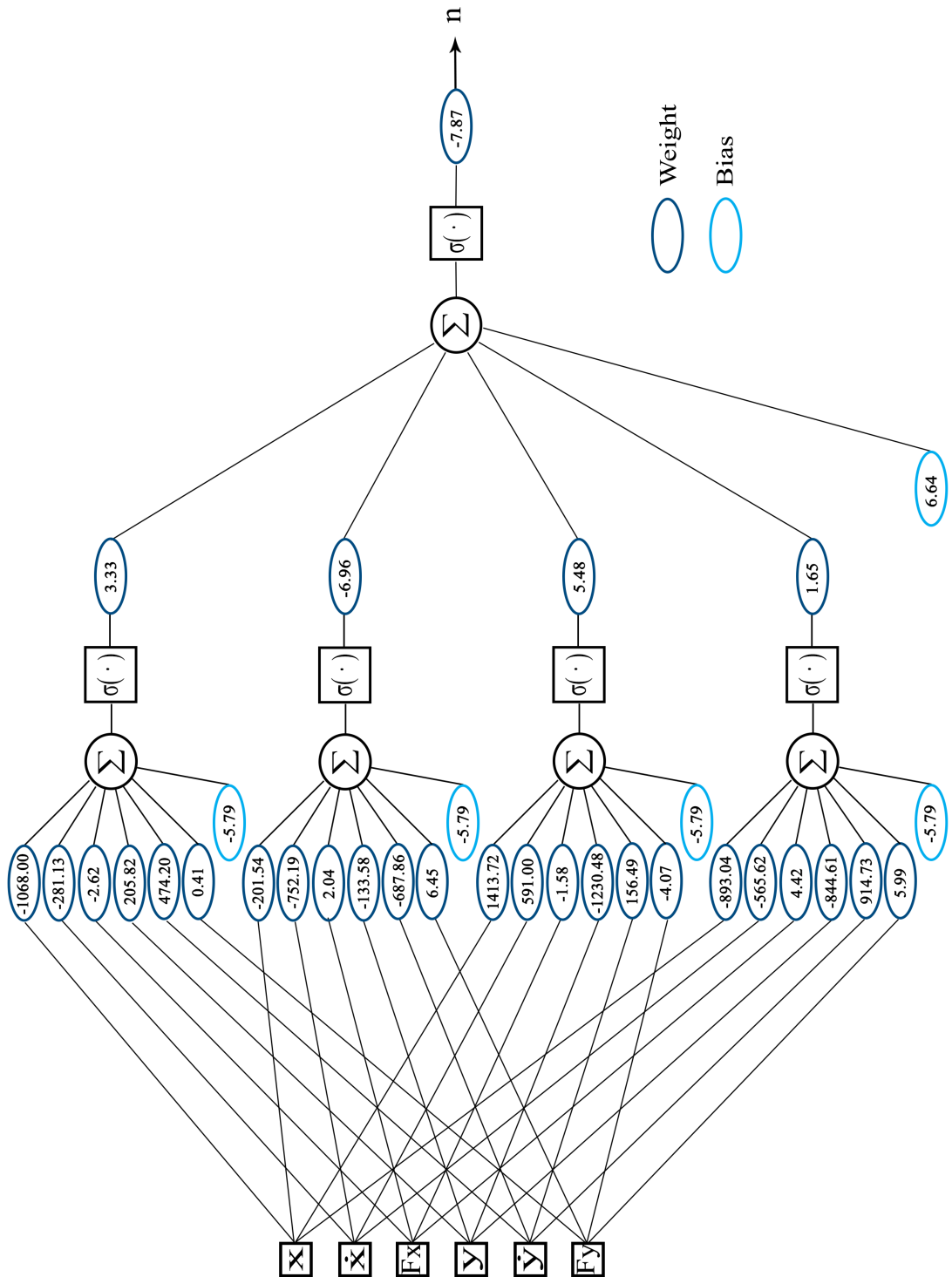


Figure 5.13: Final network weights and biases for the two d.o.f.s system





# Chapter 6

## Results

The main results of the Hybrid System with the addition of the Neural Network aimed at adaptive strategy are shown in this chapter.

It is illustrated that the proposed solution can achieve the goal of working in an unknown environment, even if time variant. Moreover the robustness of the Adaptive Hybrid System is presented.

The results are reported for both the 1 d.o.f and 2 d.o.f.s case.

### 6.1 Fixed environment stiffness

The goal of this work was the design of an adaptive system capable of setting  $n$  in order to guarantee an error in the reference trajectory as low as possible interpolating in a proper way between Impedance and Admittance Control behaviors. Indeed different performances can be obtained in different environments based on the value of the duty cycle  $n$ .

In this section the results of the Adaptive Hybrid System, Hybrid System with optimal fixed  $n$ , Admittance Control and Impedance Control are compared considering the environment stiffnesses  $k_e = 10N/m$ ,  $k_e = 700N/m$ ,  $k_e = 2100N/m$  and  $k_e = 3200N/m$  for both the single and two d.o.f.s systems. For this latter the step command position is considered in the direction orthogonal to the wall.

It is reminded that the Neural Network was trained over a stiffness range between  $10N/m$  and  $3210N/m$  with a discretization of  $200N/m$ .

Figures 6.1-6.8 show that in both the single d.o.f. and two d.o.f.s cases the adaptive solution provides an error response comparable to the one with the best fixed  $n$  both in the extrema and in the middle of the range; in any case it improves the performance of the pure Impedance and Admittance Control. The error for the 2 d.o.f.s system is considered

along the direction orthogonal to the wall where the desired impedance relation is prescribed. Along the wall the maximum measured error is around  $1mm$  and it occurs in stiff environment due to the uncertainties in the compensating gravitational term of the Impedance Control law

It can be noticed that in the single d.o.f. system the  $n$  trend varies with the different stiffness setting up near the best fixed  $n$ . Indeed for  $k_e = 10N/m$  it remains most of the time equal to 1, then for  $k_e = 700n/m$  it moves around 0.8 and so on up to  $k_e = 3200N/m$  where it assumes a value of 0.4. On the other hand, for the 2 d.o.f.s system the  $n$  parameter varies starting from 1 in soft environment and then jumping between different values as the stiffness increases. The difference between these two behaviors underlines the fact that more than one possible solution exists and the Neural Network can adapt the control system with different duty cycle time evolution.

The intermediate stiffnesses are selected not in the set used for the training of the Neural Network in order to prove that the adaptive system can work properly over the entire considered range and not only in the cases utilized in the training phase.

For the sake of completeness, in figure 6.9 the joints position evolution of the 2 d.o.f.s system are reported considering as example the cases of  $k_e = 10N/m$  and  $k_e = 3200N/m$ . Of course their trends are similar to the end-effector position behavior.

## 6.1 Fixed environment stiffness

---

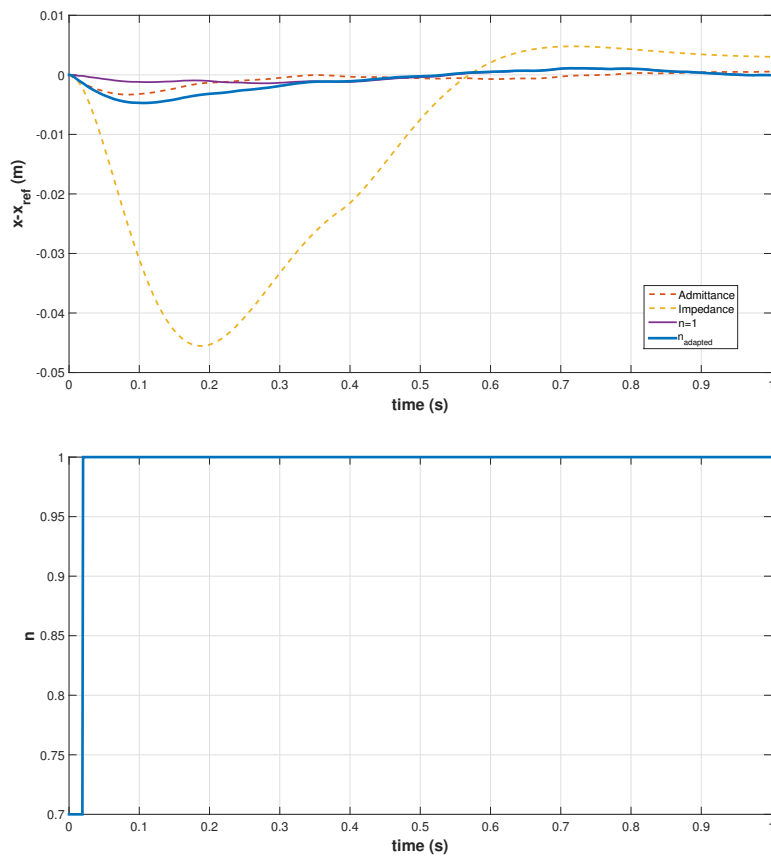


Figure 6.1: Error responses of the single d.o.f. system to a step command position from 0 to 0.5m for  $k_e = 10N/m$

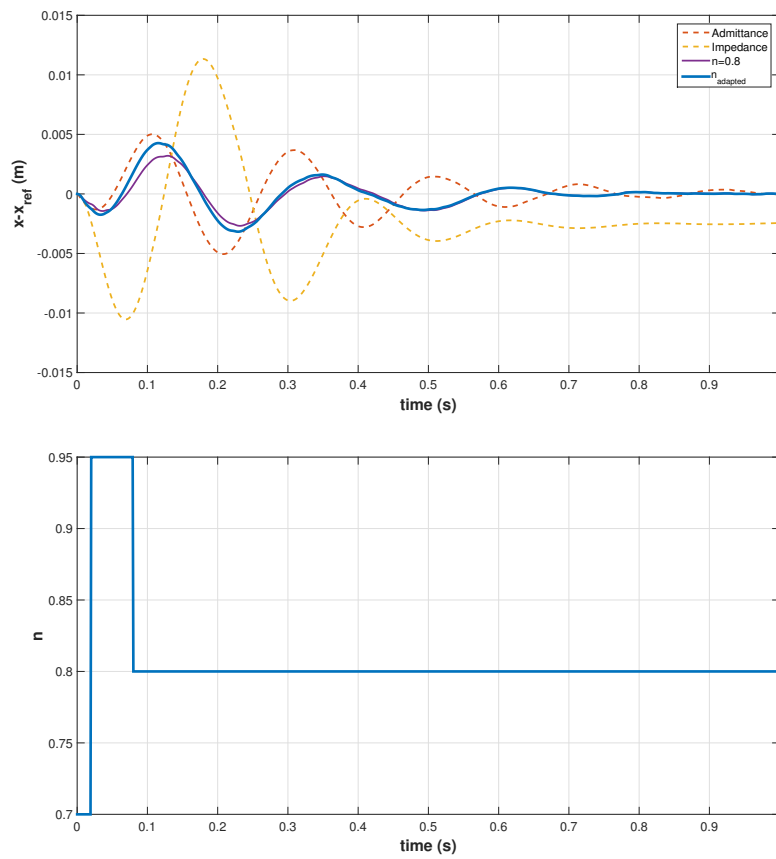


Figure 6.2: Error responses of the single d.o.f. system to a step command position from 0 to 0.5m for  $k_e = 700N/m$

## 6.1 Fixed environment stiffness

---

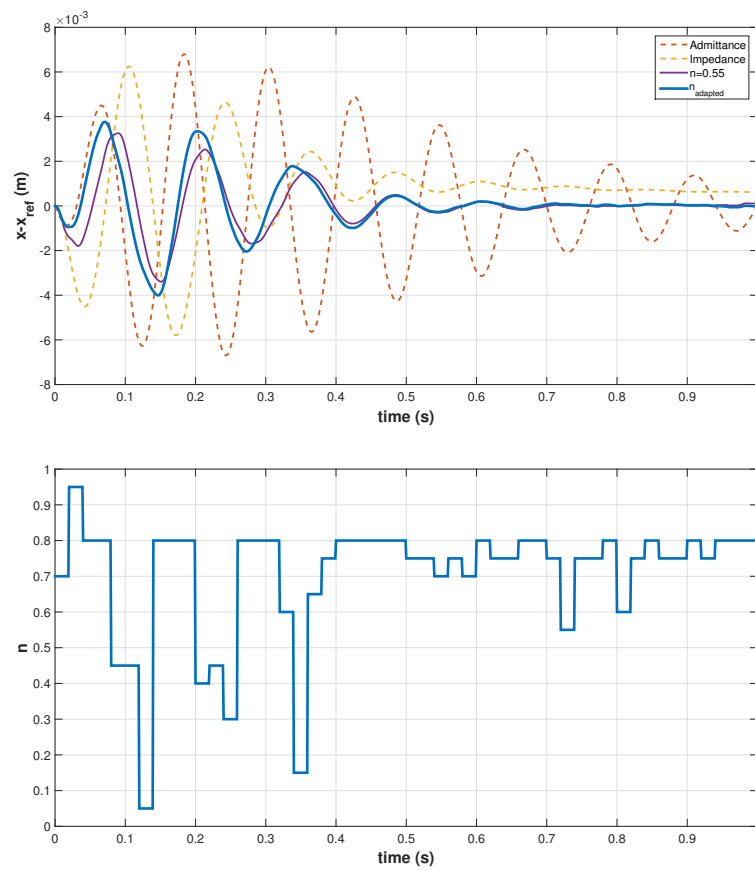


Figure 6.3: Error responses of the single d.o.f. system to a step command position from 0 to  $0.5m$  for  $k_e = 2100N/m$

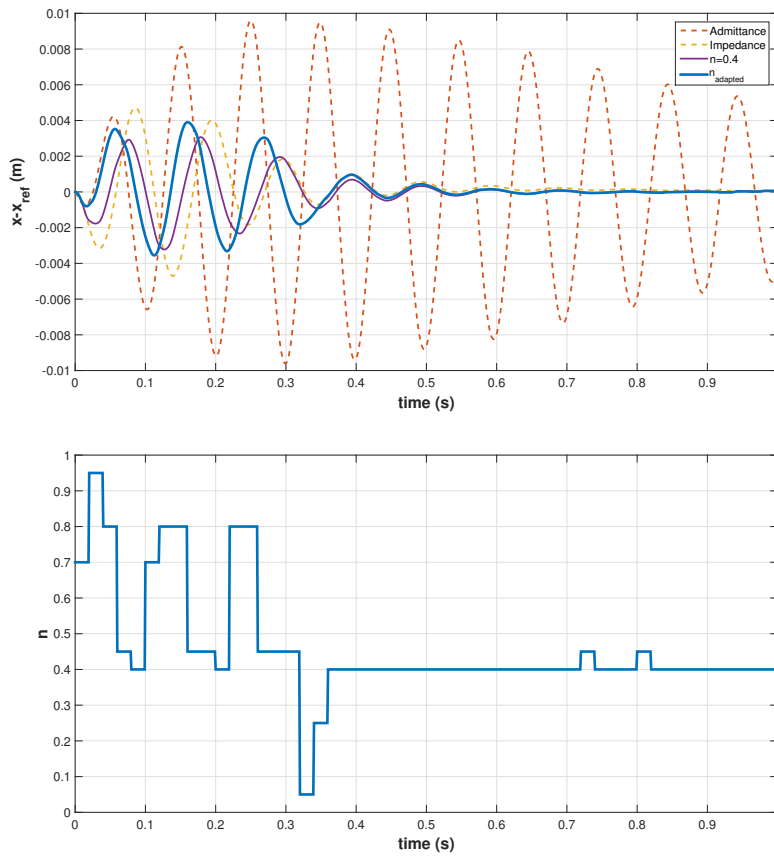


Figure 6.4: Error responses of the single d.o.f. system to a step command position from 0 to 0.5m for  $k_e = 3200N/m$

## 6.1 Fixed environment stiffness

---

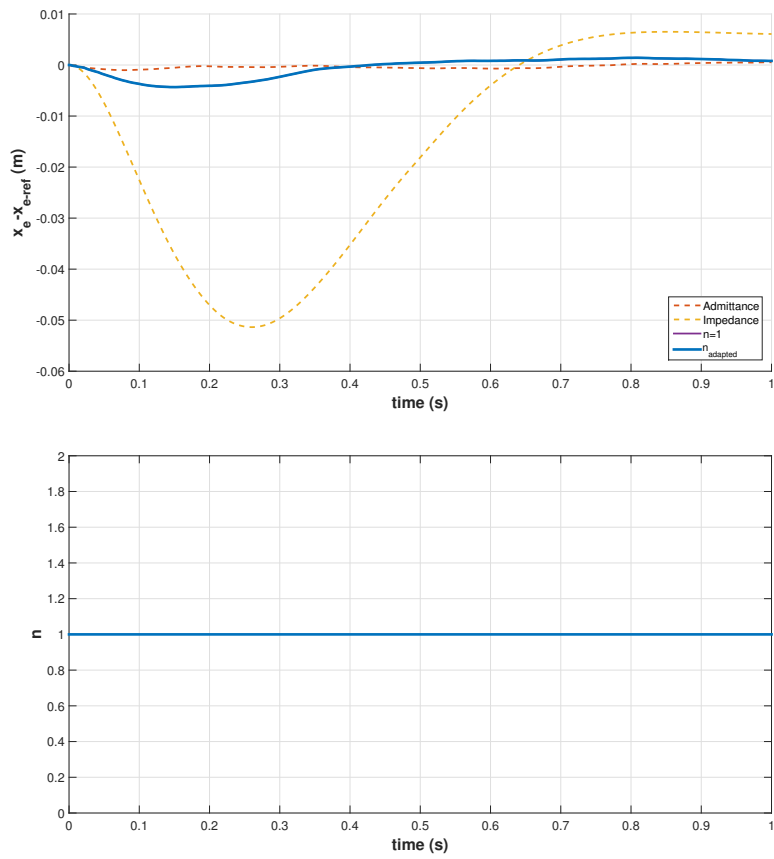


Figure 6.5: Error responses of the 2 d.o.f.s system to a step command position from 0 to 0.5m for  $k_e = 10N/m$

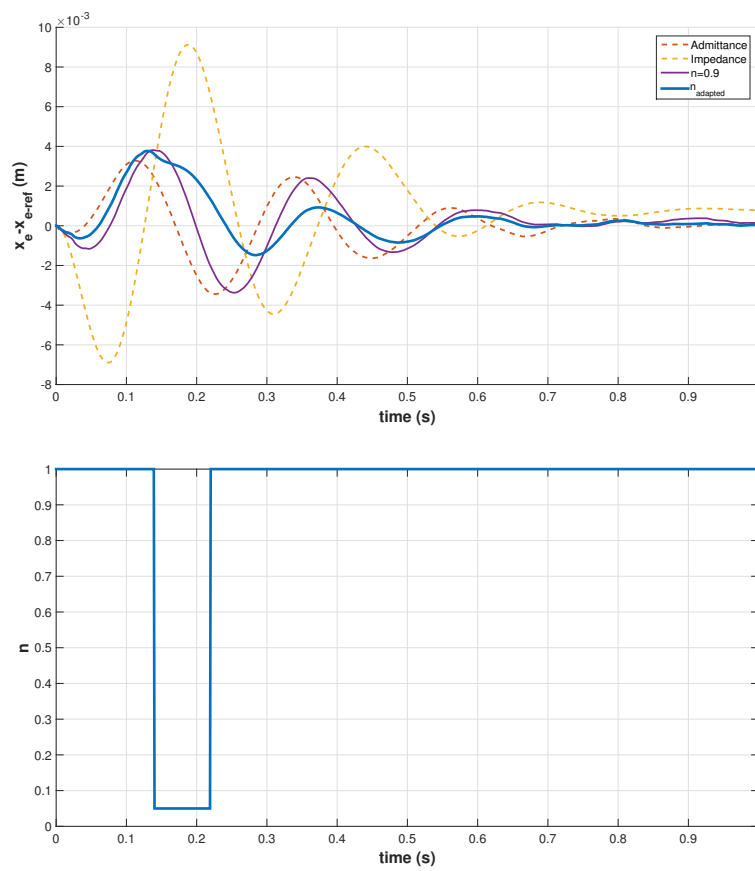


Figure 6.6: Error responses of the 2 d.o.f.s system to a step command position from 0 to 0.5m for  $k_e = 700N/m$



## 6.1 Fixed environment stiffness

---

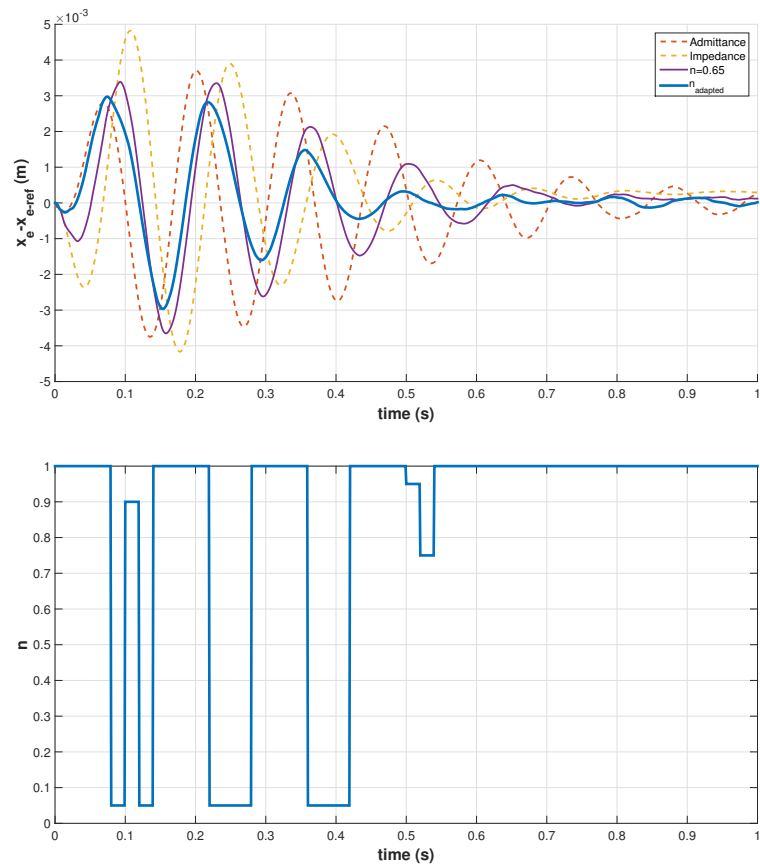


Figure 6.7: Error responses of the 2 d.o.f.s system to a step command position from 0 to  $0.5m$  for  $k_e = 2100N/m$

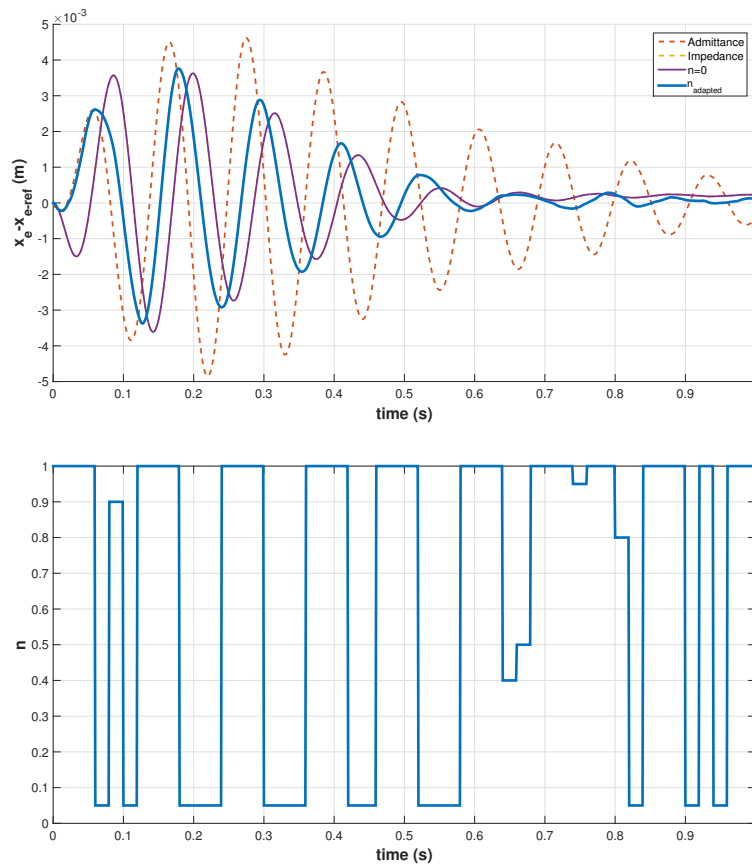


Figure 6.8: Error responses of the 2 d.o.f.s system to a step command position from 0 to  $0.5m$  for  $k_e = 3200N/m$

## 6.1 Fixed environment stiffness

---

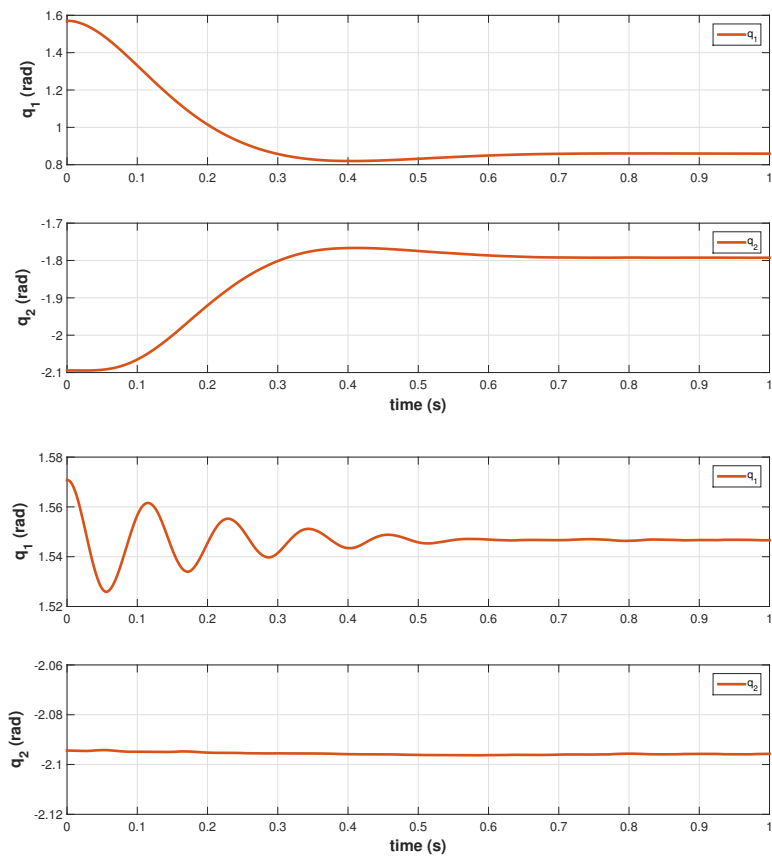


Figure 6.9: Joints coordinates of the 2 d.o.f.s system to a step command position from 0 to  $0.5m$  for  $k_e = 10 \text{ N/m}$  and  $k_e = 3200 \text{ N/m}$

## 6.2 Time-variant stiffness

Thank to the capability of the Neural Network of selecting a  $n$  depending on the states and the measured interaction force with the environment, the system can react promptly to changes in the external conditions, even if they vary suddenly.

Therefore the Adaptive Hybrid System results to be a suitable solution in case of time-variant environment stiffness, as figures 6.11, 6.13 and 6.15 show. Its error response is compared with the ones of the Impedance and Admittance Control.

The results in figure 6.11 are obtained considering a stiffness varying with a certain time law and giving to the system different consecutive unit steps (see figure 6.10). It can be seen that the proposed solution can follow the variation of the environment guaranteeing the properties of an almost zero steady state error and low overshoot in low stiffness case, typical of the Admittance Control, and an high stability in stiffer situation, characteristic of Impedance Control.

On the other hand in figure 6.13 a single unit command step is provided to the controller and the stiffness is made vary following an exponential law. One more time it can be observed that Impedance Control fails when the environment suddenly changes becoming softer due to its incapability in providing a stiff behavior. The Admittance Control instead presents instability in the stiffer situation since its limits in guaranteeing soft feature. The Adaptive Hybrid System interpolates these two characteristics and assures again almost zero steady state error with low stiffness and stability with high stiffness.

These situations are reported in order to compare their results with the ones already obtained in previous works on the hybrid system [9][10].

Figure 6.15 shows that the proposed strategy is able to adapt itself to changes in the environment condition also in the 2 d.o.f.s system. The error response is computed considering the environment evolution and the commanded displacement reported in figure 6.14. The command position is orthogonal to the wall.

Again it can be noticed that the Adaptive Hybrid System can guarantee a good damping of the response in stiff environment and a very low overshoot and steady state error in soft environment modifying its features with the Neural Network.

## 6.2 Time-variant stiffness

---

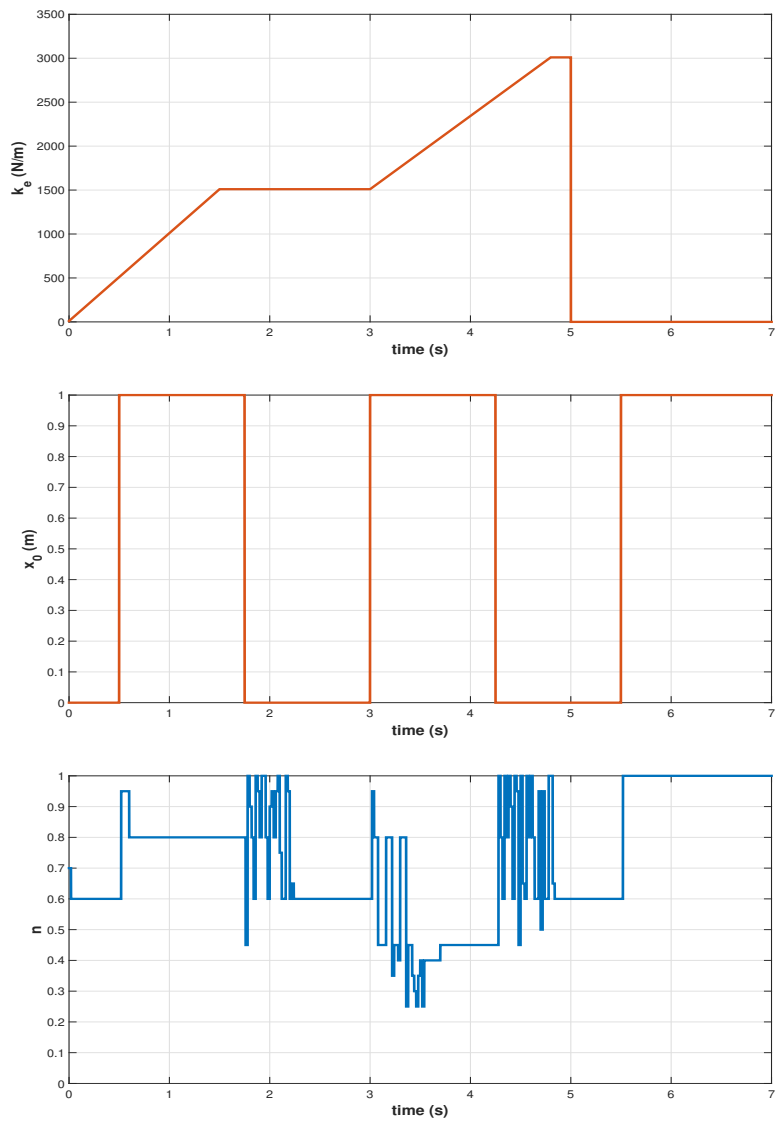


Figure 6.10: Time varying contact stiffness  $k_e$ , command position  $x_0$  and adapted  $n$  trend for the single d.o.f. system

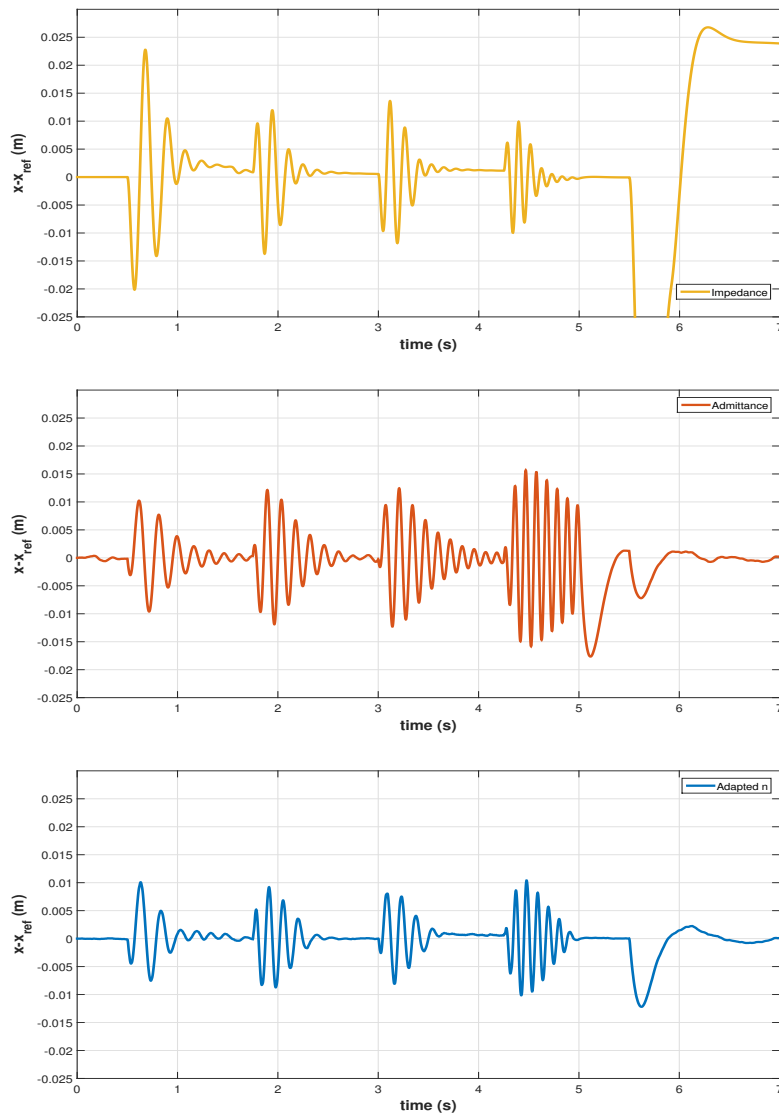


Figure 6.11: Comparison of errors for the time varying  $k_e$  for the single d.o.f. system

## 6.2 Time-variant stiffness

---

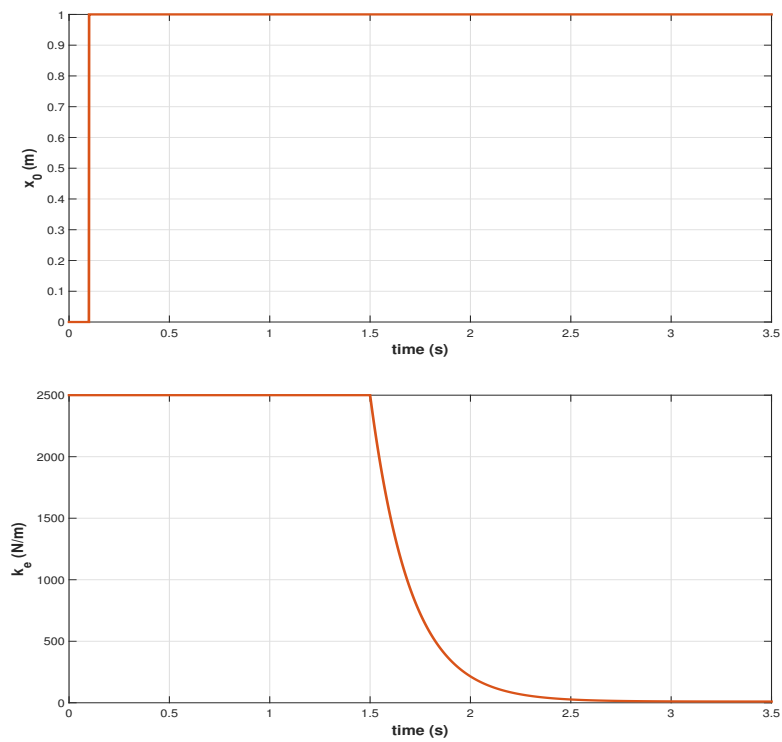


Figure 6.12: Time varying contact stiffness  $k_e$  with exponential trend and related command position  $x_0$  for the simulation in the single d.o.f. system cases

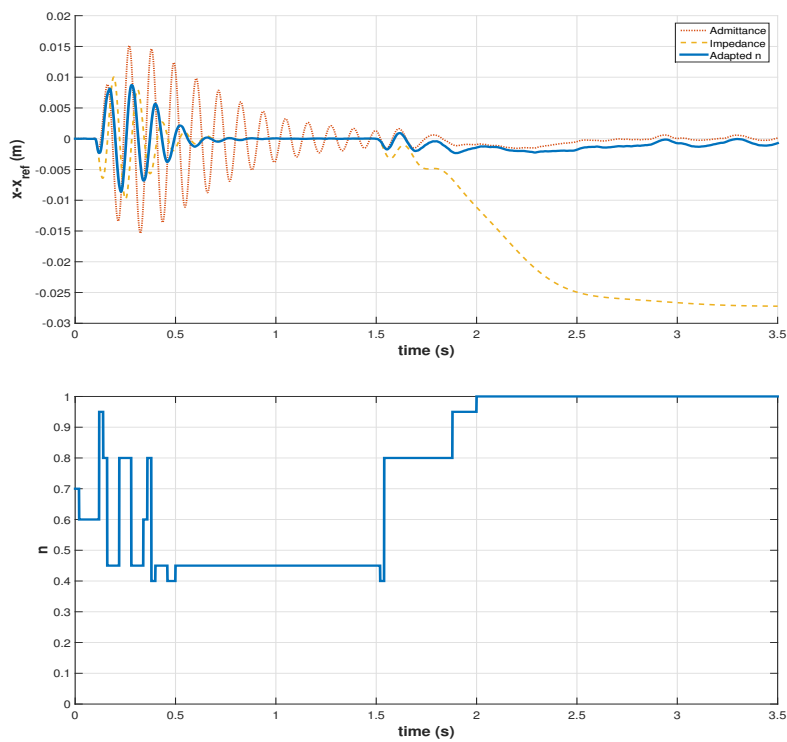


Figure 6.13: Comparison of errors for the time variant  $k_e$ , with exponential trend, in the single d.o.f. system case



## 6.2 Time-variant stiffness

---

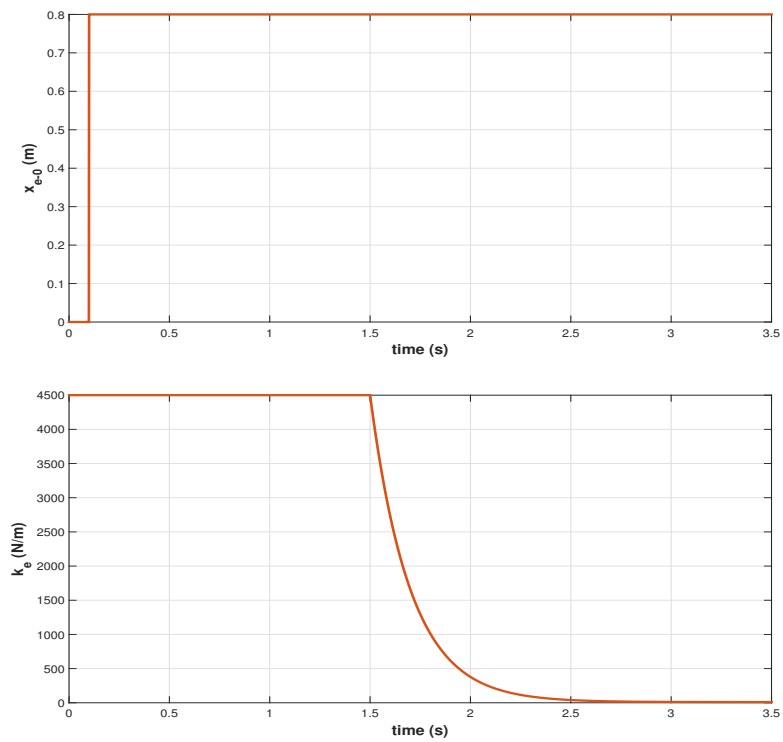


Figure 6.14: Time varying contact stiffness  $k_e$  with exponential trend and related command position  $x_{e0}$  for the simulation in the 2 d.o.f.s system cases

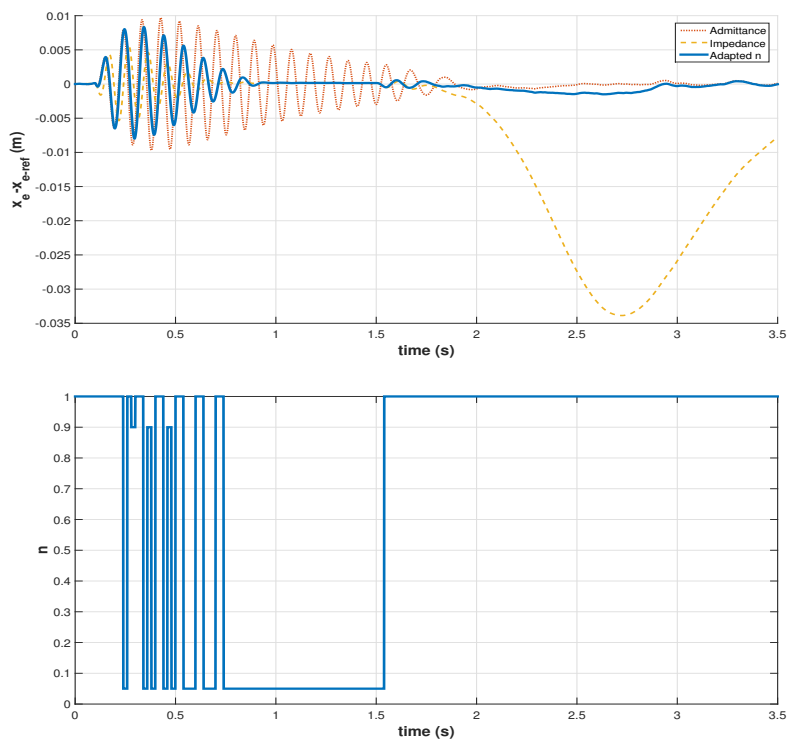


Figure 6.15: Comparison of errors for the time variant  $k_e$ , with exponential trend, in the 2 d.o.f.s system case

## 6.3 Robustness analysis

In the previous chapters it was shown that the main differences in the behavior between Impedance and Admittance Control take place when delays, uncertainties and uncompensated friction intervene in the system. For this reason the training of the Neural Network was performed introducing these effects. Moreover in the training a step command position of  $0.5m$  was used and a stiffness range between  $10N/m$  and  $3210N/m$  was considered.

In this section the robustness of the Adaptive Hybrid System is investigated simulating conditions outside the training, i.e. taking a stiffness outside the above-mentioned range, introducing different uncertainties, delays and friction and giving different command step higher than  $0.5m$ .

In figure 6.16 the error response of the single d.o.f. system in an environment with a stiffness outside the defined range is taken into account. The hybrid system with the Neural Network can guarantee good performances even in this situation. It is slightly worse than the best fixed  $n$  case, but only in terms of oscillation during the transient, indeed the settling time is almost the same. This means that the Neural Network system is robust to circumstances not foreseen in the design phase.

The same observation can be done observing the behavior of the 2 d.o.f.s system in figure 6.15. In the first instants the stiffness is  $4500N/m$  and it can be seen that the Adaptive Hybrid System responds in an appropriate way guaranteeing a certain damping. In addition, in this case a step command higher than the one utilized in the training phase was given to the system, however the controller behaves well.

Figures 6.17-6.20 show the error responses for both the single and two d.o.f.s cases increasing the uncertainties, delays and frictions with respect to the training condition. As examples, the stiffnesses  $k_e = 10N/m$ ,  $k_e = 1200N/m$ ,  $k_e = 2600N/m$  and  $k_e = 3200N/m$  are considered. Again the results of the Adaptive Hybrid System, Hybrid System with optimal fixed  $n$ , Admittance Control and Impedance Control are compared. The values used in these simulations are  $T_d = 2.5ms$ ,  $\hat{m} = 0.7*m$ ,  $c_v = 2Ns/m$  and  $F_c = 4N$  for the single d.o.f. system. Instead, as regards the two d.o.f.s case, they are  $T_d = 3ms$ ,  $\hat{M}_1 = 0.7*M_1$ ,  $\hat{M}_2 = 0.7*M_2$ ,  $\hat{J}_1 = 0.7*J_1$ ,  $\hat{J}_2 = 0.7*J_2$ ,  $c_v = 5Ns/m$  and  $F_c = 2N$ .

It can be noticed that the adaptive solution is robust when the conditions differ from the training situation. This property can be attributed to the generalization features of the Neural Network. The Adaptive Hybrid System continues to carry out its duty and interpolates between Impedance and Admittance Control correctly giving performance similar to the opti-

mal fixed  $n$  solution. Indeed the settling time is the same and the oscillations during the transient are comparable or sometimes better than the optimal fixed  $n$  response.

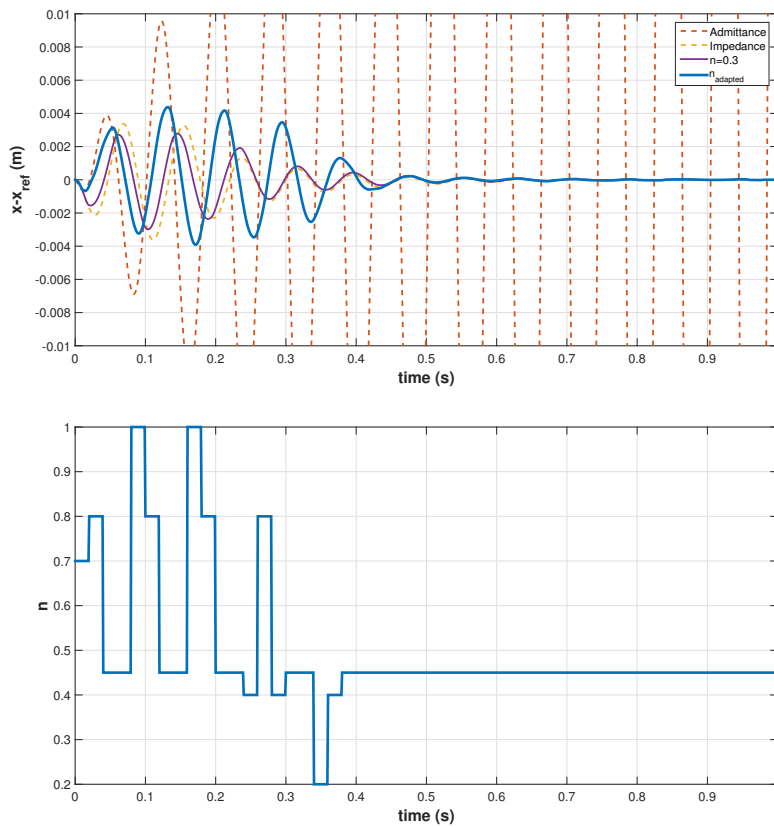


Figure 6.16: Error responses of the single d.o.f. system to a step command position from 0 to 0.5m for  $k_e = 5000N/m$  out of the training range

### 6.3 Robustness analysis

---

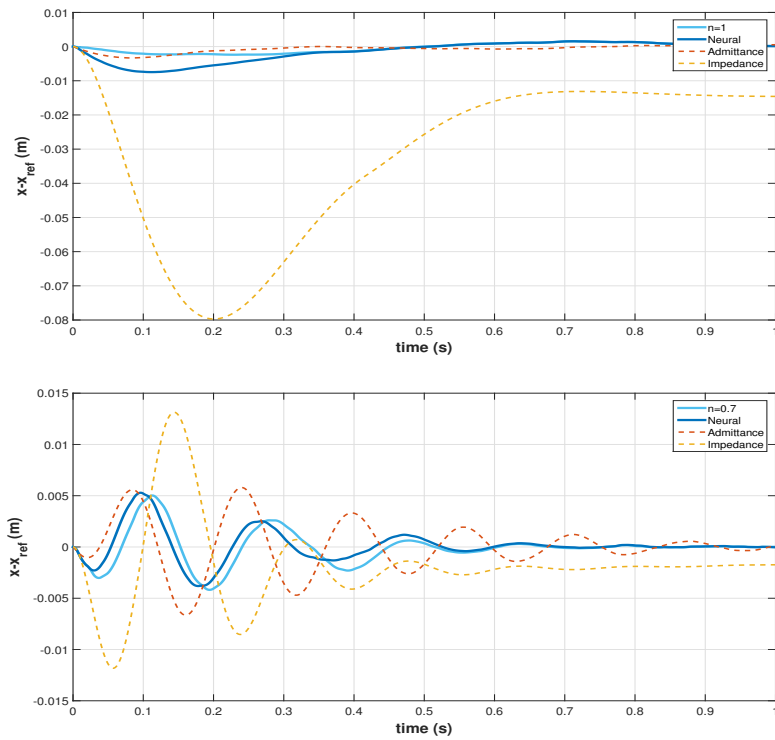


Figure 6.17: Error responses of the single d.o.f. system with increased uncertainties respectively for  $k_e = 10N/m$  and  $k_e = 1200N/m$

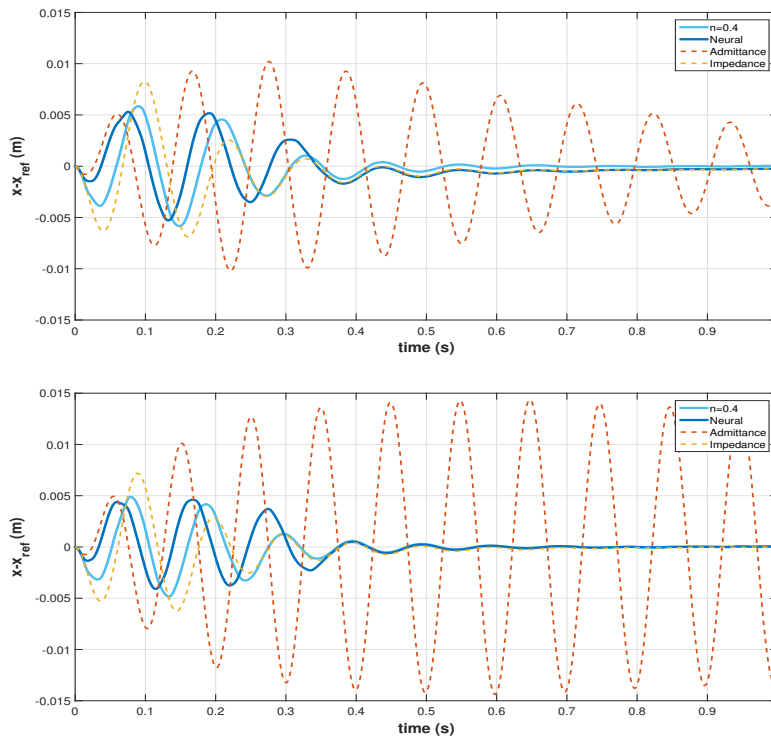


Figure 6.18: Error responses of the single d.o.f. system with increased uncertainties respectively for  $k_e = 2600N/m$  and  $k_e = 3200N/m$

### 6.3 Robustness analysis

---

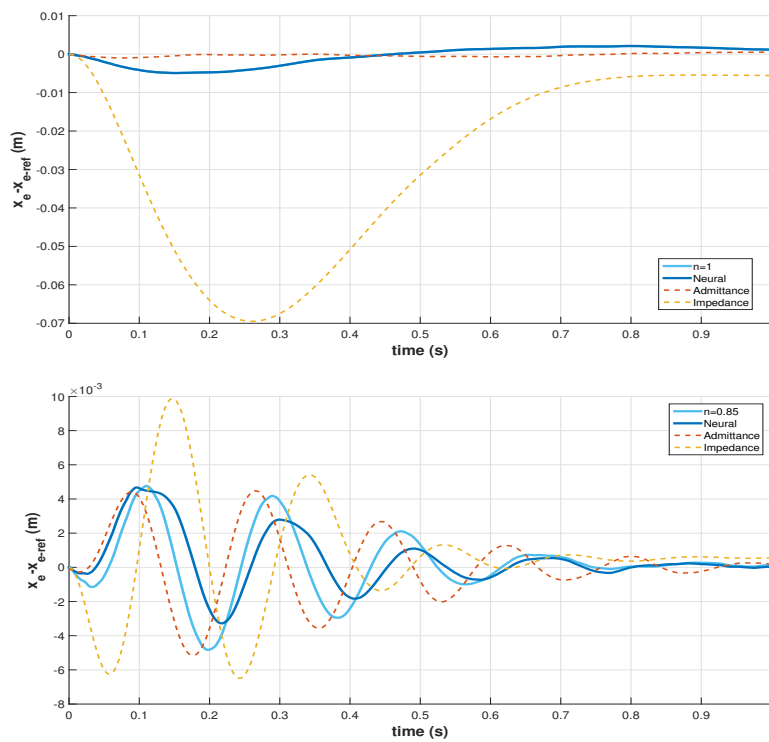


Figure 6.19: Error responses of the 2 d.o.f.s system with increased uncertainties respectively for  $k_e = 10N/m$  and  $k_e = 1200N/m$

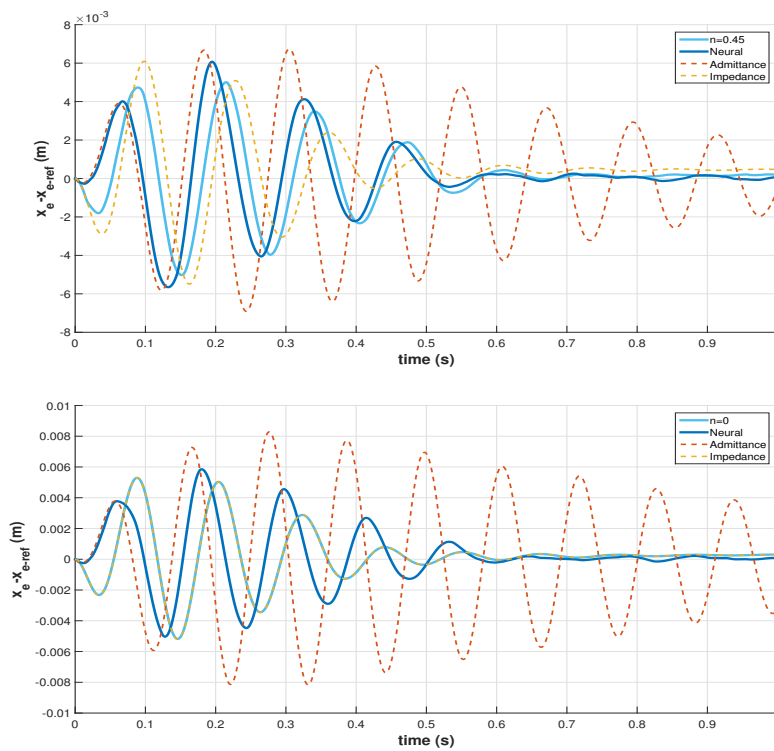


Figure 6.20: Error responses of the 2 d.o.f.s system with increased uncertainties respectively for  $k_e = 2600 N/m$  and  $k_e = 3200 N/m$



## 6.4 Specialized training

As last observation, it should be noticed that in the case the environment stiffness, either variable in time or not, is known, the training can be specialized obtaining performance higher than the pure Impedance and Admittance Control embedded in the system and higher than possible solutions with an optimal fixed  $n$ .

For example, figure 6.21 shows the error response of the single d.o.f. system with a network trained on a stiffness fixed at  $1600N/m$ . It is compared with the response of the optimal fixed  $n$  solution. It can be seen that the system with the Adaptive Hybrid Control follows better the reference trajectory.

This result is relevant whenever the environment is time-variant but known *a priori* with a certain accuracy or in case of a robot that has to accomplish different tasks working in different structured environments, fixed or not. Indeed in this latter situation it would be necessary more machines due to the different hardware requirements of the Admittance and Impedance Control. Developing the proposed strategy it could be possible to have a single robot with one controller capable of facing circumstances where an Admittance Control should be used and circumstances where an Impedance Control should be more suitable, just changing the weights of the network.

Of course also the optimal fixed  $n$  solution could be a good candidate in these situations. The choice between the two strategies should be a trade-off between the complexity of the controller and the desired performance depending on the level of knowledge of the environment stiffness.

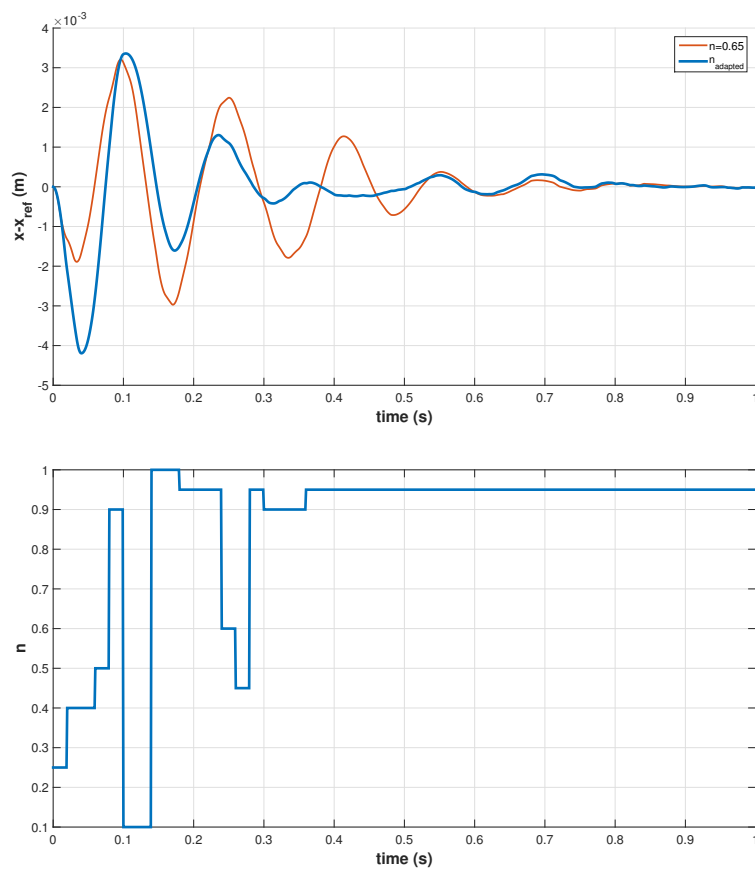


Figure 6.21: Comparison between error responses of Hybrid Control and Adaptive Hybrid Control for  $k_e = 1600N/m$

# Chapter 7

## Conclusions

The presented control framework is a new solution to the impedance control problem that continuously switches between controllers with admittance and impedance causality adapting itself to unknown environments by a continual selection of a proper duty cycle.

The time variant duty cycle allows to decide the correct contribution of each one of the two control laws. In this way it is possible to interpolate properly the features between them obtaining very good performance in different scenarios.

The system exploits a Feedforward Neural Network to adapt the control action. It gives as output the opportune duty cycle trend as a consequence of the position, velocity and interaction force evolution depending on the interacting environment.

It was proven that a Genetic Algorithm can be used successfully as optimization method in an offline training phase.

Simulation are performed for a single and a two d.o.f.s systems as first step for future developments for multiple d.o.f.s cases.

The results also show the robustness characteristics of the system. Its performance are just slightly affected by uncertainties in the physical system modeling, uncompensated friction and delay in measurements. This capability is related to the generalization feature of the Neural Network that are able to give good responses even in situation not strictly included in the training.

The system guarantees very interesting performance in time variant environments; this could make the proposed adaptive controller suitable for a wide range of possible application.

Summing up, the Adaptive Hybrid System Framework seems to be a promising alternative to already existing impedance control implementations. It unifies in a single controller the benefits from Admittance and

Impedance Control; indeed it can improve upon the steady state performance of Impedance Control and stability characteristics of Admittance Control.

The very next step for the development of this approach should be an experimental validation of the simulated results.

Moreover it should be interesting to apply the presented control strategy to a real application and compare it with other existing control laws.

As regards the analytical stability analysis, it was done for the simple system with a fixed duty cycle, in addition a linear closed loop system was considered. Therefore an extension of the analysis to a nonlinear, multi-degree-of-freedom closed-loop system could be an useful development.

Then it was seen that a Genetic Algorithm can lead to good results as concerns the determination of the Neural Network weights. However due to the problem nature, that can admits more possible solutions, and the stochastic nature of the method, the process could be slow. A deeper analysis aimed at understanding how to move towards a precise desired solution can improve the velocity and efficiency of the training phase.

In this work a physical system that remains in contact with the environment was considered. In reality, contact transitions from free motion to constraint one may occur and they are characterized by impulsive force. An important goal for future research could be the study of these situations.

Finally, as already explained, the idea behind the proposed strategy is a framework capable of interpolating the responses between two control laws with different causality. In this work simple Impedance and Admittance Control were used. It could be interesting to investigate the behavior of the system considering advanced versions of the two controllers embedded in the hybrid framework.

# Bibliography

- [1] M. H. Robert and J. J. Craig, “Hybrid position/force control of manipulators,” *ASME Journal of Dynamic Systems, Measurement, and Control*, vol. 105, pp. 126–133, 1981.
- [2] M. T. Mason, “Compliance and force control for computer controlled manipulators,” *IEEE Transactions on Systems, Man, and Cybernetics*, vol. SMC-11, no. 6, 1981.
- [3] N. Hogan, “Impedance control: An approach to manipulation,” *ASME Journal of Dynamic Systems, Measurement and Control*, vol. 107, pp. 1–7, 1985.
- [4] N. Hogan, “Impedance control: An approach to manipulation,” *ASME Journal of Dynamic Systems, Measurement and Control*, vol. 107, pp. 8–16, 1985.
- [5] N. Hogan, “Impedance control: An approach to manipulation,” *ASME Journal of Dynamic Systems, Measurement and Control*, vol. 107, pp. 17–24, 1985.
- [6] N. Hogan, “Stable execution of contact task using impedance control,” *IEEE International Conference of Robotics and Automation*, pp. 1047–1054, 1987.
- [7] R. J. Anderson and M. Spong, “Hybrid impedance control of robotic manipulators,” *IEEE Journal of Robotics and Automation*, vol. 4, no. 5, 1988.
- [8] G. J. Liu and A. A. Goldenberg, “Robust hybrid impedance control of robot manipulators,” *IEEE International Conference of Robotics and Automation*, pp. 287–292, 1991.
- [9] C. Ott, R. Mukherjee, and Y. Nakamura, “A hybrid system framework for unified impedance and admittance control,” *Journal of Intelligent and Robotic Systems*, 2014.

- [10] C. Ott, R. Mukherjee, and Y. Nakamura, “Unified impedance and admittance control,” *IEEE International Conference on Robotics and Automation*, pp. 554–561, 2010.
- [11] D. A. Lawrence, “Impedance control stability properties in common implementations,” *IEEE International Conference of Robotics and Automation*, pp. 1185–1190, 1988.
- [12] S. D. Eppinger and W. P. Seering, “Understanding bandwidth limitations in robot force control,” *IEEE International Conference of Robotics and Automation*, pp. 904–909, 1987.
- [13] C. Ott, O. Eiberger, W. Friedl, B. Bäuml, U. Hillenbrand, C. Borst, A. Albe-Schäffer, B. Brunner, H. Hirschmüller, S. Kielhöfer, R. Konietschke, M. Suppa, T. Wimbök, F. Zacharias, and G. Hirzinger, “A humanoid two-arm system for dexterous manipulation,” *Humanoids*, 2006.
- [14] G. Cheng, S.-H. Hyon, J. Morimoto, A. Ude, G. Colvin, W. Scroggin, and S. C. Jacobsen, “Cb: A humanoid research platform for exploring neuroscience,” *HUMANOIDS’06*, 2006.
- [15] J.-J. E. Slotine and W. Li, “Adaptive manipulator control: A case study,” *IEEE Transactions on Automatic Control*, vol. 33, no. 11, 1988.
- [16] W.-S. Lu and Q.-H. Meng, “Impedance control with adaptation for robotic manipulations,” *IEEE Transactions on Robotics and Automation*, vol. 7, no. 3, 1991.
- [17] S. K. Singh and D. O. Popa, “An analysis of some fundamental problems in adaptive control of force and impedance behavior: Theory and experiments,” *IEEE Transactions on Robotics and Automation*, vol. 11, no. 6, 1995.
- [18] L. J. Love and W. J. Book, “Environment estimation for enhanced impedance control,” *IEEE International Conference of Robotics and Automation*, 1995.
- [19] H. Seraji, “Adaptive admittance control: An approach to explicit force control in compliant motion,” *IEEE International Conference on Robotics and Automation*, pp. 2705–2712, 1994.

- [20] G. Cybenko, "Approximation by superpositions of a sigmoidal function," *Mathematics of Control, Signals, and Systems*, vol. 2, pp. 303–314, 1989.
- [21] K. Hornik, M. Stinchcombe, and H. White, "Multilayer feedforward networks are universal approximators," *Neural Networks*, vol. 2, pp. 359–366, 1989.
- [22] K. S. Narendra and K. Parthasarathy, "Identification and control of dynamical system using neural networks," *IEEE Transactions on Neural Networks*, vol. 1, no. 1, 1990.
- [23] P. J. Werbos, *Handbook of Intelligence Control. Neural, Fuzzy, and Adaptive Approaches*. Van Nostrand Reinhold, 1992.
- [24] S. Haykin, *Neural Networks and Learning Machines*. Pearson Prentice Hall, 2009.
- [25] G. S.-X. Cheng, "Model-free adaptive process control," 1997.
- [26] X. Aidong, Z. Yangbo, S. Yan, and L. Mingzhe, "An improved model free adaptive control algorithm," *IEEE 2009 Fifth International Conference on Natural Computation*, 2009.
- [27] S. G. Shuzhi, Z.-L. Wang, and Z.-J. Chen, "Adaptive static neural network control of robots," *IEEE International Conference Industrial Technology*, vol. 1, pp. 240–244, 1994.
- [28] X. Zhang, H. Zhang, Q. Sun, and Y. Luo, "Adaptive dynamic programming-based optimal control of unknown nonaffine nonlinear discrete-time systems with proof of convergence," *Elsevier Neurocomputing*, vol. 91, pp. 48–55, 2012.
- [29] C. Qin, H. Zhang, and Y. Luo, "Adaptive optimal control for nonlinear discrete-time systems," *IEEE Symposium on Adaptive Dynamic Programming and Reinforcement Learning*, 2013.
- [30] T. Dierks and S. Jagannathan, "Online optimal control of affine nonlinear discrete-time systems with unknown internal dynamics by using time-based policy," *IEEE Transactions on Neural Networks and Learning Systems*, vol. 23, no. 7, 2012.
- [31] H. Nakanishi, K. Yoshida, H. Ueno, N. Inaba, T. Nishimaki, and M. Oda, "Dynamics, control and impedance matching for robotic

- capture of a non-cooperative satellite,” *Advanced Robotics*, vol. 18, no. 2, pp. 175–198, 2004.
- [32] B. P. Larouche and G. Z. H. Zhu, “Investigation of impedance controller for autonomous on-orbit servicing robot,” *Canadian Aeronautics and Space Journal*, vol. 59, no. 1, pp. 15–24, 2013.
- [33] M. Diftler, J. Mehling, M. Abdallah, N. Radford, L. Bridgwater, A. Sanders, R. Askew, D. Linn, J. Yamokosi, F. Permenter, B. Hargrave, R. Platt, R. Savely, and R. Ambrose, “Robonaut 2 - the first humanoid robot in space,” *IEEE International Conference on Robotics and Automation*, 2011.
- [34] B. Siciliano and O. Khatib, *Springer Handbook of Robotics*. Springer, 2008.
- [35] M. Pelletier and M. Doyon, “On the implementation and performance of impedance control on position controlled robots,” *IEEE International Conference on Robotics and Automation*, vol. 2, pp. 1228–1233, 1994.
- [36] B. Siciliano, L. Sciavicco, L. Villani, and O. Giuseppe, *Robotics. Modeling, Planning and Control*. Springer, 2010.
- [37] P. Maciejasz, J. Eschweiler, K. Gerlach-Hann, A. Jansen-Troy, and S. Leonhardt, “A survey on robotic devices for upper limb rehabilitation,” *Journal of NeuroEngineering and Rehabilitation*, vol. 11, no. 3, 2014.
- [38] N. Diolaiti, C. Melchiorri, and S. Stramigioli, “Contact impedance estimation for robotic system,” *IEEE Transactions on Robotics*, vol. 21, no. 5, 2005.
- [39] L. Roveda, F. Vicentini, and L. Molinari Tosatti, “Deformation-tracking impedance control in interaction with uncertain environments,” *IEEE RSJ International Conference on Intelligent Robots and Systems*, 2013.
- [40] B. Yalcin and K. Ohnishi, “Environmental impedance estimation and imitation in haptics by sliding mode neural networks,” *IEEE Industrial Electronics*, pp. 4014–4019, 2006.
- [41] F. Aghili, “Robust impedance control of manipulators carrying a heavy payload,” *ASME Journal of Dynamic Systems, Measurement and Control*, vol. 132, 2010.



- [42] D. Erickson and M. Weber, “Contact stiffness and damping estimation for robotic systems,” *The International Journal of Robotics Research*, vol. 22, no. 1, pp. 41–57, 2003.
- [43] S. Jung, T. C. Hsia, and R. G. Bonitz, “Force tracking impedance control of robot manipulators under unknown environment,” *IEEE Transactions on Control System Technology*, vol. 12, no. 3, pp. 474–483, 2004.
- [44] S. Lee and H. S. Lee, “Intelligent control of manipulators interacting with an uncertain environment based on generalized impedance,” *IEEE International Symposium on Intelligent Control*, pp. 61–66, 1991.
- [45] W. S. Newman, “Stability and performance limits of interaction controllers,” *Journal of Dynamic Systems, Measurement, and Control*, vol. 114, 1992.
- [46] J. K. Salisbury, “Active stiffness control of a manipulator in cartesian coordinates,” *Proceedings of the IEEE Conference on Decision and Control*, pp. 383–388, 1980.
- [47] T. Valency and M. Zacksenhouse, “Accuracy/robustness dilemma in impedance control,” *ASME Journal of Dynamic Systems, Measurement, and Control*, vol. 125, pp. 310–319, 2003.
- [48] D. Liberian and A. S. Morse, “Basic problems in stability of switched systems,” *IEEE Control System Mag.*, pp. 59–70, 1999.
- [49] K. J. Aström and B. Wittenmark, *Adaptive Control*. Dover Publications, Inc., 2008.
- [50] I. Zelinka, V. Snasel, and A. Abraham, *Handbook of Optimization. From Classical to Modern Approach*. Springer, 2013.
- [51] A. Chipperfiel, P. Fleming, H. Pohlheim, and C. Fonseca, *Genetic Algorithm Toolbox. For Use with MATLAB*, 1994.
- [52] M. H. Beale, M. T. Hogan, and H. B. Demuth, *Neural Network Toolbox. User’s Guide.*, 2015.
- [53] H. Nakanishi and K. Yoshida, “Impedance control for free-flying space robots - basic equations and applications,” *International Conference on Intelligent Robots and Systems*, 2006.